UNIVERSIDADE DE SÃO PAULO
FACULDADE DE MEDICINA DE RIBEIRÃO PRETO
DEPARTAMENTO DE GENÉTICA

Flaviane Maria Galvão Rocha

Desafios impostos ao dermatófito *Trichophyton rubrum* pela sertralina, um fármaco utilizado como antidepressivo

Ribeirão Preto - SP
2023

Flaviane Maria Galvão Rocha

Desafios impostos ao dermatófito *Trichophyton rubrum* pela sertralina, um fármaco utilizado como antidepressivo

Tese apresentada ao programa de pós-graduação em Ciências Biológicas da Faculdade de Medicina de Ribeirão Preto da Universidade de São Paulo para obtenção do título de doutora em Ciências.
Área de concentração: Genética

Orientador: Prof. Dr. Antonio Rossi Filho
Co-orientadora: Profª Dra. Nilce Maria Martinez Rossi

Ribeirão Preto - SP
2023

Rocha, Flaviane Maria Galvão

Desafios impostos ao dermatófito *Trichophyton rubrum* pela sertralina, um fármaco utilizado como antidepressivo. Ribeirão Preto, 2023.

131 p. : il. ; 30 cm

Tese de Doutorado, apresentada à Faculdade de Medicina de Ribeirão Preto/USP. Área de concentração: Ciências biológicas (Genética).

Orientador: Rossi Filho, Antonio.

1.Sertralina 2. Reposicionamento 3. *Trichophyton rubrum* 4. *Splicing* alternativo 5. RNAseq

APOIO E SUPORTE FINANCEIRO

Este projeto foi realizado com o apoio financeiro das seguintes entidades e instituições:
Fundação de Amparo à Pesquisa do Estado de São Paulo – FAPESP- Projeto temático (2019/22596-9)
Coordenação de Aperfeiçoamento de Pessoal do Ensino Superior – CAPES- Bolsa de Doutorado (Demanda social - 001)
Conselho Nacional de Desenvolvimento Científico e Tecnológico – CNPq (Nº 307876/2021-7)
Fundação de Apoio ao Ensino, Pesquisa e Assistência – FAEPA (FMRP-USP)
Comitê de Ética do Hospital Universitário da Faculdade de Medicina de Ribeirão Preto - HCFMRP-USP (Protocolo nº 4.278.367/2020).
Programa de Aperfeiçoamento de Ensino – PAE – 2º semestre de 2022 e 1º semestre de 2023.

Ficha de aprovação

Nome: Flaviane Maria Galvão Rocha
Título: Desafios impostos ao dermatófito *Trichophyton rubrum* pela sertralina, um fármaco utilizado como antidepressivo

Tese apresentada ao programa de pós-graduação em Ciências Biológicas da Faculdade de Medicina de Ribeirão Preto da Universidade de São Paulo, para obtenção do título de doutora em Ciências.
Área de concentração: Genética

Aprovada em ____/____/_____.

Banca Examinadora

Prof. Dr.: _____ Instituição: _____
Julgamento: _____ Assinatura: _____

Prof. Dr.: _____ Instituição: _____
Julgamento: _____ Assinatura: _____

Prof. Dr.: _____ Instituição: _____
Julgamento: _____ Assinatura: _____

Prof. Dr.: _____ Instituição: _____
Julgamento: _____ Assinatura: _____

Normalização Adotada
Este documento foi elaborado de acordo com:
As normas brasileiras em documentação do Comitê Brasileiro (ABNT/CB-14): NBR 6023, NBR 6024, NBR 6027 e NBR 6028.
Universidade de São Paulo. Sistema Integrado de Bibliotecas. Diretrizes para apresentação de dissertações e teses da USP: documento eletrônico e impresso Parte I (ABNT), São Paulo, 2020.

Dedico este trabalho especialmente ao meu pai, Antônio de Sousa Rocha (*In memorium*), grande incentivador do meu crescimento profissional e pessoal, foi quem me ensinou a nunca desistir.

Agradecimentos

Agradeço a Deus por todas as bênçãos a mim concedidas e força para superar as adversidades.

Agradeço imensamente a Dra. Nilce M. Martinez-Rossi por permitir que eu compusesse sua equipe, a todo apoio, confiança, incentivo e orientação na condução deste projeto, discussão de resultados, a toda dedicação nas correções, sugestões em artigos, resumos de congresso e de minha tese, e toda valiosa atenção que foram de fundamental importância para a construção e execução deste projeto.

Ao meu orientador Dr. Antonio Rossi Filho toda dedicação, compartilhamento de conhecimento, confiança na execução de experimentos, incentivo, atenção especial em minha orientação e discussão de resultados que foram cruciais para a execução deste projeto.

Sou grata a toda a equipe do laboratório, aos técnicos Marcos Diogo Martins, Vanderci Massaro Oliveira, Mendelson Mazucato por toda ajuda no preparo dos materiais, auxílio na execução de experimentos, colaboração e atenção. Tudo isso foi fundamental para a execução deste projeto.

Agradeço imensamente ao Dr. Pablo R. Sanches por estar sempre de prontidão para ajudar com as análises de bioinformática e colaboração neste projeto.

À Dra. Maíra Martins, sou grata pela ajuda enquanto esteve no laboratório, apesar de breve foi significativa para meu crescimento profissional. Agradeço sua dedicação em me explicar procedimentos, conceitos, discussões de resultados, contribuição na redação do meu projeto de doutorado e na construção das bibliotecas do RNA-seq.

À Dra. Tamíres A. Bitencourt por sua ajuda na construção das bibliotecas do RNA-seq, protocolos, sugestões e a todos os momentos de grande aprendizado quando era pós-doutoranda do laboratório.

Ao Dr. Matthew S. Sachs, docente da Texas A&M University, USA, pelas sugestões e contribuição neste projeto.

À Dra. Monise F. Petrucelli e ao Dr. Leonardo M. Santana pela atenção, sugestões, e contribuições, importantes para a construção desta tese. Aos demais colegas do laboratório, aos professores da pós-graduação e toda infraestrutura da Universidade de São Paulo que propiciou a execução deste projeto.

Agradeço ao coordenador da pós-graduação Dr. Klaus Hartmann Hartfelder e a Chefe do departamento Dra. Ester Silveira Ramos por toda atenção, disposição, respeito e ajuda

recebida essenciais para o bom desenvolvimento deste projeto. Agradeço também a toda equipe da secretaria da pós-graduação.

Sou grata a toda a minha família por me dar forças para continuar. A minha mãe agradeço todo o esforço, amor e carinho ao longo de toda a minha vida. Aos meus irmãos, agradeço todo cuidado e dedicação em minha criação. Sou grata as minhas sobrinhas lindas Dalila, Débora e Amália por darem força para a "titia vi" em todos os momentos. Ao meu sobrinho Arthur por todo carinho. Meus cunhados Danilo, Amaral e minha cunhada Núbia por me tratarem sempre muito bem, muito obrigada. Por último, mas não menos importante, minha tia Dalva por toda ajuda no processo de despedida do meu pai, uma dando força para a outra, ajudando a superar essa perda irreparável em nossas almas. Agradeço aos meus familiares da parte de meu esposo, meus sogros Maria e Raimundo, minhas cunhadas, sobrinhos e sobrinhas por toda alegria que trouxeram para minha vida. Todo o apoio emocional recebido por vocês foi crucial para o desenvolvimento deste projeto.

Agradeço imensamente meu esposo Carlos Henrique, grande companheiro de bancada, da vida, sempre ao meu lado. Contribuiu para este projeto sugerindo experimentos, padronizando técnicas, discutindo todos os resultados obtidos, analisando todos os dados comigo, calculando comigo desde uma diluição seriada até padronização de *primers*, construindo todos os gráficos comigo com toda paciência e dedicação que somente ele tem, e por todos os momentos compartilhados no laboratório de incomensurável importância para este projeto.

A todos que contribuíram direta ou indiretamente neste trabalho!

RESUMO

ROCHA, F.M.G. **Desafios impostos ao dermatófito *Trichophyton rubrum* pela sertralina, um fármaco utilizado como antidepressivo.** Tese (Doutorado) – Faculdade de Medicina de Ribeirão Preto, Universidade de São Paulo, Ribeirão Preto, 2023.

O número limitado de alvos celulares para os fármacos em uso, e a resistência a eles, dificulta o tratamento das infecções fúngicas. *Trichophyton rubrum* é responsável pela maioria das infecções cutâneas denominadas dermatofitoses, que representam um problema de saúde pública crescente. Por isso, a identificação de novos compostos com atividade antifúngica se faz necessária, mas seu desenvolvimento é demorado e caro. O reposicionamento de fármacos em uso apresenta-se como uma das abordagens de menor custo para sua implementação. Neste contexto, a sertralina (SRT), um antidepressivo, apresenta-se como candidato para prescrição como antifúngico. Nesse sentido, os efeitos do fármaco SRT no transcriptoma do dermatófito *T. rubrum* foram estudados através do sequenciamento de RNA (RNA-seq). A SRT revelou a expressão diferencial de genes e suas isoformas alternativas através do mecanismo de *Splicing* alternativo (SA) como um dos efeitos marcantes de sua toxicidade em *T. rubrum*. Foi prevalente a retenção de íntrons entre os eventos de SA. Os resultados obtidos com a dosagem de ergosterol evidenciaram que a membrana plasmática foi prejudicada. SRT também modulou genes que codificam enzimas relacionadas ao metabolismo energético fúngico, desintoxicação celular e defesa contra o estresse oxidativo. A SRT induz ou reprime a retenção de íntrons em genes que codificam para quinases, fatores de transcrição, transportadores, chaperonas, dentre outros, relacionados à patogênese e adaptação fúngica. Desta forma, foi confirmada a atividade antifúngica da SRT contra *T. rubrum* mostrando potenciais alvos para seu uso estratégico no tratamento das dermatofitoses.

Palavras chave: RNA-seq; reposicionamento; dermatofitose; sertralina; *Trichophyton rubrum*

ABSTRACT

ROCHA, F.M.G. **Challenges posed to the dermatophyte *Trichophyton rubrum* by sertraline, a drug used as an antidepressant.** Tese (Doutorado) – Faculdade de Medicina de Ribeirão Preto, Universidade de São Paulo, Ribeirão Preto, 2023.

The limited number of cellular targets for the drugs in use, and the resistance to them, makes the treatment of fungal infections difficult. *Trichophyton rubrum* is responsible for most cutaneous fungal infections called dermatophytoses, representing a growing public health problem. Therefore, identifying new compounds with antifungal activity is necessary, but their development is time-consuming and expensive. The repositioning of drugs in use is one of the lowest-cost approaches for their implementation. Sertraline (SRT), an antidepressant, is a candidate for prescription as an antifungal. In this sense, we studied the effects of SRT on the transcriptome of *T. rubrum* through RNA sequencing (RNA-seq). The results showed that the fungal cell wall was impaired. SRT revealed the differential expression of genes and their alternative isoforms through alternative Splicing (AS) as a hallmark effect of its toxicity in *T. rubrum*. Intron retention was the prevalent type of AS event mechanism. The results obtained with the ergosterol dosage showed that the plasmatic membrane was harmed. SRT also modulated genes encoding enzymes related to fungal energy metabolism, cellular detoxification, and defense against oxidative stress. SRT induces or represses intron retention in genes coding for the kinases, transcription factors, transporters, and chaperones, among others, related to fungal pathogenesis and adaptation. SRT also modulated genes encoding enzymes related to fungal energy metabolism, cellular detoxification, and defense against oxidative stress. Thus, the antifungal activity of SRT against *T. rubrum* was confirmed, showing potential targets for its strategic use in treating dermatophytoses.

Keywords: RNA-seq; repositioning; dermatophytosis; sertraline; *Trichophyton rubrum*

Lista de figuras

Lista de tabelas

Sumário

Introdução

1. Introdução

1.1 O dermatófito *Trichophyton rubrum*

Trichophyton rubrum é um fungo filamentoso capaz de infectar estruturas queratinizadas do hospedeiro humano. É o responsável por quadros clínicos de progressão lenta e recalcitrantes. Na maioria das vezes é restrita ao estrato córneo (camada mais externa da pele), porém, o fungo pode progredir para camadas mais profundas da pele causando quadros graves em pacientes com algum comprometimento imunológico. É o fungo mais comum em casos de dermatofitoses e sua abrangência corresponde a quase um quarto da população mundial. Devido ao aumento de sua incidência e dificuldades na remissão clínica completa, as dermatofitoses são um grave problema de saúde pública (Martinez-Rossi *et al.*, 2021; Gupta and Venkataraman, 2022).

Durante o processo de infecção, *T. rubrum* deve superar as defesas naturais do hospedeiro, como por exemplo, o espessamento do estrato córneo, a regeneração contínua da pele (descamação), a composição de ácidos graxos, os peptídeos antimicrobianos, o pH moderadamente ácido e a competição com a microbiota residente. Este dermatófito utiliza mecanismos que dificultam seu reconhecimento pelas células especializadas do sistema imunológico do hospedeiro. A resposta efetora das células do sistema imune é prejudicada com a secreção de vesículas extracelulares, secreção de enzimas hidrolíticas e remodelação da parede celular. Mecanismos de resistência antifúngica têm sido relatados em dermatófitos, incluindo mutações pontuais com alteração nos sítios-alvo de enzimas, aumento da atividade mediada por transportadores para efluxo dos fármacos, aumento da depuração do fármaco devido indução da expressão de genes que codificam para enzimas neutralizantes, formação de biofilmes e *splicing* alternativo (SA) (Martinez-Rossi *et al.*, 2021; Osset-Trénor *et al.*, 2023) (**Figura 1**).

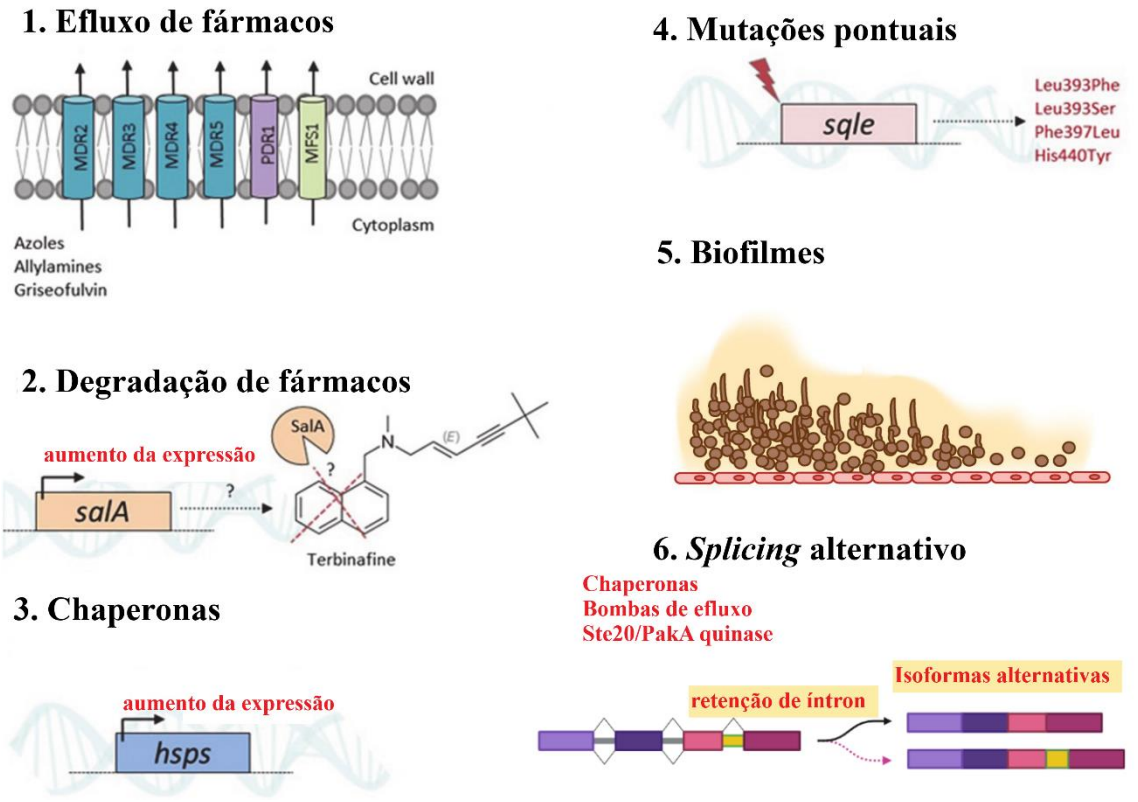

Figura 1. Estratégias empregadas por *Trichophyton rubrum* para superar a toxicidade de antifúngicos. **Adaptado** (Hokken *et al.*, 2019; Martinez-Rossi *et al.*, 2021).

1.2 Desafios para o tratamento das dermatofitoses

Os antifúngicos disponíveis na prática médica contra dermatófitos são poucos. Atualmente terbinafina é o principal antifúngico de escolha para o tratamento das dermatofitoses. Outros fármacos como o itraconazol, fluconazol e posaconazol também são utilizados. Estes antifúngicos possuem mecanismos de ação intimamente relacionados, atuando na inibição da biossíntese do ergosterol (**Figura 2**). Dados da literatura relatam a ocorrência de linhagens resistentes a esses antifúngicos, principalmente quando sua prescrição ocorre por longos períodos. Tratamentos prolongados e descontinuados podem levar a infecções recalcitrantes favorecendo a seleção de linhagens resistentes (Martinez-Rossi *et al.*, 2021; Osset-Trénor *et al.*, 2023).

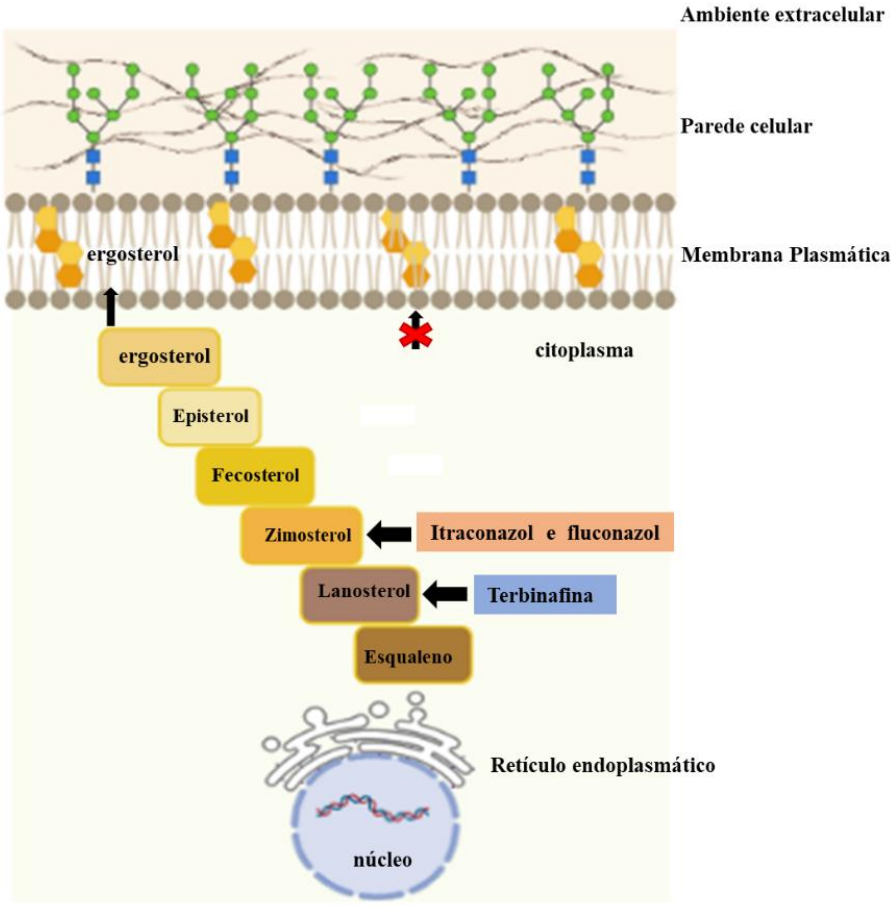

Figura 2. Via de biossíntese de ergosterol e antifúngicos. Os azólicos itraconazol e fluconazol, e a alilamina terbinafina reduzem o conteúdo de ergosterol na célula fúngica através da inibição de sua síntese (representado em vermelho (X) **Fonte**: O autor, 2023.

O número disponível de antifúngicos para uso clínico, a ocorrência de resistência e o limitado número de alvos terapêuticos torna necessária a busca de novas estratégias para o tratamento das dermatofitoses. Dentre as alternativas possíveis destaca-se o reposicionamento de fármacos e a combinação de fármacos com ação sinérgica como muito vantajosas.

1.3 Reposicionamento de fármacos

A utilização de um medicamento já aprovado com propriedades farmacológicas conhecidas que possa ser utilizado como antifúngico é extremamente vantajosa. Pelo reposicionamento é possível ampliar as opções terapêuticas com significativa economia de tempo e recursos financeiros (Ashburn and Thor, 2004) (**Figura 3**).

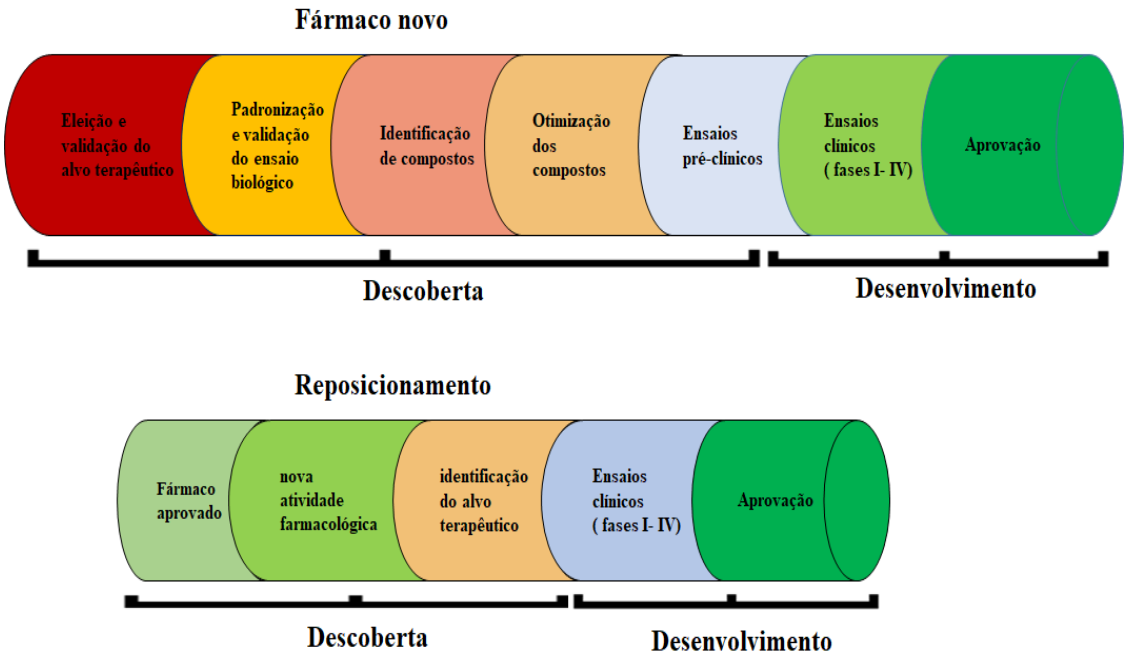

Figura 3. Resumo das etapas da descoberta de um fármaco e do reposicionamento de um fármaco em uso na prática médica. **Fonte**: Adaptado (Ashburn and Thor, 2004).

Neste contexto, o fármaco sertralina (SRT), um antidepressivo pertencente ao grupo dos inibidores seletivos da recaptação da serotonina (Devane *et al.*, 2002) (**Figura 4**), apresenta potencial para prescrição alternativa como antifúngico. Além disso, a inexistência de gene homólogo que codifica para o transportador de serotonina em fungos, indica que a ação inibitória da SRT seja em diferente alvo celular (Ayaz *et al.*, 2015; Trevino-Rangel *et al.*, 2019).

O potencial uso da SRT como fármaco antifúngico foi observado pela primeira vez em pacientes submetidas a este antidepressivo para tratamento de transtorno disfórico pré-menstrual. Durante esse tratamento as pacientes apresentaram melhora no quadro de candidíase vulvovaginal, que recrudesceu após interrupção do uso do fármaco (Lass-Flörl *et al.*, 2001). Relatos posteriores reforçaram a ação fungicida da SRT em diversos patógenos como *Candida* (Lass-Flörl *et al.*, 2003) *Aspergillus* (Heller *et al.*, 2004) e *Cryptococcus* (Zhai *et al.*, 2012).

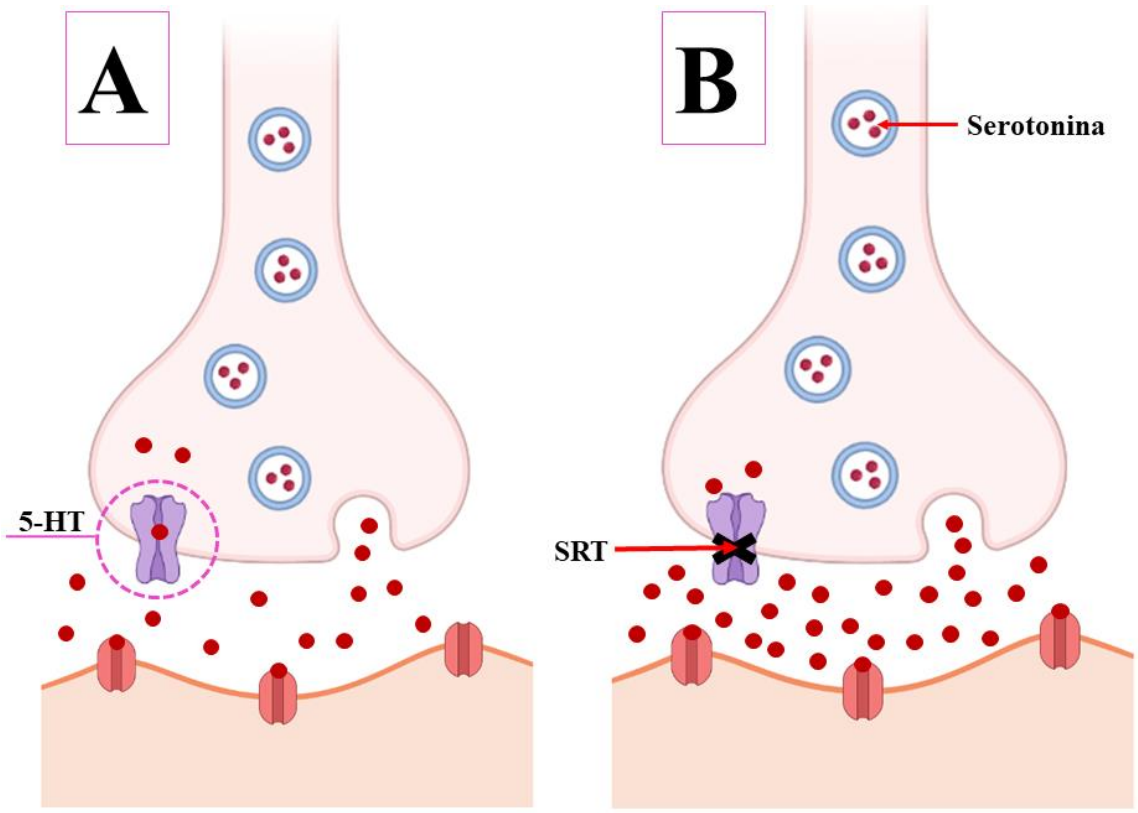

Figura 4. Mecanismo de ação do antidepressivo sertralina em neurônios humanos. O neurotransmissor serotonina é sintetizado pelos neurônios e liberado na fenda sináptica. Após período de excitação o neurotransmissor é recuperado pelo transportador 5-HT presente na membrana do neurônio que o sintetizou (**A**). O fármaco SRT complexa ao transportador 5-HT impedindo sua absorção disponibilizando mais serotonina na fenda sináptica (**B**). **Fonte**: Autor, 2023.

Nossa hipótese foi que a ampla atividade antifúngica do fármaco SRT pudesse ser também extrapolada para os dermatófitos. Sendo um grupo numeroso e disseminado de fungos com alta capacidade de transmissão por contato direto e indireto, os dermatófitos produzem um impacto significativo sobre a saúde humana sendo importantes alvos para novos tratamentos (Havlickova *et al.*, 2008; White *et al.*, 2014).

Os mecanismos subjacentes responsáveis pela atividade antifúngica do fármaco SRT permanecem desconhecidos. Porém, os resultados positivos obtidos com a inibição do desenvolvimento de fungos patogênicos sustentam o potencial deste antidepressivo no tratamento de infecções fúngicas. Os estudos voltados para a compreensão dos

mecanismos inibitórios da SRT mostram que sua atividade está relacionada a múltiplos alvos, o que explica sua atividade antimicrobiana extensa. Sua atividade antifúngica em *Saccharomyces cerevisiae* foi relacionada à alteração da composição da membrana mitocondrial e no transporte mediado por vesículas (Rainey *et al.*, 2010). Além disso, sua atividade fungicida contra *Cryptococcus* foi atribuída à inibição da síntese proteica via interação com o fator de iniciação da tradução Tif*3* e alteração do metabolismo lipídico (Zhai *et al.*, 2012; Breuer *et al.*, 2022).

Os efeitos inibitórios da SRT também se estendem aos protozoários como *Leishmania donovani* (Palit and Ali, 2008), *Leishmania infantum* (Lima *et al.*, 2018), e *Trypanosoma cruzi* (Ferreira *et al.*, 2018). O modo de ação da SRT em *T. cruzi* foi atribuído a alteração da integridade mitocondrial e a diminuição dos níveis citoplasmáticos de ATP, causando disfunção mitocondrial e dano irreversível que pode levar à morte celular por apoptose. *T. rubrum* modula a expressão gênica para sua sobrevivência na presença de agentes antifúngicos (Ferreira *et al.*, 2018; Mendes *et al.*, 2018), logo, a avaliação em nível transcricional de como as vias metabólicas respondem à STR vai auxiliar no entendimento de como este fármaco atua e como o fungo se defende, favorecendo seu possível uso como uma nova estratégia terapêutica.

A estratégia mais informativa para estudar expressão gênica é o Sequenciamento de RNA (RNA-seq). RNA-seq é vantajoso devido sua abrangência que permite não somente a análise do perfil transcricional e quantificação da expressão gênica, mas também a identificação de novos transcritos e isoformas (Wang *et al.*, 2009). Esta técnica foi utilizada nos estudos com *T. rubrum* para este fim por nosso grupo, identificando alvos de fármacos após exposição à acriflavina e ao ácido undecanóico (Persinoti *et al.*, 2014; Mendes *et al.*, 2018). Nestes trabalhos revelou-se que genes que codificam para componentes de parede celular, enzimas de biossíntese de ergosterol, transportadores de

membrana, proteínas ribossomais, processos de oxidação-redução, e genes envolvidos na patogenicidade foram modulados. Além disso, eventos de SA que ocorreram quando o fungo foi exposto a estes fármacos foram validados.

1.5 *Splicing* alternativo em *Trichophyton rubrum*

O processamento do mRNA em eucariotos consiste na excisão de sequências não codificantes (íntrons) e junção das sequências codificantes (exons) para produzir mRNAs maduros. O mecanismo de SA modifica a sequência nucleotídica do pré-mRNA, por consequência altera a composição do mRNA maduro. O processamento do pré-mRNA pode ser realizado pelas mais variadas formas, como a exclusão de éxons, sítios doadores 5' alternativos, sítios receptores 3' alternativos, éxons mutuamente exclusivos e retenção de íntrons. Dentre eles, a retenção de íntrons (RI) é o mecanismo mais comum em fungos (Muzafar *et al.*, 2021) (**Figura 5**).

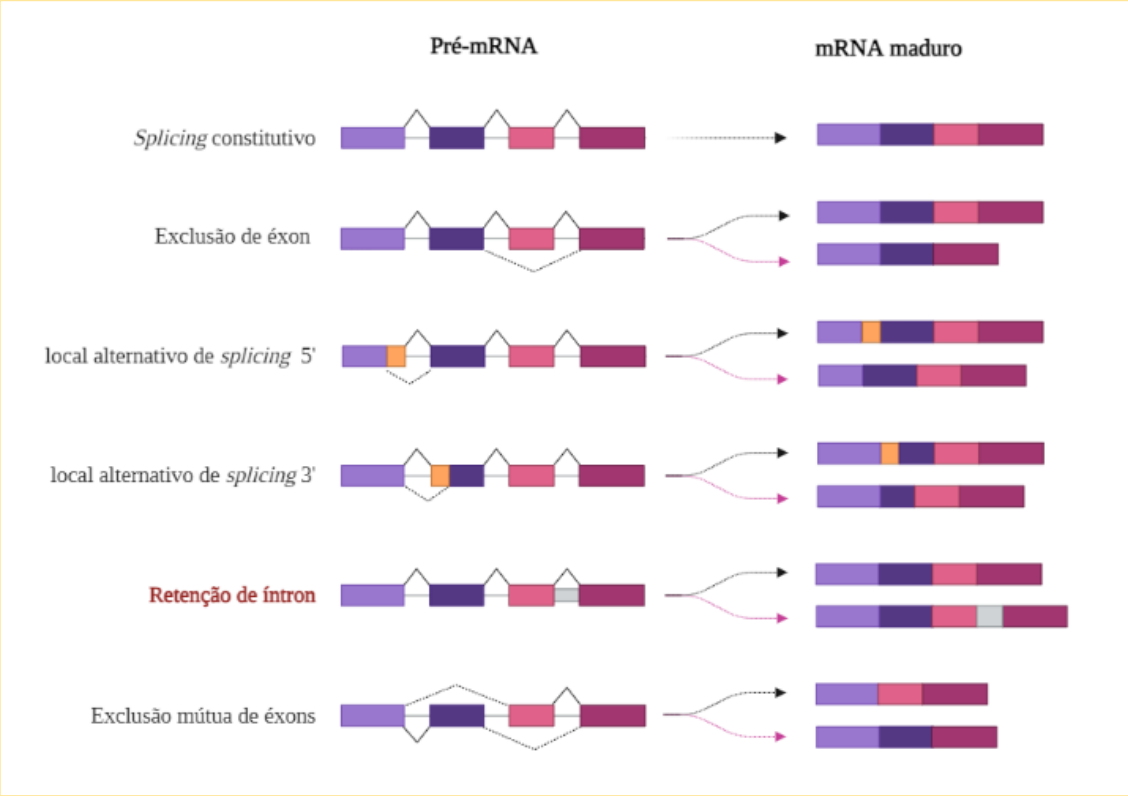

Figura 5. Tipos de *Splicing* alternativo. **Adaptado** (Muzafar *et al.*, 2021).

Por consequência, SA pode alterar o repertório proteico através de proteínas diferenciadas de suas formas canônicas. O SA pode atuar também como um mecanismo celular regulatório por meio de proteínas modificadas ou RNAs não codificantes, alterando as vias de transdução de sinal, úteis para homeostase celular. Além disto, pode ocorrer a localização subcelular diferenciada de proteínas oriundas do mesmo pré-mRNA com funções modificadas devido perda ou ganho de domínios (Kretova *et al.*, 2023).

O SA é também substrato para o processo evolutivo através da inovação do repertório molecular. Se uma nova isoforma alternativa é expressa, mesmo que em níveis baixos, a pressão de seleção negativa contra ela é relaxada porque a isoforma ancestral continua a ser expressa em níveis normais. Em confronto com um novo ambiente, a isoforma menos expressa pode ter valor adaptativo, podendo ser selecionada e aumentar sua frequência na população (Singh and Ahi, 2022).

O SA é um dos processos mais importantes na regulação pós-transcricional. Em humanos, variantes anormais de SA correspondem a mais da metade das doenças genéticas (Kretova *et al.*, 2023). Mutações pontuais que suprimem os sítios de *splicing*, criam um sítio críptico para *splicing* ou *splicings* aberrantes afetam vias metabólicas relacionadas a absorção ou metabolismo de quimioterápicos em células cancerígenas. Ativação de receptores nucleares, processo de apoptose, variantes de *splicing* em células cancerígenas e ausentes em células normais, dentre outros, constituem mecanismos atuantes para a falha do tratamento contra o câncer (Bradley and Anczuków, 2023).

Em fungos, o SA pode contribuir para diferenças adaptativas ao hospedeiro através do ganho, perda ou troca de alguns domínios funcionais de proteínas que podem alterar a função proteica, e ser determinante para sobrevivência a estressores ambientais, patogenicidade, modulação da imunidade do hospedeiro, resistência aos antifúngicos,

dentre outros mecanismos (Mendes *et al.*, 2016; Muzafar *et al.*, 2020; Martinez-Rossi *et al.*, 2021; Martins-Santana *et al.*, 2022).

Eventos de SA no transcriptoma do dermatófito *T. rubrum* após desafio com fármacos foram previamente documentados (Persinoti *et al.*, 2014; Gomes *et al.*, 2018; Mendes *et al.*, 2018; Neves-Da-Rocha *et al.*, 2019; Lopes *et al.*, 2022). Os resultados obtidos sugerem que as isoformas alternativas são atuantes nos mecanismos de resistência e adaptação aos fármacos. Ademais, genes que codificam proteases são alvos de SA na presença de queratina. Foi relatado que o fator de transcrição StuA e os mecanismos reguladores de SA podem interagir para promover um balanço para a transcrição destas proteases (Martins-Santana *et al.*, 2022). Apesar dos mecanismos de SA serem documentados no dermatófito *T. rubrum*, o entendimento desse mecanismo ainda precisa de aprofundamento.

Justificativa

2. Justificativa

As infecções causadas por *T. rubrum* são difíceis de tratar e contribuem significativamente para um decréscimo na qualidade de vida do paciente. O número de antifúngicos atualmente disponíveis para o tratamento das dermatofitoses é relativamente limitado. Semelhanças significativas compartilhadas entre células de mamíferos e fungos restringem o uso de possíveis alvos celulares, e associada à ocorrência de resistência a múltiplas drogas, vem direcionando pesquisas para a avaliação do uso alternativo de compostos terapêuticos comercialmente existentes (Zhai *et al.*, 2012; Martinez-Rossi *et al.*, 2018). Sabe-se que um número significativo de drogas usadas no tratamento de condições não infecciosas, como inflamação, depressão e doenças cardiovasculares, exibe atividade antimicrobiana. Entre eles, a SRT revelou potencial atividade antifúngica contra diferentes organismos patogênicos. Sendo um fármaco já existente, bem tolerado, e com evidentes atividades alternativas, incluindo atividade antifúngica, o estudo de sua atuação contra dermatófitos permitirá melhor compreensão dos mecanismos de ação e de adaptação fúngica ao fármaco. Sua possível utilização contra dermatófitos permitirá uma nova opção terapêutica, além de reduzir gastos e tempo no desenvolvimento de novos fármacos. Informações sobre o modo de ação da SRT em dermatófitos pode contribuir para a implementação de uma nova abordagem terapêutica, isoladamente ou em combinação com outros fármacos já existentes.

Hipótese

3. Hipótese

O antidepressivo SRT constitui uma estratégia terapêutica contra o dermatófito *T. rubrum* no tratamento de dermatofitoses.

Objetivo e estratégias

4. Objetivo e estratégias

4.1 Objetivo

Analisar o transcriptoma do dermatófito *T. rubrum* em função da exposição à SRT utilizando sequenciamento de RNA (RNA-seq) para avaliar os mecanismos de ação deste fármaco bem como os mecanismos de adaptação fúngica a este desafio.

4.2 Estratégias

- Estabelecer o perfil de susceptibilidade antifúngica de *T. rubrum* após exposição à SRT.
- Traçar o perfil transcricional do dermatófito *T. rubrum* após tratamento com SRT utilizando a tecnologia do RNA-seq.
- Identificar alvos/vias metabólicas diretamente envolvidas no modo de ação da SRT e na adaptação fúngica.
- Analisar e validar a ocorrência de eventos de SA após exposição à SRT nos resultados obtidos no RNA-seq.
- Realizar testes bioquímicos em função da expressão diferencial de genes relacionados a categorias que se julgar importante para o entendimento do modo de ação da SRT.

Material e Métodos

5. Material e Métodos

5.1 Linhagem e condições de crescimento

O isolado de referência de *Trichophyton rubrum* CBS 118892 obtido das *Centraalbureau Voor Schimmelcultures* na Holanda, foi cultivado em meio de cultura ágar com extrato de malte (MEA) durante 20 dias a 28 ° C em placas de Petri. O meio de cultivo foi preparado em frasco reagente de vidro Boro 3.3 com capacidade para 1000ml. Foi pesada a quantidade de 20g de extrato de malte, 20g de glicose, 1g de peptona, 2% de ágar bacteriológico (v/v), pH ajustado para 5,7 e o volume da solução foi completado para 1L com água destilada. Seguiu-se com esterilização pelo método de autoclavagem a 120° C com pressão de 1atm por 20 minutos.

Após o período de cultivo em MEA, os micélios foram coletados com auxílio de espátulas de aço, transferidos para tubo para centrífuga tipo Falcon de 50ml contendo 10 mL de solução salina 0,9%. Depois, as amostras foram agitadas vigorosamente por 5 minutos em vórtex. Após período de agitação, a solução foi transferida para um funil com lã de vidro acoplado a um frasco Erlenmeyer boca estreita de vidro boro 3.3. O filtrado foi transferido para tubo de centrífuga tipo Falcon de 15ml, centrifugado a 4000 rpm por 10 minutos a 28° C. O sobrenadante foi descartado e ao sedimento celular foram acrescentados 2 mL de solução salina 0,9%. Foi retirada uma alíquota de 50 µL para a realização das diluições de 10^{-1} para a contagem dos conídios em câmera de Neubauer em microscópio óptico. A concentração do inóculo foi padronizada em aproximadamente $1x10^{6}$ conídios/mL para todos os experimentos.

5.2 Perfil de susceptibilidade antifúngica

5.2.1 Determinação da concentração inibitória mínima (CIM)

Para a determinação da CIM da SRT, foi realizado o ensaio de microdiluição de acordo com as diretrizes do documento M38-A (CLSI, 2008) com adaptações, em meio

Sabouraud líquido (SDB). O meio foi preparado em frasco reagente de vidro Boro 3.3 com capacidade para 1000ml. Foi pesada a quantidade de 20g de glicose, 10g de peptona, pH ajustado para 5,7 e o volume da solução foi completado para 1L com água destilada. Seguiu-se com esterilização pelo método de autoclavagem a 120° C com pressão de 1atm por 20 minutos. O experimento foi realizado diluindo-se a SRT serialmente com fator de diluição 2 em SDB, as concentrações testadas variaram de 100 µg/mL a 0,195µg/mL. Posteriormente, essas concentrações foram transferidas para placas de 96 poços, e foram acrescentados 100 µL da suspensão de conídios previamente padronizada (**subitem 5.1**). O controle de crescimento fúngico foi estabelecido acrescentando os conídios ao meio SDB, sem a presença da SRT. A CIM foi definida como a menor concentração onde não houve crescimento visível do fungo.

5.2.2 Condições de Cultivo para o sequenciamento

O isolado *Trichophyton rubrum* CBS 118892 foi cultivado em MEA e o inóculo foi padronizado como descrito no subitem **5.1**. Foi transferido 1 mL da suspensão de conídios para 100 mL de meio SDB reservado em frascos Erlenmeyer boca estreita de vidro boro 3.3. Os frascos foram mantidos a 28°C sob agitação de 120 rpm por 96 horas. Após esse período, os micélios foram transferidos para novos frascos contendo 100 mL de SDB na presença da SRT na concentração correspondente a 70% da CIM. Os micélios foram mantidos a 28°C sob agitação de 120 rpm durante 3 ou 12 h. O controle sem SRT foi realizado nas mesmas condições de temperatura e agitação. Decorrido o período de incubação, os micélios foram coletados por filtração a vácuo, congelados em nitrogênio líquido e armazenados -80 ° C até a realização da extração do RNA.

5.3 Extração de RNA e sequenciamento

O RNA total foi extraído com o kit de extração Illustra RNAspin Mini (GE Healthcare, EUA) seguindo as recomendações do fabricante. Após a extração, com o

objetivo de evitar contaminação por DNA genômico, as amostras foram tratadas com DNAse I livre de RNAse (Invitrogen, EUA), de acordo com as diretrizes do fabricante. A pureza e concentração do RNA foram determinadas usando um espectrofotômetro NanoDrop ND-1000, e a integridade das amostras foi determinada usando-se Agilent 2100 Bioanalyzer (Agilent Technologies, EUA). RNAs de três repetições biológicas, em cultivos independentes para cada condição, foram utilizadas no sequenciamento. As bibliotecas foram sequenciadas na plataforma Illumina HiSeq 2000 (Illumina, USA), usando a metodologia de enriquecimento por PCR para gerar bibliotecas pareadas com fragmentos de 150 bp.

5.4 Análise dos dados

Os dados obtidos do sequenciamento foram analisados inicialmente quanto à sua qualidade empregando o software *FastQC* e cortados usando Trimmomatic (Bolger *et al.*, 2014) para remover os adaptadores e sequencias específicas necessárias ao sequenciamento. As sequências de boa qualidade de cada amostra foram alinhadas ao genoma de referência de *T. rubrum* (ftp://ftp.broadinstitute.org/pub/annotation/fungi) usando o alinhador STAR (Dobin *et al.*, 2013). Foram geradas contagens de leitura em nível de gene por STAR usando a opção quantModeGeneCounts. A cobertura média dos transcritos e alinhamentos foram inspecionados pelo software *Interative genomics viewir* (IGV) (Robinson *et al.*, 2011; Thorvaldsdottir *et al.*, 2012). A expressão diferencial foi analisada usando o pacote DESeq2 Bioconductor. A correção de Benjamini-Hochberg foi aplicada ($p < 0,05$) (Benjamini and Hochberg, 1995), e o limite de corte de ± 1,5 Log2 foi definido para revelar diferenças de expressão estatisticamente significativas (genes que ultrapassam esses limites são referidos como genes diferencialmente expressos (DEs))(Persinoti *et al.*, 2014). Seguiu-se com a categorização funcional usando os termos Gene Ontology (GO) atribuídos pelo algoritmo Blast2GO. As categorias altamente

representadas foram determinadas por análise de enriquecimento usando o algoritmo BayGO (Vêncio *et al.*, 2006).

Para identificar as vias metabólicas, nos quais os genes modulados em resposta a SRT poderiam estar envolvidos, foi realizada análise com *Kegg Orthology* utilizando-se o KAAS (*Kegg Automatic Annotation Server*), para esta análise o organismo modelo de referência foi *Trichophyton verrucosum* (Kanehisa *et al.*, 2016).

5.5 Validação por RT-qPCR

A expressão diferencial dos genes foi validada por RT-qPCR com o sistema StepOnePlus Real time PCR (Applied Biosystems, EUA). Para isto, foi realizado um cultivo nas mesmas condições descritas no subitem **5.2.2**. O RNA total foi extraído com o reagente Trizol (Sigma Aldrich). Para remover qualquer contaminação de DNA genômico, após a extração, 1 μL do RNA total foi utilizado para o tratamento com DNAse 1 Amplification Grade ® (Sigma Aldrich), seguindo as recomendações do fabricante. Para certificação de que todo DNA genômico foi digerido pela enzima, foi realizada uma Reação em cadeia da polimerase (PCR) utilizando oligonucleotídeos flanqueando o gene da β-tubulina (Fwd: CCGTATGATGGCCACTTTCT; Rev: AAGATGGCAGAGCAGGTAAGGT). Os produtos gerados na reação foram observados em gel de agarose 2%. Quando constatado que nenhuma amplificação ocorreu nas amostras, seguiu-se para a síntese de cDNA. Para isto, foi utilizando o kit Transcrição Reversa ® de cDNA de alta capacidade (Applied Biosystems) seguindo as instruções do fabricante. Após a síntese de cDNA, para verificar que a síntese foi satisfatória, bem como a integridade das amostras, uma PCR foi realizada como descrito anteriormente. Após a verificação, seguiu-se para a reação de RT- qPCR (Rocha *et al.*, 2022).

Para a validação dos dados obtidos no RNA-seq 13 genes foram selecionados aleatoriamente com o objetivo de retirar qualquer viés no processo de confirmação. Os

iniciadores foram construídos utilizando o software primer3 (https://primer3plus.com/cgi-bin/dev/primer3plus.cgi) (**Tabela 1**). A reação foi padronizada pela realização do ensaio de curva padrão. A expressão diferencial entre os tratamentos foi avaliada com base na quantificação relativa de genes responsivos. Os ensaios foram normalizados utilizando-se os genes *DNA-dependent RNA polimerase* e *glyceraldehyde 3-phosphate dehydrogenase* como controles endógenos (Jacob *et al.*, 2012). Dados da expressão gênica foram analisados estatisticamente por *test t* com *post test* de *Tukey* utilizando o software *GraphPad Prism* v. 5.1 (GraphPad Software, USA). O nível de significância de 95% foi considerado para que as medidas fossem estatisticamente diferentes ($p < 0,05$). A correlação dos dados obtidos no RT- qPCR e no RNA-seq foi analisada aplicando-se a correlação de *Pearson*.

Tabela 1. Lista dos oligonucleotídeos utilizados nos ensaios de RT-qPCR.

ID	Nome do produto do gene	Primers (5' - 3')	Eficiência (%)
TERG_05742	DNA-dependent RNA polymerase II RPB140	FW: TGCAGGAGCTGGTGGAAGA REV:GCTGGGAGGTACTGTTTGATCAA	94,99
TERG_04402	glyceraldehyde 3-phosphate dehydrogenase	FW: GCGTGACCCAGCCAACA REV:CGGTGGACTCGACGATGTAGT	99,90
TERG_11735	microtubule associated protein (*T. tonsurans*)	FW: GGGCCAAAGAAACAACAACA REV: CGCTCGGCATATTACCCTAA	98,2
TERG_07544	lipase (*T. tonsurans*)	FW: CTTGACGGATGGAAAAAGGA REV: CACCGTTATTTGGATCAGCA	101,6
TERG_06673	pachytene checkpoint component Pch2 (*T. tonsurans*)	FW: ATGGGGAGATGCAGTTATGG REV: ACAACGCTCACTTGTGCAAC	102,8
TERG_01762	sulfite reductase (NADPH) hemoprotein. beta-component	FW: ACGTGGATTCTGGGAAACAG REV: AGGCCGAAAACGGAATACTT	95,3
TERG_05522	lysophospholipase (*T. equinum*)	FW: CAACGCGGACAATGTCTCTA REV:CTCCATTCATCAAAGCACGA	104,0
TERG_11924	ankyrin repeat protein (*T. tonsurans*)	FW: GACCGGAAAGGTGGATGTTA REV: CTCGTGTCGATAGCTTGCAG	100,0
TERG_06548	hypothetical protein	FW: ATCCGGTTCACAGACCAAAC REV: GCTGGATTGAAAGGAGGACA	102,0
TERG_03936	CAMK protein kinase	FW: AGACAGCTGGCTTGCAAAAT REV: TGAAACAGTCGTTTGGGACA	98,9
TERG_06540	glutathione transferase (*T. tonsurans*)	FW: AGGGATTGAACAAAGCCAGA REV: AGGACCAATCTCATCCATCG	102,0
TERG_07570	G-protein signaling regulator. putative (*T. verrucosum*)	FW: TGGCATCAAGCACAAACTGT REV: CTTTTTGGGCTTTGGACTTG	103,0

TERG_07539	multidrug resistance protein (*T. tonsurans*)	FW: CTCCTACCACCCCATTGCTA REV: CTCAAGGCCGATAAGGAACA	100,0
TERG_03815	subtilisin-like protease 3	FW: TGGTGTTGACACCGGTATTG REV: GTTGCCATCAGTGTTGTCGT	102,0

5.6 Dosagem do conteúdo de Ergosterol total

A cepa de *T. rubrum* CBS118892 foi cultivada em ágar *Sabouraud* dextrose (SDA) por 17 dias a 28 ◦C. Os micélios obtidos foram transferidos para 50 mL de SDB e cultivados por 24 h a 28 ◦C com agitação (200 rpm). Após esse período, o micélio foi recuperado, inoculado em 20 mL de SDB contendo uma concentração subinibitória da SRT (6,25 µg/mL), cetoconazol (KTC, 4 µg/mL; Sigma-Aldrich), ou anfotericina B (AMB, 1,25 µg/mL; Sigma-Aldrich), e incubados por 48 h a 28 ◦C, 200 rpm. Micélios também foram inoculados em SDB sem fármacos (controle). Os micélios resultantes foram filtrados, retirado o excesso de água e pesados. O conteúdo de ergosterol total foi determinado. Resumidamente, 3 mL de solução alcoólica de hidróxido de potássio a 25% foram adicionados aos micélios secos e misturados em vórtex por 5 min. As amostras foram incubadas a 85 ◦C por 1 h. Os tubos foram resfriados à temperatura ambiente e 1 mL de água destilada e 3 mL de *n*-heptano foram adicionados, seguido de agitação vigorosa em vórtice para 5 min. A camada de heptano foi transferida para um tubo de poliestireno limpo, e uma alíquota de 20 µL foi diluída cinco vezes em etanol 100% e lida em um espectrofotômetro entre 230 e 300 nm (Arthington-Skaggs *et al.*, 1999). A redução no teor de ergosterol foi calculada como a diferença nos tratamentos comparados às amostras de controle. Os resultados foram expressos como uma porcentagem do conteúdo de ergosterol nos micélios desafiados com os fármacos em comparação com o controle de crescimento. O teste ANOVA *one-way* foi usado para determinar a quantidade de ergosterol no controle comparado aos tratamentos, seguido do teste *post-hoc* de *Tukey*. O nível de significância de 95% foi considerado para que as medidas fossem

estatisticamente diferentes ($p < 0,05$). O *software* Prism v. 5.1 foi utilizado para gerar os gráficos e realizar as análises estatísticas.

5.7 Análise dos eventos de SA

Os eventos de *splicing* alternativo (SA) foram mapeados como descrito anteriormente (Martins-Santana *et al.*, 2022). Os eventos foram analisados em R com o pacote *ASpli* (Mancini *et al.*, 2021). Resumidamente, as leituras provenientes da análise do sequenciamento de RNA foram mapeadas com o genoma de referência de *T. rubrum* usando o alinhador de sequências STAR (Dobin *et al.*, 2013). As leituras alinhadas ao genoma de referência foram processadas usando o pacote ASpli para identificar eventos de SA. A análise de expressão diferencial foi realizada usando o pacote DESeq2 Bioconductor (Love *et al.*, 2014). O valor de *p* ajustado por Benjamini-Hochberg foi definido como 0,05, e um corte de ±1,5 Log2 foi aplicado para identificar os níveis de expressão gênica significativamente modulados entre a abundância de transcritos (Martins *et al.*, 2020; Bitencourt *et al.*, 2021; Martins-Santana *et al.*, 2022). Os transcritos que apresentaram valor ajustado de *p* menor que 0,05 foram identificados como diferencialmente expressos (TDEs) (Sieber *et al.*, 2018).

Para a validação dos eventos de SA foi selecionado o gene TERG_07061, que codifica uma CMGC/SRPK *protein kinase* e que apresentou retenção do íntron 3 nos ensaios de RNA-seq. Inicialmente, os iniciadores foram desenhados flanqueando a região intrônica para os ensaios de RT-PCR (**Tabela 2**). Foi realizada a verificação da temperatura ótima de anelamento dos oligos para certificação de bandas correspondentes aos eventos de retenção. Para isso, o intervalo de temperatura variando de 50 a 60 ^{o}C foi testado. Após o estabelecimento dos parâmetros de ciclagem, ambos os tempos de exposição à SRT foram testados, além de seus respectivos controles na ausência do antidepressivo. Os produtos de PCR e todos os ensaios foram visualizados em gel de agarose 2% com preparo

seguindo as instruções do fabricante. A expressão diferencial dos transcritos foi avaliada por RT-qPCR conforme descrito anteriormente no item **5.5**. Os iniciadores utilizados nos ensaios foram projetados dentro de regiões específicas dos transcritos gerados com e sem a retenção do íntron 3, respectivamente (**Figura 6**), e suas sequências encontram-se na T**abela 2**.

Tabela 2. Lista dos oligonucleotídeos utilizados nos ensaios de RT-PCR e RT-qPCR para validação da retenção do íntron 3 no gene que codifica uma CMGC/SRPK *protein kinase* em *Trichophyton rubrum*.

ID	Primers (5' - 3')
RT-PCR	FW: CTTCGGAGAGGCAAGAATTG REV: CATACGCCTGACCATCCTCT
Transcrito sem retenção	FW: TTACAGCCTGGGACTTGC REV: GAACCGCATCATACGCCTGA
Transcrito com retenção	FW: CCTTTCATCGCTATACTGGT REV: GAACCGCATCATACGCCTGA

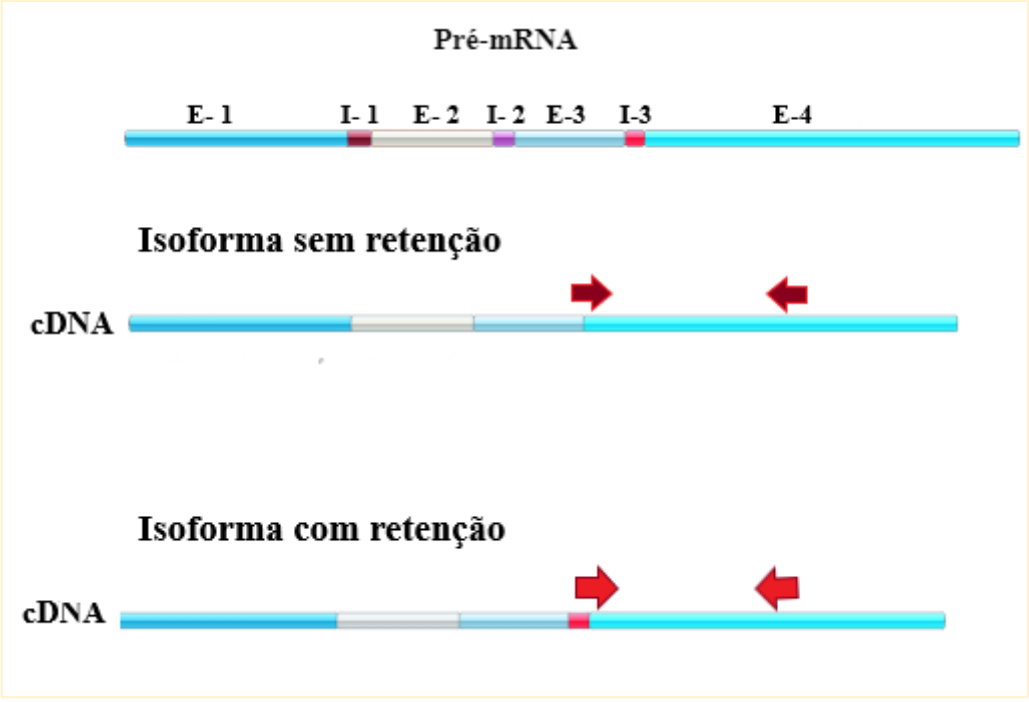

Figura 6. Regiões de anelamento dos oligonucloeotídeos utilizados nos ensaios de RT-qPCR. *Splicing* sem retenção foram avaliados através de iniciadores complementares às regiões de junção E-3/E-4, enquanto que *splicing* com retenção do íntron 3 os iniciadores eram complementares às regiões de junção I-3/ E-4. Setas vermelhas indicam regiões complementares aos iniciadores. E-1: Éxon 1; I-1: Íntron 1; E-2: Éxon 2; I-2: Íntron 2; E-3: Éxon 3: I-3: Íntron.

5.8 Caracterização *in silico* da retenção de íntron

Inicialmente a sequência do gene TERG_07061 foi identificada utilizando o banco de dados *EnsemblFungi* seguindo as coordenadas de localização para o íntron retido (*Start*:209028 –*End*: 209083). Primeiro, os quadros de leitura aberta foram preditos com a utilização da ferramenta *Expasy - Translate tool*. Depois, uma análise funcional foi realizada utilizando a base de dados *InterPro* com a busca por domínios de assinatura para as sequências.

Resultados

6. Resultados

6.1 Perfil transcricional de *Trichophyton rubrum* desafiado pela SRT

O RNA-seq foi utilizado para analisar de forma abrangente os genes do dermatófito *T. rubrum* modulados em resposta ao antidepressivo SRT. O fungo foi desafiado em 3h e 12h de exposição com a concentração do fármaco SRT correspondente a 70% da concentração inibitória mínima, ou seja, a menor concentração da SRT que inibe visivelmente o crescimento de *T.rubrum*. Aproximadamente 535,5 milhões de leituras de alta qualidade de sequências *paired-end* de 150 pb foram obtidas (**Tabela 3**). As correlações entre as réplicas em cada ponto de tempo foram fortemente positivas, variaram de 0,96 a 0,99 (**Tabela 4**).

Tabela 3. Características gerais de leituras de RNA-seq mapeadas para o genoma de referência de *Trichophyton rubrum*.

Amostra	Dados brutos	Leituras de alta qualidade	Leituras mapeadas	Total de leituras mapeadas (%)
TRSAB 3 horas I	49,001,399	46,661,059	45,099,456	96,65
TRSAB 3 horas II	53,711,149	50,929,711	48,747,310	95,71
TRSAB 3 horas III	54,065,522	51,244,460	48,776,743	95,18
TRSAB 12 horas I	49,723,884	47,231,185	45,011,034	95,30
TRSAB 12 horas II	48,820,202	46,313,505	38,542,411	83,22
TRSAB 12 horas III	49,378,560	46,733,086	38,063,153	81,45
TRSAB Str 3 horas I	44,238,209	41,936,258	40,012,345	95,41
TRSAB Str 3 horas II	46,989,637	44,653,620	41,137,174	92,13
TRSAB Str 3 horas III	46,798,013	44,244,584	42,078,809	95,10
TRSAB Str 12 horas I	42,267,590	40,220,692	38,407,036	95,49
TRSAB Str 12 horas II	43,358,547	41,011,155	38,955,931	94,99
TRSAB Str 12 horas III	36,247,455	34,371,291	32,688,609	95,10

Tabela 4. Similaridade entre as réplicas biológicas submetidas ao sequenciamento.

Amostras	I *vs.* II	I *vs.* III	II *vs.* III
TRSAB 3 horas	0,97	0,98	0,97
TRSAB 12 horas	0,98	0,99	0,99
TRSAB Str 3 horas	0,98	0,96	0,99
TRSAB Str 12 horas	0,99	0,99	0,99

Em resposta à exposição ao fármaco SRT, foram quantificados 169 e 1197 genes que foram modulados em 3 e 12 h, respectivamente, quando comparados aos níveis de expressão do controle. Trezentos e setenta e dois genes foram modulados em ambos os momentos, totalizando 1738 genes que responderam ao fármaco SRT (**Figura 7A**). Dos genes modulados após 3h de tratamento com SRT, a maior parte é regulado positivamente. Este perfil se inverte em 12 h de exposição à SRT. No entanto, o número de genes que são modulados (positiva ou negativamente) neste tempo é cerca de 3 vezes maior que em 3h (**Figura 7B**).

A

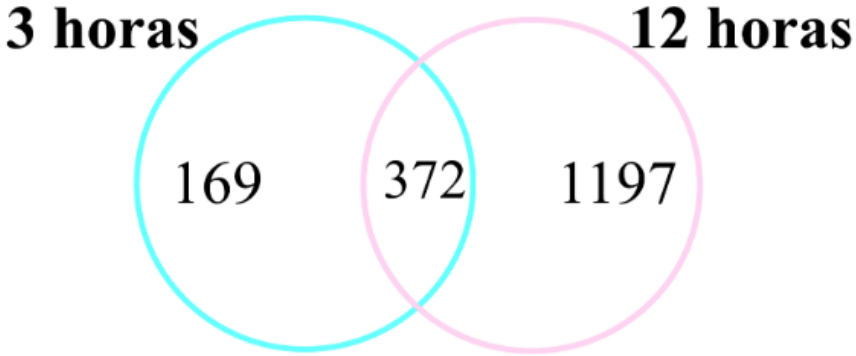

B

Exposição	Total de genes	Induzidos	Reprimidos
3 horas	541	452	89
12 horas	1569	768	801

Figura 7. Expressão gênica diferencial induzida pelo antidepressivo sertralina. (**A**) Diagrama de Venn representando a expressão diferencial dependente do tempo de 1.738 genes após exposição a doses subletais da SRT por 3 h e 12 h, em comparação com a amostra controle (ausência da SRT). (**B**) Total de genes induzidos e reprimidos em cada período de exposição ao fármaco SRT.

Os genes que apresentaram os níveis mais significativos de modulação positiva ou negativa em resposta à SRT, no RNA-seq, estão na **Tabela 5**.

Tabela 5. Genes de *Trichophyton rubrum* com maior modulação em sua expressão após a exposição ao antidepressivo sertralina.

		Log2 (Fold change)	
ID	**Produto do gene**	**3h**	**12h**
TERG_06548	hypothetical protein	10,86	11,80
TERG_00785	endoplasmic reticulum vesicle protein 25	8,60	
TERG_01782	hypothetical protein	8,34	9,02
TERG_00010	amidase family protein (*T. verrucosum*)		8,72
TERG_03829	FAD binding domain-containing protein (*T. equinum*)		6,92
TERG_04952	Multidrug resistance protein (*T. equinum*)	6,87	7,69
TERG_08954	hypothetical protein	6,61	
TERG_06106	sulfate permease 2 (*T. tonsurans*)		6,45
TERG_08751	ABC multidrug transporter, putative (*A. benhamiae*)	5,82	6,33
TERG_01543	s-adenosylmethionine (SAM)-dependent methyl transferase (*M. gypseum*)	5,42	7,48
TERG_08041	aminotransferase, putative (*A. benhamiae*)	5,42	
TERG_04937	alpha/beta hydrolase (*T. equinum*)	5,41	6,40
TERG_07830	hypothetical protein	5,41	8,22
TERG_02653	hypothetical protein	-6,21	
TERG_02652	O-methyltransferase, putative (*T. verrucosum*)	-4,91	
TERG_04066	filamentation protein (Rhf1), putative (*T. verrucosum*)	-4,67	
TERG_02959	hypothetical protein	-4,16	
TERG_05816	hypothetical protein	-3,74	
TERG_02650	NmrA family protein (*T. equinum*)	-3,56	
TERG_12339	hypothetical protein	-3,31	
TERG_01619	toxin biosynthesis protein (Tri7), putative (*T. verrucosum*)	-3,20	
TERG_00490	erythromycin esterase (*T. tonsurans*)	-3,13	-5,24
TERG_03826	hypothetical protein	-2,77	
TERG_02959	hypothetical protein		-5,90
TERG_11536	hypothetical protein		-5,69
TERG_11771	hypothetical protein		-5,51
TERG_04742	hypothetical protein		-5,29
TERG_01148	hypothetical protein		-5,26
TERG_03919	phytoene dehydrogenase (*T. equinum*)		-5,20
TERG_01599	hypothetical protein		-4,95
TERG_12035	NB-ARC and TPR domain protein (*A. benhamiae*)		-4,87
TERG_11963	hypothetical protein		-4,79

A categorização funcional dos genes modulados revelou genes relacionados aos mecanismos moleculares pelos quais *T. rubrum* detecta e responde à SRT (**Figura 8**). Análise de função gênica foi enriquecida principalmente nos termos de função molecular após 3 h de tratamento. Atividade catalítica, atividade hidrolase, e ligação a íons metálicos

foram induzidas, enquanto que genes codificantes para produtos relacionados a atividade transferase e metiltransferase foram reprimidos. Dos cerca de 70 genes com atividade oxidorredutase que foram modulados após 3 h de exposição à SRT cerca de 55 foram induzidos (**Figura 8A**). Os genes associados à componentes da membrana celular regulados positivamente aumentaram em 12 h em comparação tratamento de 3h. Os genes relacionados à tradução que foram modulados mostraram-se todos inibidos em 12h. O número de genes associados à atividade hidrolase e ao transporte transmembrana aumentou em 12h comparado a condição de 3 h, permanecendo induzido em resposta a exposição à SRT (**Figura 8B**).

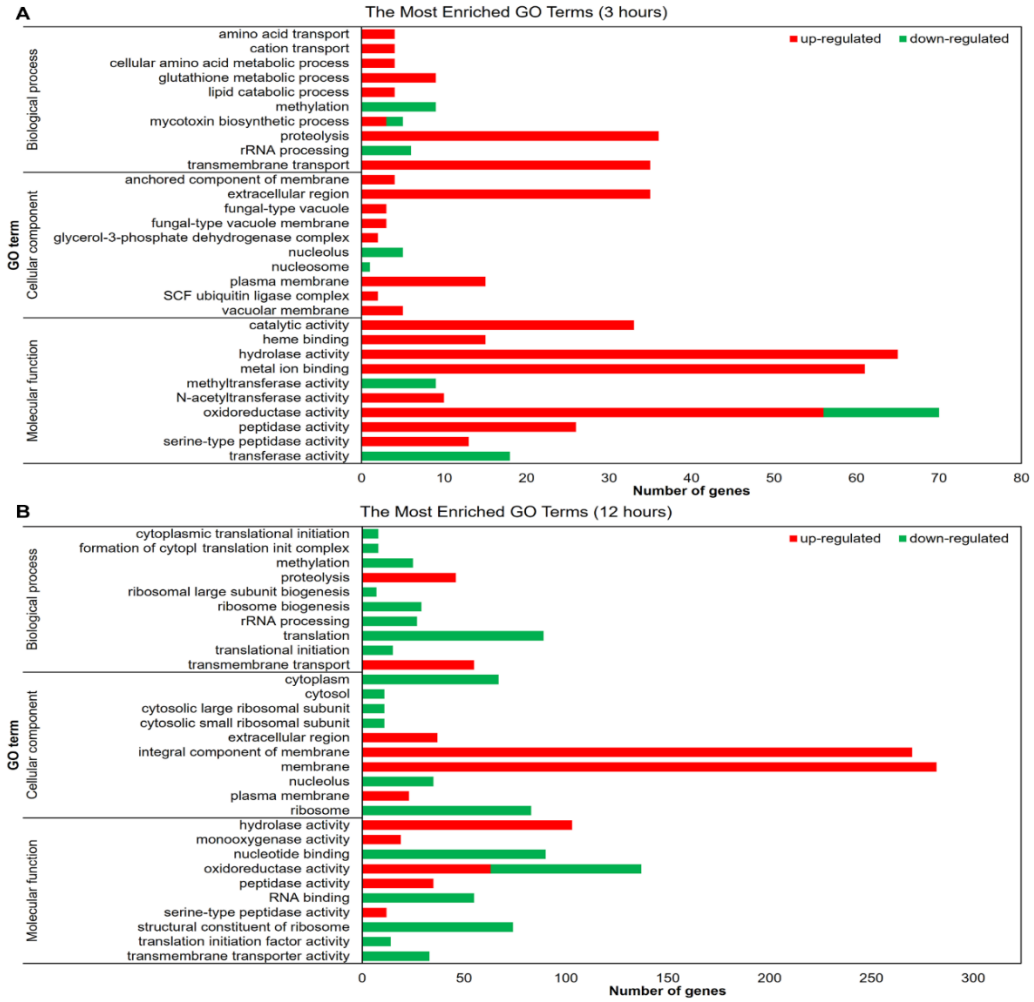

Figura 8. Categorização funcional baseada na ontologia dos genes diferencialmente expressos. As barras vermelhas e verdes indicam o número de genes induzidos e reprimidos em resposta ao fármaco SRT ($p < 0,05$). Os resultados mostram os genes após

3 h (A) e 12 h (B) de exposição ao antidepressivo em comparação com o controle sem SRT.

6.2 Confirmação da expressão diferencial por RT-qPCR

Para validar os resultados do RNA-seq, selecionamos 13 genes diferencialmente expressos relacionados a processos como atividade catalítica, atividade de transferase e transporte transmembrana para submete-los ao RT-qPCR (**Figura 9**). Os dados das réplicas biológicas revelam a confiabilidade dos resultados (correlação de Pearson, r > 0,92, p < 0,001) (**Tabela 6**).

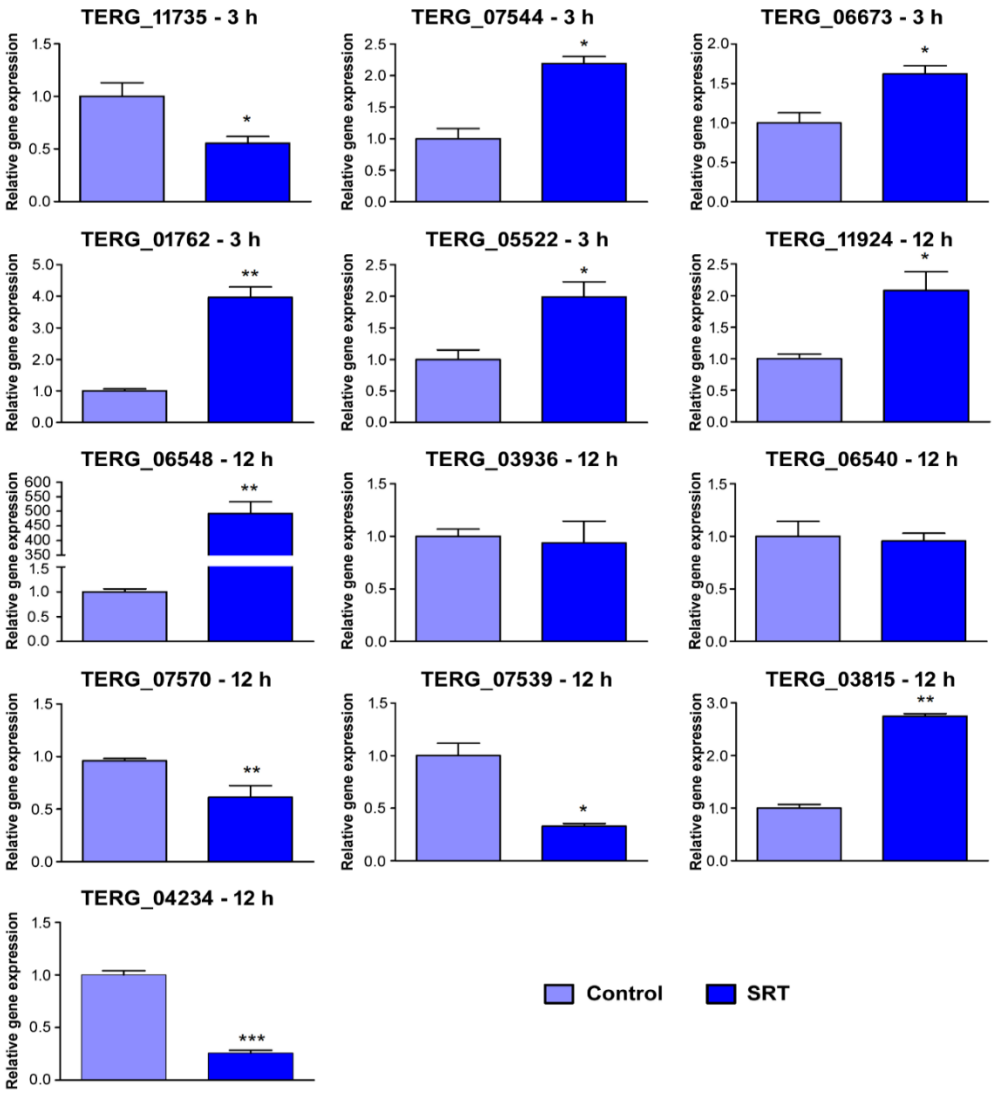

Figura 9. Validação dos dados de RNA-seq por RT-qPCR. Um total de 13 genes diferencialmente expressos em resposta à exposição ao fármaco SRT foram analisados. Gráficos plotados de acordo com *fold change* de Log2 em cada período de tempo

representa mudanças no nível de expressão de cada gene em relação ao controle sem SRT. Os asteriscos indicam a significância estatística determinada pelo teste *t* seguido pelo teste *post-hoc* de *Tukey* (* $p < 0,05$; ** $p < 0,01$; *** $p < 0,001$). A identificação dos genes se encontra na **Tabela 6**.

Tabela 6. Comparação dos níveis de expressão gênica avaliados por RNA-seq e RT-qPCR.

ID	Condição	Produto do gene	RNA-seq	qRT-PCR
TERG_11735	3h	microtubule-associated protein (*T. tonsurans*)	-2,4	-1,41
TERG_07544	3h	lipase (*T. tonsurans*)	2,02	1,13
TERG_06673	3h	pachytene checkpoint component Pch2 (*T. tonsurans*)	2,0	0,70
TERG_01762	3h	sulfitereductase (NADPH) hemoprot. beta-component	2,14	1,99
TERG_05522	3h	lysophospholipase (*T. equinum*)	1,55	0,97
TERG_11924	12h	ankyrin repeat protein (*T. tonsurans*)	3,85	1,06
TERG_06548	12h	hypothetical protein	11,8	8,63
TERG_03936	12h	CAMK protein kinase	-4,19	-0,09
TERG_06540	12h	glutathione transferase (*T. tonsurans*)	-3,44	-0,07
TERG_07570	12h	G-prot. signaling regulator putative (*T. verrucosum*)	-3,47	-0,70
TERG_04234	12h	hydrophobin. putative (*T. verrucosum*)	-3,41	-1,98
TERG_07539	12h	multidrug resistance protein (*T. tonsurans*)	-1,72	-1,61
TERG_03815	12h	subtilisin-like protease 3	1,78	1,46

6.3 SRT interfere na sinalização de *T. rubrum*

Genes que codificam para proteínas quinases e fatores de transcrição são enriquecidos no genoma de dermatófitos antropofílicos (Martinez *et al.*, 2012), sugerindo que a modulação das vias de sinalização e a regulação transcricional são importantes na especificidade ao hospedeiro. O quinoma de *T. rubrum* (membros da superfamília da proteína quinase) compreende 170 genes codificantes (Martinez *et al.*, 2012). No presente trabalho, 81 quinases foram moduladas (**Tabela 7**), codificando principalmente para proteínas quinases serina/treonina e quinases pertencentes ao grupo CMGC (quinases dependentes de ciclina (CDKs)). Entre os 15 genes de serina/treonina-proteína quinase modulados, apenas TERG_07509 foi reprimido após 12 h de tratamento. Entre os oito genes que codificam quinases do tipo CMGC moduladas após exposição à SRT, TERG_12259 (proteína CMGC/CLK quinase), TERG_05893 (proteína quinase CMGC) e TERG_07061 (proteína CMGC/SRPK quinase) foram reprimidos.

A maioria dos fatores de transcrição modulados pela SRT codifica proteínas contendo domínio dedo de zinco e são preferencialmente reprimidos, principalmente após 12 h de exposição (incluindo TERG_02532, TERG_01042 e TERG_05497 (**Tabela 8**).

Tabela 7. Genes que codificam para proteínas quinase no genoma de *Trichophyton rubrum* modulados em resposta ao fármaco Sertralina.

ID	Produto do gene	3 h	12 h
TERG_00199	serine/threonine protein kinase	**2,32**	**2,61**
TERG_00620	NAD+ kinase Utr1 (*T. equinum*)	0,74	**2,30**
TERG_00689	AUR protein kinase	-1,16	**-3,75**
TERG_00694	glutamate 5-kinase	**-1,77**	**-3,65**
TERG_00783	guanine nucleotide-binding protein subunit beta-like protein	-1,03	**-2,40**
TERG_00875	glutamate-cysteine ligase	**1,76**	0,73
TERG_00962	protein kinase subdomain-containing protein (*T. tonsurans*)	-0,94	**-1,91**
TERG_01105	serine/threonine protein kinase (*T. tonsurans*)	1,24	**1,60**
TERG_01322	NEK protein kinase (*T. tonsurans*)	-1,45	**-2.98**
TERG_01761	hypothetical protein	-0,98	**-1,54**
TERG_01822	serine/threonine protein kinase	0,62	**2,21**
TERG_01856	CMGC/SRPK protein kinase	0,74	**1,62**
TERG_01919	serine/threonine protein kinase	**1,92**	**2,96**
TERG_01925	hypothetical protein	**1,77**	**3,53**
TERG_01996	serine/threonine protein kinase	0,90	**1,60**
TERG_02018	hypothetical protein	1,27	**2,02**
TERG_02211	serine/threonine protein kinase (*T. tonsurans*)	0,78	**1,88**
TERG_02263	hypothetical protein	-0,09	**-2,16**
TERG_02655	hypothetical protein	**2,48**	0,91
TERG_02759	hexokinase XprF (*T. equinum*)	-0,65	**-1,98**
TERG_03182	serine/threonine protein kinase (*T. equinum*)	0,92	**1,65**
TERG_03229	hexokinase (*T. tonsurans*)	**1,92**	**1,65**
TERG_03415	serine/threonine protein kinase	1,02	**2,33**
TERG_03628	serine/threonine protein kinase (*T. tonsurans*)	0,99	**2,30**
TERG_03684	stress activated MAP kinase interacting protein (*T. equinum*)	1,08	**1,82**
TERG_03871	phosphotransferase (*M. canis*)	**1,60**	0,08
TERG_03892	CAMK/CAMKL protein kinase (*T. tonsurans*)	**1,78**	**1.62**
TERG_03936	CAMK protein kinase	-1,13	**-4,19**
TERG_04036	adenosine kinase (*T. tonsurans*)	-1,31	**-2,34**
TERG_04103	hypothetical protein	0,62	**1,63**
TERG_04210	CAMKK/CAMKK-META protein kinase	0,81	**1,57**
TERG_04374	STE/STE20/YSK protein kinase	-1,34	**-3,18**
TERG_04385	serine/threonine protein kinase (*T. tonsurans*)	0,87	**1,74**
TERG_04429	MORN repeat-containing protein (*T. equinum*)	0,79	**1,84**
TERG_04447	protein kinase subdomain-containing protein (*T. equinum*)	**1,54**	1,34

TERG_04448	CMGC/DYRK protein kinase (*M. gypseum*)	**1,97**	0,06
TERG_04558	nucleoside diphosphate kinase	**-1,57**	**-2,48**
TERG_04941	mitochondrial pyruvate dehydrogenase kinase (*T. tonsurans*)	0,95	**2,08**
TERG_05098	arginine metabolism regulation protein iii (*T. verrucosum*)	0,35	**1,74**
TERG_05251	phosphoglycerate kinase	-0,91	**-2,28**
TERG_05544	plk/plk-unclassified protein kinase (*T. tonsurans*)	-1,08	**-2,36**
TERG_05552	DNA mismatch repair protein MutL (*T. tonsurans*)	1,14	**1,53**
TERG_05553	integral membrane protein (*T. equinum*)	0,33	**1,90**
TERG_05615	hsp70-like protein (*T. equinum*)	0,92	**-2,55**
TERG_05813	1-phosphatidylinositol-3-phosphate 5-kinase (*T. equinum*)	0,26	**1,55**
TERG_05893	CMGC protein kinase (*T. tonsurans*)	-0,46	**-2,37**
TERG_05948	protein kinase subdomain-containing protein (*T. equinum*)	-0,15	**-1,68**
TERG_06366	CAMK protein kinase	-0,72	**-1,54**
TERG_06403	HASPIN protein kinase	-1,12	**-2,97**
TERG_06407	protein kinase subdomain-containing protein (*M. canis*)	**2,11**	**1,95**
TERG_06539	fructosamine-3-kinase (*T. equinum*)	-1,32	**-1,90**
TERG_06761	CAMK protein kinase (*T. tonsurans*)	**1,53**	1,31
TERG_06765	ULK/ULK protein kinase	0,39	**1,58**
TERG_06836	CAMK/CAMK1/CAMK1-RCK protein kinase	0,60	**1,56**
TERG_06969	CMGC/CDK/CDK5 protein kinase	1,34	**2,17**
TERG_07012	rRNA 2'-O-methyltransferase fibrillarin	-1,20	**-1,97**
TERG_07061	CMGC/SRPK protein kinase	-0,97	**-1,61**
TERG_07134	serine/threonine protein kinase	**2,05**	**2,67**
TERG_07273	glycerol kinase (*T. equinum*)	0,91	**2,29**
TERG_07509	serine/threonine protein kinase (*M. canis*)	-0,76	**-2,09**
TERG_07547	RGS domain-containing protein (*T. tonsurans*)	-1,03	**-1,73**
TERG_07616	diphosphomevalonate decarboxylase	-1,33	**-1,68**
TERG_07639	atypical/ABC1/ABC1-B protein kinase (*T. tonsurans*)	-1,28	**-2,65**
TERG_07782	GA-binding protein beta chain (*M. gypseum*)	**2,19**	0,56
TERG_07921	adenylylsulfate kinase	1,24	**2,18**
TERG_08066	STE/STE7 protein kinase	0,59	**1,57**
TERG_08278	serine/threonine protein kinase (*T. tonsurans*)	0,71	**2,19**
TERG_08368	TTK protein kinase	-0,88	**-1,69**
TERG_08538	Diacylglycerol kinase domain-containing protein (*T. equinum*)	0,77	**2,06**
TERG_08539	Diacylglycerol kinase domain-containing protein (*T. equinum*)	**2.51**	**4.42**
TERG_08568	CMGC/SRPK protein kinase	**1,75**	**2,47**
TERG_08794	pyruvate dehydrogenase kinase (*T. equinum*)	0,16	**-1,94**
TERG_11505	phosphoenolpyruvate carboxykinase [ATP]	-0,06	**-3,77**
TERG_11506	phosphoenolpyruvate carboxykinase [ATP]	0,08	**-3,27**
TERG_11690	protein kinase subdomain-containing protein (*T. tonsurans*)	-1,35	**-1,86**
TERG_11800	serine/threonine protein kinase (*T. equinum*)	**1,74**	1,19
TERG_11801	serine/threonine protein kinase (*T. equinum*)	**2,06**	**1,70**
TERG_12033	atypical/RIO/RIO1 protein kinase (*T. tonsurans*)	-0,77	**-2,49**
TERG_12071	AGC/DMPK protein kinase (*T. equinum*)	**-1,70**	0,94
TERG_12259	CMGC/CLK protein kinase (*T. equinum*)	-0,62	**-2,00**
TERG_12322	CMGC/SRPK protein kinase (*M. gypseum*)	**2,05**	**1,96**

(*) Valores em log2 FC. Em vermelho valores iguais ou acima de 1,50. Em verde valores iguais ou abaixo de -1,50.

Tabela 8. Fatores de transcrição de *Trichophyton rubrum* modulados em resposta à exposição ao fármaco sertralina.

ID	Produto do gene	3 h	12 h
TERG_00218	C2H2 transcription factor (Swi5), putative (*A. benhamiae*)	-0,97	**-3,97**
TERG_01042	C6 transcription factor, putative (*T. verrucosum*)	**2,14**	**2,91**
TERG_01310	nascent polypeptide-associated complex subunit beta	-0,80	**-1,69**
TERG_02061	C2H2 transcription factor (Ace1), putative (*T. verrucosum*)	1,20	**1,89**
TERG_02532	C6 transcription factor, putative (*T. verrucosum*)	**2,72**	**4,90**
TERG_02843	C6 transcription factor (*T. equinum*)	-0,73	**1,62**
TERG_02955	CP2 transcription factor, putative (*A. benhamiae*)	-0,56	**-1,53**
TERG_03333	transcription factor RfeD, putative (*A. benhamiae*)	**1,72**	**2,26**
TERG_03619	transcription factor Tos4 (*T. equinum*)	-1,44	**-2,27**
TERG_03861	C2H2 transcription factor (*T. tonsurans*)	0,96	**2,03**
TERG_04089	RfxA protein (*T. equinum*)	-1,03	**-2,32**
TERG_04600	fungal specific transc. factor domain-cont. prot. (*T. equinum*)	1,34	**2,96**
TERG_05021	C6 transcription factor, putative (*A. benhamiae*)	-0,31	**-1,88**
TERG_05032	C6 transcription factor (*T. equinum*)	1,32	**2,36**
TERG_06802	hypothetical protein	1,49	**1,79**
TERG_06815	bZIP transcription factor (*T. tonsurans*)	-0,92	**-2,11**
TERG_06884	C6 transcription factor (War1), putative (*T. verrucosum*)	0,95	**1,54**
TERG_07077	C6 transcription factor (*T. equinum*)	1,14	**1,70**
TERG_07493	Zinc knuckle transcription factor (CnjB) (*T. tonsurans*)	-1,49	**-2,21**
TERG_08262	C6 transcription factor, putative (*A. benhamiae*)	0,63	**2,06**
TERG_08825	bZIP transcription factor JlbA/IDI-4 (*T. verrucosum*)	**1,58**	**1,93**
TERG_11817	Transc. initiat. factor TFIID sub. 7, putative (*T. verrucosum*)	1,41	**2,91**
TERG_11920	Vesic. med. transp. prot. Bfr2/Che-1, putative (*T. verrucosum*)	**-1,68**	**3,68**

(*) Valores em log2 FC. Em vermelho valores iguais ou acima de 1,50. Em verde valores iguais ou abaixo de -1,50.

6.4 A parede celular e a estrutura da membrana são afetadas pela SRT

A SRT modulou a expressão de genes associados à formação de glucanos e quitinas, que são polissacarídeos estruturais importantes na parede celular fúngica. Esses genes incluem endoglucanases (TERG_08178, TERG_03353, TERG_06189 e TERG_04268), quitinases (TERG_05626 e TERG_05625) e quitina sintases (TERG_12318 e TERG_12319). Enquanto os genes relacionados ao glucano foram predominantemente induzidos, os genes associados à quitina foram reprimidos após 12 h

de tratamento com a SRT. O gene que codifica a hidrofobina (TERG_04234) foi reprimido após apenas 12 h de exposição à SRT. Além disso, SRT regula negativamente a expressão de genes que codificam componentes da via biossintética do ergosterol em *T. rubrum*. Após 12 h, os genes que codificam para difosfomevalonato descarboxilase (erg19; TERG_07616), C-8 esterol isomerase (erg1; TERG_06755), c-14 esterol redutase (erg24; TERG_04382), C-4 metilsterol oxidase (erg25; TERG_08545), proteína de biossíntese de ergosterol (erg28; TERG_04740) e esterol 24-Cmetiltransferase/Delta (24(24[1]))-sterol redutase (erg4; TERG_06528/TERG_03102) foram reprimidos. O gene codificador de esqualeno epoxidase (erg1; TERG_05717) foi reprimido após 3 e 12h.

O baixo conteúdo de ergosterol após tratamento com SRT confirmou a inibição da via Biosintética desse esterol (**Figura 10**). Ainda, a modulação da esfingomielinase D (TERG_01406), fosfolipase lisossômica A2 (TERG_03747), B (TERG_05522) e D (TERG_05303) e regulação positiva da fosfolipase A2 secretora (TERG_00127) foram observadas.

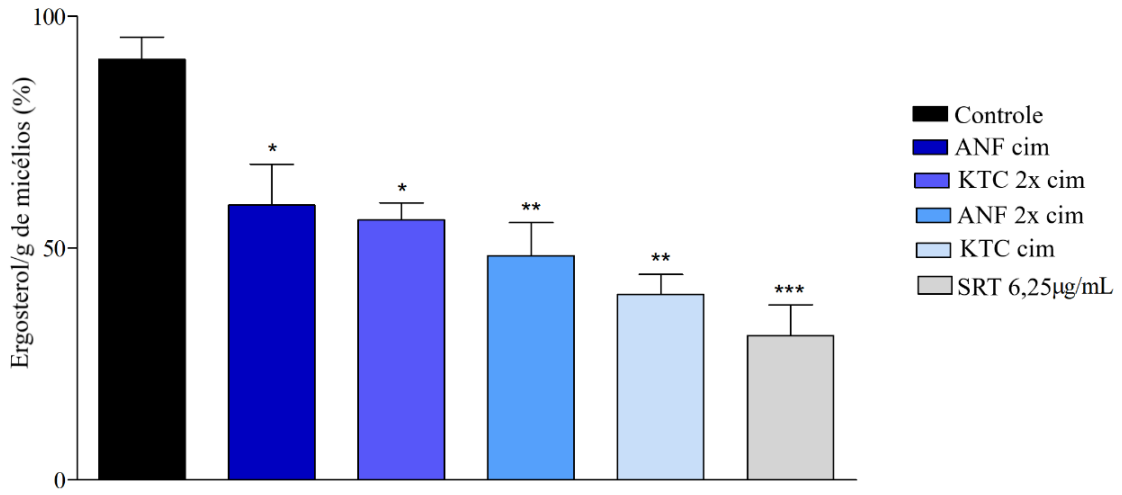

Figura 10. Efeito do fármaco sertralina no teor de ergosterol total como porcentagem do peso úmido do micélio de *Trichophyton rubrum*. Controle (ausência de fármacos), presença dos antifúngicos anfotericina B (ANF cim e ANF 2x cim), cetoconazol (KTC

cim e KTC 2x cim) como controles positivos e SRT na concentração subinibitória (6,25 µg/mL). Os asteriscos representam diferença estatística * $p < 0,05$, ** $p < 0,01$ e *** $p < 0,001$ em comparação ao controle.

A exposição à SRT levou ao acúmulo de transcritos de alguns genes que codificam transportadores de membrana. O número de genes modulados aumentou ao longo do tempo. Genes que codificam os transportadores do tipo MFS foram preferencialmente inibidos em ambos os pontos de tempo. Entre os genes regulados positivamente, 23 permaneceram induzidos após 3 e 12 h de desafio com SRT (**Tabela 9**).

Tabela 9. Genes que codificam transportadores no genoma de *Trichophyton rubrum* modulados em resposta à exposição ao fármaco sertralina.

ID	Produto do gene	3h	12h
TERG_00286	ABC transporter (*T. tonsurans*)	0,52	**1,53**
TERG_00402	ABC multidrug transporter, putative (*T. verrucosum*)	**2,49**	**3,00**
TERG_00955	ABC drug exporter AtrF (*T. verrucosum*)	**2,07**	**1,62**
TERG_01443	ABC multidrug transporter (*T. tonsurans*)	-0,02	**-1,61**
TERG_01718	cell division control protein Cdc6 (*T. tonsurans*)	-1,35	**-2,19**
TERG_02186	ABC multidrug transporter, putative (*A. benhamiae*)	**1,91**	**3,47**
TERG_02867	ribosome biogenesis ATPase RIX7 (*T. tonsurans*)	-1,05	**-1,91**
TERG_04224	ABC transporter	**2,32**	**3,96**
TERG_04952	multidrug resistance protein (*T. equinum*)	**6,87**	**7,69**
TERG_05126	ABC multidrug transporter, putative (*A. benhamiae*)	1,17	**2,27**
TERG_05254	translation initiation factor RLI1	-0,84	**-1,60**
TERG_08130	ABC ATPase (*T. equinum*)	**2,36**	0,54
TERG_08299	multidrug resist.-associated prot. 1 transporter (*M. canis*)	**1,96**	**3,30**
TERG_08613	ABC multidrug transporter, putative (*A. benhamiae*)	1,16	**3,50**
TERG_08751	ABC multidrug transporter, putative (*A. benhamiae*)	**5,82**	**6,33**
TERG_12373	multidrug resistance protein (*T. tonsurans*)	0,57	**-1,73**
TERG_12595	ABC multidrug transporter SitT (*T. tonsurans*)	0,15	**3,60**
TERG_00008	MFS phospholipid transporter (*T. tonsurans*)	-0,19	**-1,53**
TERG_00162	MFS multidrug transporter, putative (*A. benhamiae*)	**2,30**	**2,26**
TERG_00574	MFS multidrug transporter, putative (*T. verrucosum*)	**1,86**	**3,07**
TERG_00776	MFS transporter (*T. tonsurans*)	0,83	**1,82**
TERG_01053	MFS monocarboxylate transp., putative (*T. verrucosum*)	**1,76**	**2,39**
TERG_01336	MFS transporter (*T. equinum*)	0,06	**-2,30**
TERG_01480	MFS multidrug transporter, putative (*A. benhamiae*)	1,11	**-3,74**
TERG_01623	MFS transporter (*T. equinum*)	**1,54**	**2,98**
TERG_01634	MFS multidrug transporter, putative (*T. verrucosum*)	-1,17	**-2,40**

TERG_01912	MFS transporter (*T. equinum*)	0,32	**-2,29**
TERG_02265	MFS multidrug transporter (*T. equinum*)	1,15	**2,02**
TERG_02283	MFS transporter, putative (*T. verrucosum*)	-0,05	**-2,18**
TERG_02369	MFS transporter (*T. tonsurans*)	0,68	**1,51**
TERG_02545	MFS monocarboxylate transporter (*T, equinum*)	0,26	**-2,14**
TERG_02616	integral membrane protein (*T, equinum*)	0,55	**-1,63**
TERG_02844	major facilitator superfamily transporter (*T. tonsurans*)	**-2,51**	0,19
TERG_03055	MFS transporter, putative (*T. verrucosum*)	**2,51**	**2,25**
TERG_03174	MFS siderochrome iron transporter MirB (*T. verrucosum*)	-0,30	**-1,57**
TERG_03240	transmembrane efflux protein (*T. tonsurans*)	**1,64**	**1,70**
TERG_03965	MFS nicotinic acid transporter (*T. tonsurans*)	1,49	**2,31**
TERG_04308	MFS sugar transporter (*T. tonsurans*)	-0,10	**-2,59**
TERG_04399	MFS transporter, putative (*A. benhamiae*)	**2,31**	**1,81**
TERG_04764	MFS transporter (*T. tonsurans*)	**1,93**	0,88
TERG_04765	MFS transporter, putative (*A. benhamiae*)	**1,70**	1,30
TERG_04875	monocarboxylate permease (*T. equinum*)	-1,07	**-1,88**
TERG_05104	MFS transporter of unknown specificity (*T. verrucosum*)	**1,96**	**1,67**
TERG_05199	MFS gliotoxin efflux transporter GliA (*T. verrucosum*)	**2,20**	**2,70**
TERG_05202	MFS drug efflux transporter (*T. equinum*)	-0,07	**-2,58**
TERG_05342	MFS multidrug transporter, putative (*A. benhamiae*)	-0,44	**-1,91**
TERG_05429	MFS multidrug transporter, putative (*T. verrucosum*)	0,94	**2,33**
TERG_05466	MFS transporter, putative (*T. verrucosum*)	**3,12**	**3,90**
TERG_05575	MFS multidrug transporter (*T. tonsurans*)	1,12	**1,98**
TERG_05891	MFS phosphate transporter (*T. equinum*)	-1,23	**-1,65**
TERG_06650	MFS monocarboxylate transp., putative (*A. benhamiae*)	**1,53**	**1,63**
TERG_06679	MFS transporter, putative (*A. benhamiae*)	1,45	**2,64**
TERG_07040	MFS drug efflux transporter (*T. equinum*)	**2,07**	0,32
TERG_07492	sugar transporter STL1 (*T. tonsurans*)	0,35	**1,50**
TERG_07539	multidrug resistance protein (*T. tonsurans*)	-0,04	**-1,72**
TERG_07654	MFS transporter, putative (*T. verrucosum*)	1,48	**3,48**
TERG_08095	MFS multidrug transporter, putative (*A. benhamiae*)	0,48	**-2,19**
TERG_08336	MFS multidrug transporter, putative (*A. benhamiae*)	**1,53**	0,49
TERG_08700	DUF895 domain membrane protein (*T. equinum*)	**2,83**	**1,79**
TERG_11600	MFS transporter (*T. tonsurans*)	-0,46	**-1,78**
TERG_11753	MFS transporter (*T. tonsurans*)	-0,40	**-2,28**
TERG_11943	MFS maltose permease (*T. tonsurans*)	1,31	**1,55**
TERG_12017	MFS sugar transporter, putative (*A. benhamiae*)	-0,82	**-3,68**
TERG_12018	MFS sugar transporter, putative (*A. benhamiae*)	-1,06	**-3,85**
TERG_12193	MFS sugar transporter (*T. equinum*)	**-1,84**	**-2,38**
TERG_12194	MFS monosaccharide transport., putative (*T. verrucosum*)	**-2,01**	**-2,53**
TERG_12270	MFS multidrug transporter, putative (*A. benhamiae*)	**2,00**	-0,02
TERG_12370	MFS multidrug transporter, putative (*A. benhamiae*)	1,38	**1,72**
TERG_12503	polyamine transporter 2	0,12	**-1,71**
TERG_12504	MFS multidrug transporter (*T. equinum*)	0,26	**-1,54**
TERG_12511	MFS multidrug transporter (*T. equinum*)	-0,05	**-1,95**
TERG_00616	potassium/sodium efflux P-type ATPase, fungal-type	**1,98**	**5,04**

TERG_02565	sulfate transporter (*T. equinum*)	**1,77**	**1,82**
TERG_03396	phospholipid-transporting ATPase (*T. equinum*)	1,38	**2,11**
TERG_03401	high affinity nickel transporter (*T. tonsurans*)	-0,54	**-1,95**
TERG_03408	ZIP metal ion transporter (*T. equinum*)	0,69	**1,58**
TERG_03714	NCS1 nucleoside transporter (*T. tonsurans*)	1,30	**2,53**
TERG_04778	Ribos. assembly and trans. prot. Srp40 (*T. verrucosum*)	-1,30	**-2,12**
TERG_04790	arsenical-resistance protein	-1,29	**-1,81**
TERG_05023	calcium/proton exchanger	**3,86**	**2,95**
TERG_05141	NCS1 nucleoside transporter (*T. equinum*)	-1,15	**-3,13**
TERG_05701	C4-dicarboxylate transp./malic acid protein (*T. verrucosum*)	-0,70	**-1,62**
TERG_05837	Plasm. memb. ammonium trans. (Ato3), putativ. (*A. benhamiae*)	0,46	**2,12**
TERG_07174	vesicle transport V-snare protein (*T. equinum*)	0,42	**1,53**
TERG_07921	adenylylsulfate kinase	1,24	**2,18**
TERG_07942	calcium channel subunit Cch1 (*T. tonsurans*)	1,15	**2,01**
TERG_08377	copper transporter Ctr (*T. tonsurans*)	1,21	**2,92**
TERG_11885	ABC bile acid transporter, putative (*T. verrucosum*)	0,98	**1,61**
TERG_11920	vesicle-med. transp.prot.Bfr2/Che-1 (*T. verrucosum*)	**-1,68**	**3,68**
TERG_12058	transporter smf2 (*T. tonsurans*)	-0,71	**-2,38**
TERG_12059	transporter smf2 (*T. tonsurans*)	-0,33	**-1,83**
TERG_12342	membrane zinc transporter (*T. tonsurans*)	0,29	**-3,13**
TERG_12436	monocarboxylate transporter (*M. canis*)	1,31	**1,88**
TERG_12559	copper-transporting ATPase (*T. tonsurans*)	**1,67**	**2,82**

(*) Valores expressos em log2 FC ± 1,5 estão destacados em vermelho para genes induzidos e em verde para genes reprimidos na presença do fármaco SRT.

6.5 SRT afeta a transcrição de genes de estresse oxidativo em *T. rubrum*

Através da regulação positiva dos genes da glutationa S-transferase (GST) (TERG 03390, TERG 04960, TERG 01405, TERG 07326, TERG 02041, TERG 00579, TERG 08208 e TERG 05135), *T. rubrum* pode ter uma resposta alterada ao estresse oxidativo quando exposto ao fármaco SRT. Na presença da SRT, dois outros genes GST (TERG_06540 e TERG_06578), bem como genes codificando catalase A (TERG_01252) e Fe-superóxido dismutase (TERG_04819), foram regulados negativamente. Além disso, SRT regulou positivamente o gene que codifica a tioredoxina redutase (TERG_08849) e regulou negativamente o gene da tiorredoxina (TERG_05849). Tioredoxinas (TRX) são pequenas proteínas redox onipresentes que desempenham papéis-chave na sinalização redox e respostas ao estresse oxidativo. Os genes responsáveis pela conversão da

melatonina em dois metabólitos, 6-hidroximelatonina e N-acetil-N-formil-5-metoxiquinuramina, foram também regulados positivamente pela SRT (**Figura 11**). Finalmente, o gene mais induzido em ambos os momentos (TERG_06548) foi um ortólogo oxidoredutase identificado em *Microsporum canis*.

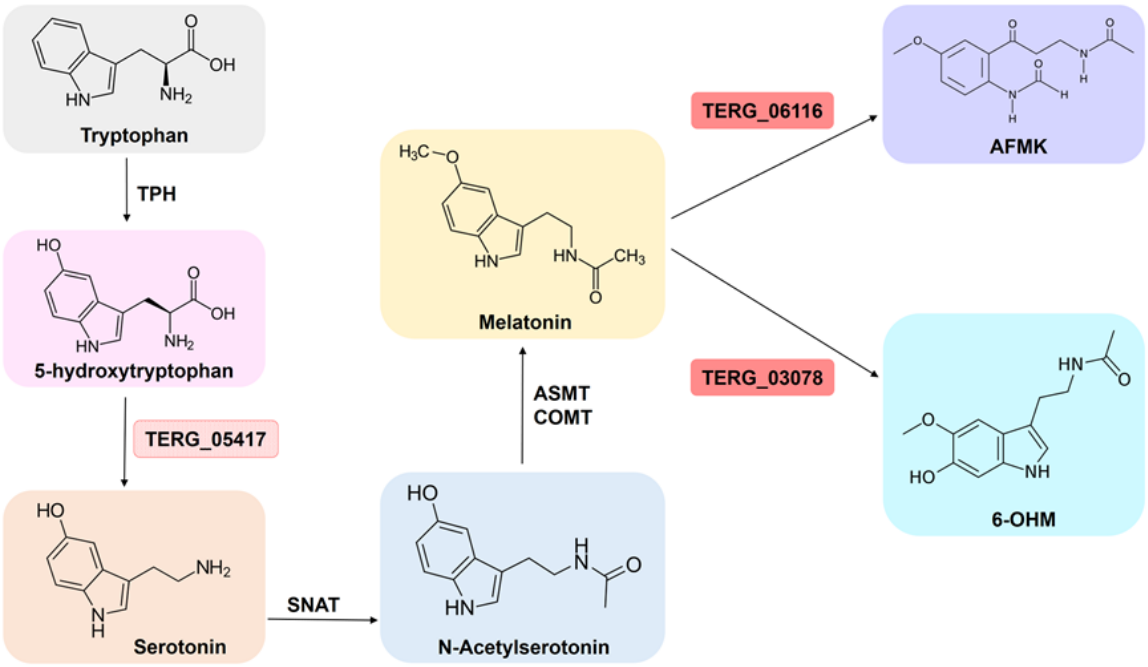

Figura 11. A via biossintética envolvida na síntese de melatonina a partir do triptofano. Etapas enzimáticas do triptofano à melatonina e os metabólitos correlacionados.

6.6 Efeito da SRT no Metabolismo de *T. rubrum*

SRT aparentemente interfere com o metabolismo primário de *T. rubrum*. Enquanto os genes envolvidos na glicólise foram reprimidos, os genes envolvidos no ciclo do glioxilato, etanol e biossíntese de glicerol e desramificação de glicogênio foram induzidos. O antidepressivo faz *T. rubrum* desviar do metabolismo de carbono padrão para caminhos alternativos (**Figura 12**). Este efeito repressivo nos genes da via da glicólise neutraliza a etapa inicial realizada pela hexoquinase (TERG_03229), que foi induzida. A reprogramação metabólica induziu a expressão de genes associados ao ciclo do glioxilato (TERG_11639, TERG_01281, TERG_08288 e TERG_08287) e biossíntese

de glicerol (TERG_07273, TERG_12172 e TERG_12173). Além disso, SRT modulou genes relacionados ao catabolismo de etanol e glicerol e induziu uma enzima desramificadora (TERG_06681). Essa enzima facilita a quebra do glicogênio, que serve como reserva de glicose.

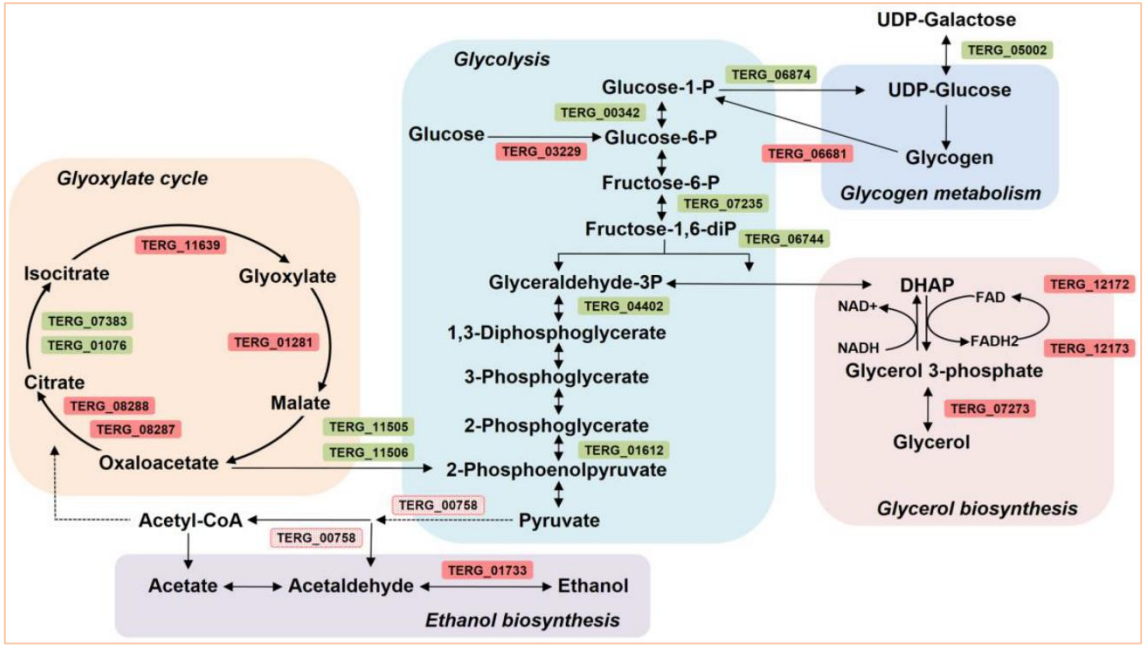

Figura 12. Visão geral do efeito do fármaco sertralina no metabolismo de *Trichophyton rubrum*. Genes induzidos (vermelho) ou reprimidos (verde) considerando ± 1,5 Log2 FC. Em amarelo, o acúmulo de transcrição está abaixo do limiar de ± 1,5 Log2 FC (correspondente a 1,47 *fold change*).

6.7 Eventos de SA na presença do fármaco SRT

O RNA-seq revelou a expressão diferencial de transcritos alternativos em 288 genes em 3h e em 679 genes em 12h na presença da SRT. Portanto, a maioria dos genes responsivos ao desafio concentrou-se em 12h (**Figura 13**).

Os genes com as maiores modulações de eventos de SA estão listados na **Tabela 10**. Transportadores de membrana, fatores de transcrição e proteínas quinase continuaram como grupos proeminentes, porém, não há necessariamente relação entre a indução ou repressão dos genes com os eventos de SA.

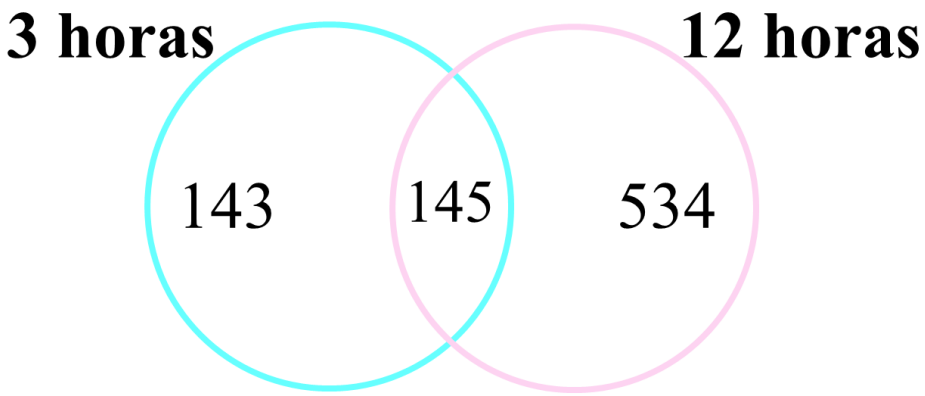

Figura 13. Diagrama de Venn apresentando os genes que sofreram *splicing* alternativo após exposição à dose subletal da SRT por 3 h e 12 h em comparação com as amostras de controle sem SRT.

Tabela 10. Os eventos de *splicing* alternativo mais significativamente regulados.

		Log2 Fold change	
ID	**Produto do gene**	**3h**	**12h**
TERG_07560	hypothetical protein	4,02	3,19
TERG_00243	pathogenesis associated protein Cap20, putative (*T. verrucosum*)	2,88	5,46
TERG_08430	Neurofilament heavy polypeptide (*T. tonsurans*)	2,77	2,86
TERG_08333	1-pyrroline-5-carboxylate dehydrogenase	2,70	3,27
TERG_04145	ATP synthase subunit beta, mitochondrial	2,12	3,45
TERG_06358	dicer (*T. tonsurans*)	2,04	
TERG_03566	GYF domain-containing protein (*T. equinum*)	2,02	
TERG_07169	hypothetical protein	2,01	
TERG_07200	C2 domain-containing protein (*T. tonsurans*)	1,91	
TERG_03599	metalloproteinase (*T. equinum*)	1,90	
TERG_07656	lupus La protein (*T. equinum*)		3,09
TERG_03642	hypothetical protein		2,97
TERG_07330	chromatin regulatory protein sir2 (*T. tonsurans*)		2,73
TERG_01957	proteinase T (*M. gypseum*)		2,72
TERG_07753	hypothetical protein		2,69
TERG_06810	hypothetical protein	-1,93	
TERG_08093	inositolphosphorylceramide-B C-26 hydroxylase (*T. equinum*)	-1,96	
TERG_06041	hypothetical protein	-1,98	
TERG_03829	FAD binding domain-containing protein (*T. equinum*)	-1,99	
TERG_00146	Phospholip.-translocating P-type ATPase domain-containing protein (*T. equinum*)	-2,00	
TERG_00362	glutaminase (T. equinum)	-2,02	
TERG_00412	CMGC/SRPK protein kinase (*T. tonsurans*)	-2,07	
TERG_02483	hypothetical protein	-2,19	

TERG_07283	GABA permease (*T. equinum*)	-2,25	
TERG_00553	amino acid permease (*T. equinum*)	-2,42	
TERG_07238	zinc-binding oxidoreductase, putative (*A. benhamiae*)		-3,58
TERG_08672	HFR-3 (*M. canis*)		-3,61
TERG_01479	GTPase activating protein (*T. tonsurans*)		-3,82
TERG_07070	meiotically up-regulated 62 protein (*M. gypseum*)		-3,94
TERG_08189	CMGC/CLK protein kinase		-3,99
TERG_07319	metacaspase 1B (*T. tonsurans*)		-4,00
TERG_02909	acyl-CoA oxidase, putative (*T. verrucosum*)		-4,17
TERG_04324	extracellular metalloproteinase 4		-4,51
TERG_08416	DUF1339 domain-containing protein (*T. equinum*)		-5,18
TERG_00745	fes/CIP4 y domain-containing protein (*T. equinum*)		-5,19

Para validar o SA um gene codificador da quinase CMGC/SRPK, TERG_07061, foi selecionado pois ele apresentou repressão de sua expressão na presença da SRT em 3h e 12h (**Tabela 7**) e indução da retenção do íntron 3 em 3h (1,43 log2 FC) e 12h (2,50 log2 FC). O resultado do teste de variação da temperatura de anelamento dos primers demonstra que os iniciadores se ligam especificadamente nas regiões determinadas. Apenas duas bandas foram visualizadas após a amplificação do produto do cDNA com *primers* que flanqueiam o intron 3. A banda de maior tamanho corresponde ao produto de amplificação do transcrito com retenção do íntron com 253pb, e a banda de menor tamanho corresponde ao transcrito processado com 197pb (**Figura 14**).

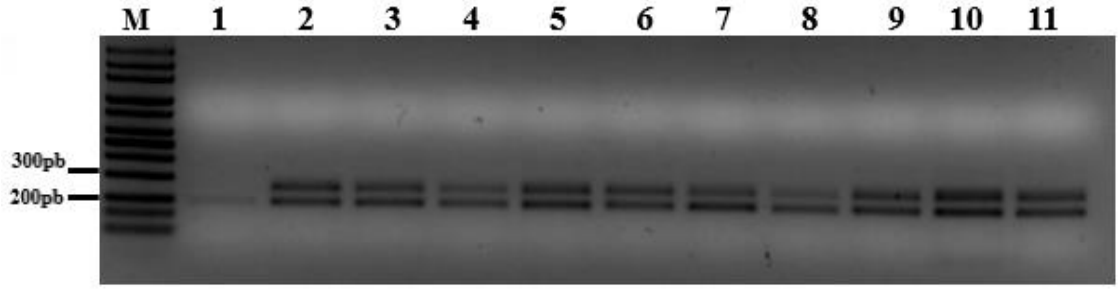

Figura 14. Eletroforese em gel de agarose realizada com produtos RT-PCR. Teste do gradiente de temperatura do passo de anelamento dos oligonucleotídeos. Da esquerda para direita, M: marcador de peso molecular (100pb); 1: 50 °C; 2: 50,3°C; 3: 50,9°C; 4: 51,1°C; 5: 53,1°C; 6: 54,4°C; 7: 55,6°C; 8: 56,9°C; 9: 58,2°C; 10: 59,1; 11: 59,7°C. Todos os produtos de amplificação de cDNA foram obtidos de micélios cultivados na ausência da SRT.

Os resultados obtidos confirmam os eventos de retenção do íntron para os tempos 3h e 12h, na presença e na ausência do fármaco SRT, como revelado nos dados do RNA-seq (**Figura 15B)**.

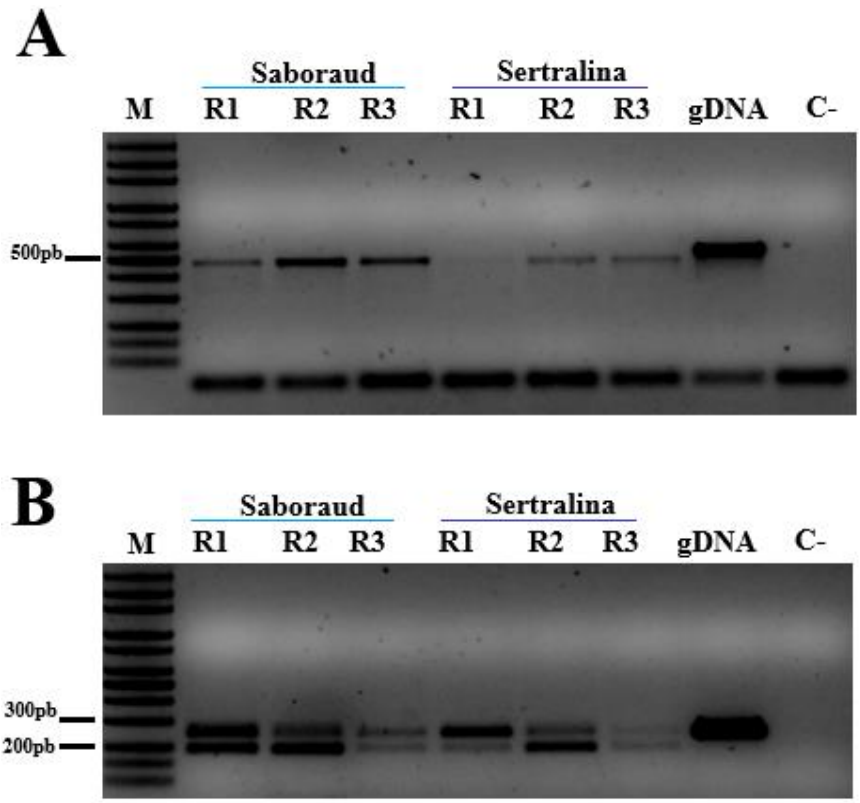

Figura 15. Produtos de amplificação de cDNA obtido de micélios de *Trichophyton rubrum* na presença de 70% da CIM do fármaco sertralina. **A**) Produto de amplificação de cDNA utilizando oligonucleotídeos que flanqueiam um íntron do gene da β-tubulina de *T. rubrum*. **B**) Produto de amplificação de cDNA utilizando oligonucleotídeos que flanqueiam o íntron 3 do gene TERG_07061 codificador da quinase CMGC/SRPK de *T. rubrum*. M: marcador de peso molecular (100pb); *Saboraud* R1, R2 e R3 cDNA extraído de micélios crescidos na ausência do fármaco SRT; Sertralina R1, R2 e R3 cDNA extraído de micélios crescidos na presença do fármaco SRT; gDNA: DNA extraído de micélios crescidos na ausência do fármaco utilizado como controle positivo; C-: controle negativo.

Conforme revelado nos dados de RNA-seq, houve indução significativa da retenção do intron 3 em 12h de exposição à SRT. Apesar da expressão da isoforma sem retenção também estar induzida em 12h, os valores de expressão relativa são maiores para a isoforma com retenção do íntron 3 (**Figura 16**). Adicionalmente, dos 81 genes

codificadores de proteína quinase que foram modulados pela SRT (**Tabela 7**). Apenas 38 genes sofreram SA mostrando que não é um fenômeno geral para todas as quinases.

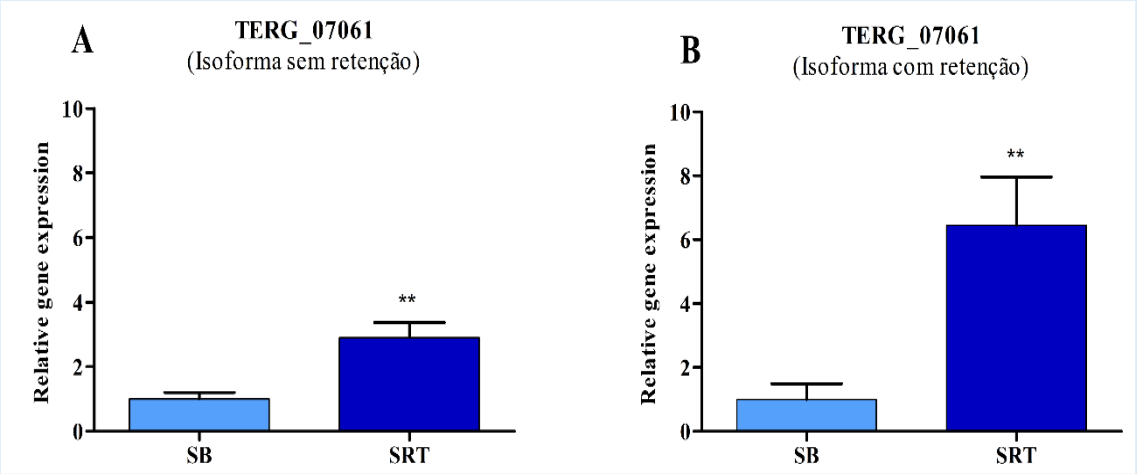

Figura 16. Nível de expressão relativa das isoformas do gene TERG_07061 codificador da quinase CMGC/SRPK em *Trichophyton rubrum*. (A) Expressão relativa da isoforma sem retenção do íntron 3 após 12h de tratamento em comparação com controle na ausência do fármaco SRT. (B) Isoforma com retenção do íntron 3 após 12h de tratamento em comparação com o controle na ausência do fármaco SRT. Os asteriscos indicam a significância estatística determinada pelo *teste t* seguido de *post-hoc* de *Tukey* (** $p < 0,01$).

6.8 Caracterização das isoformas do gene SRPK

O gene TERG_07061 codifica para uma proteína quinase CMGC/SRPK e tem 2.246 pares de base. Apenas uma isoforma proteica contendo 400 aminoácidos está descrita. Quando o íntron 3 é retido a proteína tem 67 resíduos de aminoácidos a menos em comparação com a isoforma descrita no *EnsemblFungi*.

Portanto, a busca por domínios revelou proteínas com tamanhos diferentes. A isoforma com retenção do íntron é menor, porém, possui em sua estrutura pelo menos parte dos domínios de assinatura para proteína quinase. Além disso, as análises de predição de domínios mostraram que o sítio de ligação ao ATP foi mantido, permanecendo do mesmo tamanho e posição na proteína com retenção (**Figura 17**).

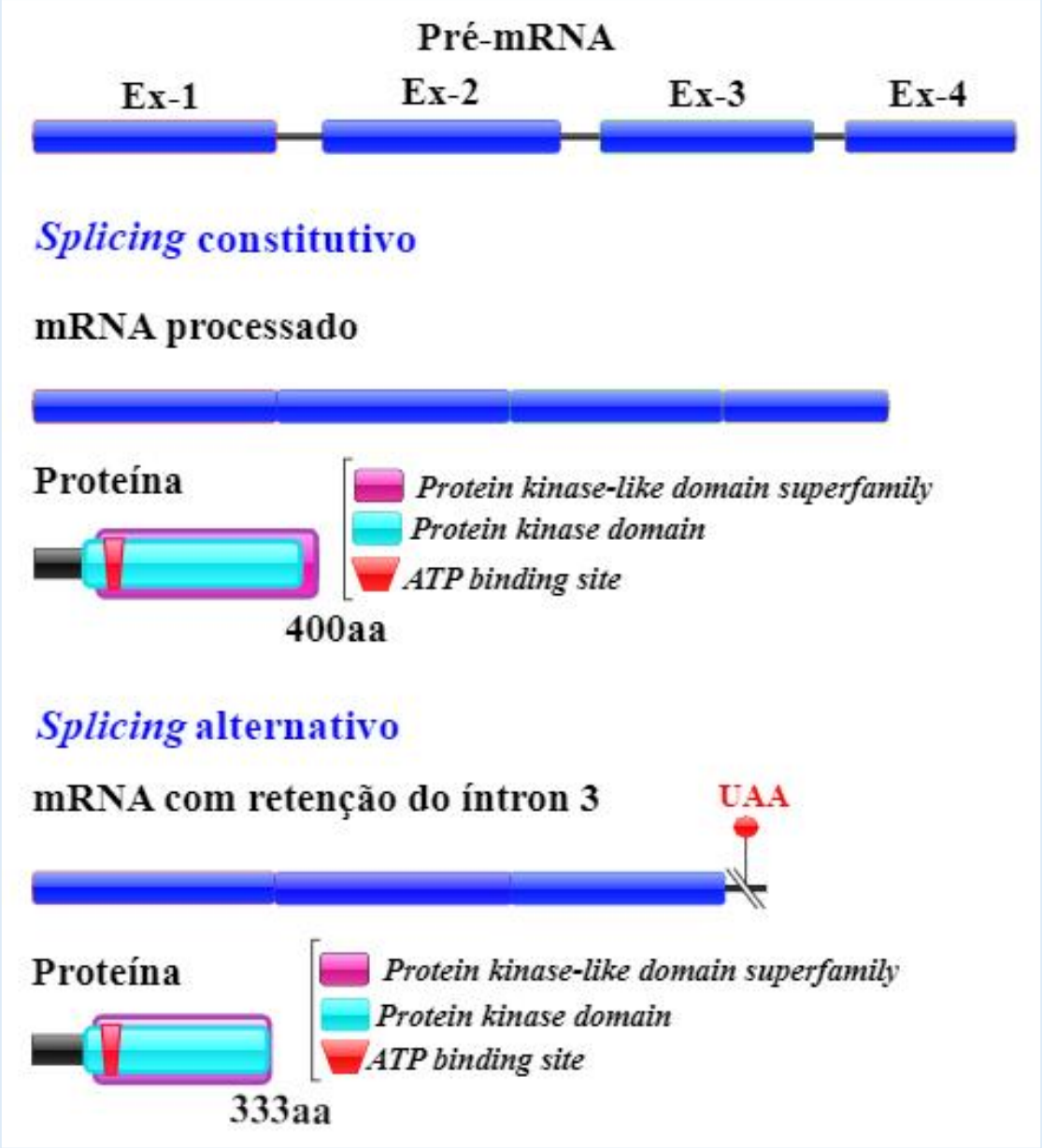

Figura 17. Comparação entre isoformas do gene SRPK. Análise dos domínios das isoformas derivadas do *splicing* convencional e *splicing* com retenção de íntron 3. Ex-1: Éxon 1; Ex-2: Éxon 2; Ex-3: Éxon 3 e E-4: Éxon 4. **UAA**: códon de parada.

Discussão

7. Discussão

Conhecer os possíveis mecanismos relacionados à resposta dos patógenos ao candidato a fármaco facilitará a otimização do seu reposicionamento. Portanto, realizamos uma análise abrangente dos efeitos do antidepressivo SRT no transcriptoma do agente etiológico mais comum das dermatofitoses, o dermatófito *T. rubrum*.

Além de seu uso como antidepressivo, o fármaco SRT também tem sido explorado para outras aplicações terapêuticas. Estudos *in vitro e in vivo* demonstraram seu potencial de aplicação no tratamento de osteomielite e câncer (Muthu *et al.*, 2019; Baú-Carneiro *et al.*, 2022). Além disso, a SRT apresenta atividades antiparasitárias, antibacterianas e antifúngicas contra vários fungos patogênicos, incluindo *C. neoformans*, *Aspergillus fumigatus*, *Trichosporon asahii*, *Sporothrix schenckii* e *T. rubrum* (Lass-Flörl *et al.*, 2001; Cong *et al.*, 2016; Ferreira *et al.*, 2018; Muthu *et al.*, 2019; Villanueva-Lozano *et al.*, 2019; Breuer *et al.*, 2022; Rocha *et al.*, 2022). A SRT também é eficaz isoladamente ou como terapia adjuvante contra a formação de biofilme de *T. rubrum*, *in vitro* e em modelo de unha humana, isoladamente ou em combinação com caspofungina (Rocha *et al.*, 2022).

7.1 Sequenciamento

O RNA-seq é uma tecnologia confiável que usa 3 réplicas técnicas e 3 réplicas biológicas. No entanto, devido ao grande volume de dados obtidos é recomendável usar uma outra técnica para validar o experimento. Nós utilizamos o RT-qPCR, e selecionamos 13 genes aleatoriamente, sem predileção de vias, tipo de modulação ou tempo de exposição, com o intuito de obter uma amostra a mais heterogênea possível.

Os resultados obtidos demonstraram a confiabilidade do RNA-seq. As leituras de alta qualidade, bem como a correlação entre RT-qPCR e RNA-seq, justificam seu uso nesse e em outros estudos sobre os efeitos de fármacos antidermatofíticos. (Persinoti *et al.*, 2014; Mendes *et al.*, 2018; Martins *et al.*, 2019).

7.2 SRT afeta sinalização celular e a transcrição em *T. rubrum*

O enriquecimento do domínio da proteína quinase serina/treonina (IPR002290), o catalisador domínio da proteína quinase tirosina e o domínio de ligação ao DNA semelhante a fungos Zn(2)-C(6) (IPR001138) foi relatado em fungos antropofílicos (Martinez *et al.*, 2012). O perfil transcricional de *T. rubrum* após ser desafiado com a SRT forneceu evidências de que quinases e os genes associados à regulação transcricional, quando modulados, foram preferencialmente induzidas, principalmente em 12 h de desafio.

A fosforilação por proteínas quinases é um mecanismo crítico que ajusta as atividades celulares como proliferação, metabolismo, apoptose e expressão gênica. Essas proteínas funcionam como interruptores moleculares ligando e desligando vias através de eventos de fosforilação (Watson *et al.*, 2020). A indução da transcrição resultante da exposição à SRT sugere ativação de vias de sinalização específicas. Os resultados obtidos indicam a ativação do *splicing* através da fosforilação reversível de proteínas SR. Essa fosforilação depende das famílias SRPK e CLK. A família SRPK fosforila proteínas SR, promovendo a importação nuclear de proteínas SR. Uma vez no núcleo, as proteínas SR podem ser fosforiladas pela família CLK de quinases, que compreende uma sequência de eventos essenciais para o *splicing* do pré-mRNA (Zhou and Fu, 2013). Por outro lado, o número significativo de genes codificadores de proteínas quinases modulados negativamente, sugere a desativação de outras vias. Essa estratégia de desativação pode representar uma demanda de conservação de energia suportada pela regulação negativa da biogênese ribossomal (**Figura 8**). Biogênese de ribossomos é energeticamente cara para as células. Consequentemente, condições ambientais desfavoráveis inibem tais processos (Piazzi *et al.*, 2019).

Os fatores de transcrição também estão associados à especificidade dos dermatófitos por determinados hospedeiros (Martinez *et al.*, 2012). Um pequeno número de fatores de transcrição foi modulado, a maioria dos quais tinha um motivo estrutural de dedo de zinco. Os fatores de transcrição são importantes para controlar a expressão gênica e regular as redes de transcrição moldando a fisiologia celular. Os fatores de transcrição foram descritos em *T. rubrum* como envolvidos na regulação de aquisição de nutrientes no hospedeiro, morfogênese, formação de biofilme, ajuste de pH, secreção de proteases, infecção em unhas, modulação da produção e secreção de citocinas em cultivo com queratinócitos humanos, regulação do processo de SA, dentre outros, que são determinantes para o sucesso do processo infeccioso e neutralização de fármacos (Bitencourt *et al.*, 2020; Lang *et al.*, 2020; Martins *et al.*, 2020; Bitencourt *et al.*, 2021; Martins-Santana *et al.*, 2022; Peres *et al.*, 2022). Considerando a relevância da regulação de fatores de transcrição e seu papel fundamental na patogênese de dermatófitos antropofílicos, é provável que SRT desencadeie a regulação direta ou indiretamente da transcrição, limitando o gasto de energia em condições desfavoráveis.

7.3 SRT perturba a parede celular e a membrana do *Trichophyton rubrum*

A parede celular fúngica é a primeira estrutura que os fármacos encontram antes de entrar na célula. É uma estrutura composta por proteínas de sinalização altamente especializadas em detectar vários estímulos essenciais para a manutenção da homeostase celular e a pressão osmótica. Essa estrutura possui alta plasticidade sendo fonte de diferentes respostas adaptativas. Várias moléculas que formam as paredes e membranas celulares são exclusivas dos fungos e constituem alvos adequados para o desenvolvimento de antifúngicos, no entanto, alcançar essa estrutura não é uma tarefa fácil, os fungos desenvolveram ao longo de sua jornada várias estratégias para manter sua estabilidade (Martins *et al.*, 2019).

A parede celular fúngica é constituída por β-1,3-glucano, quitina e glicoproteínas, que são principalmente responsáveis pelas interações entre a célula e o ambiente. Esta parede está associada com uma membrana celular composta predominantemente por glicerofosfolípidos, esteróis e esfingolipídios. A exposição à SRT afeta a expressão de genes codificadores de enzimas hidrolíticas em *T. rubrum*, o que pode contribuir para mudanças na estrutura da parede celular. Além disso, a repressão de uma beta-1,6 glucana sintetase que atua como um ligante glicosídico sugere uma instabilidade imposta na montagem da parede celular (Roncero and Vázquez De Aldana, 2020). Os efeitos repressivos gerais da SRT nos níveis de transcrição para quitina sintases e quitinases podem funcionar como um mecanismo compensatório para manter a integridade da parede celular. Este perfil modulador é semelhante aos efeitos dos antifúngicos pertencente ao grupo das equinocandinas nas células fúngicas. As equinocandinas têm como alvo o gene β-1,3-glucano sintase, esgotando o conteúdo de glucano da parede celular e aumentando o conteúdo de quitina (Martinez-Rossi *et al.*, 2021). N-acetiltransferases (GNAT) são enzimas que catalisam reações de acetilação transferindo uma porção acil da acil-coenzima A para diversos substratos (Choudhary *et al.*, 2014). Todos os genes que codificam GNAT (TERG_05545, TERG_07987, TERG_07408 e outros) foram regulados positivamente quando o fungo estava na presença da SRT. As hidrofobinas são proteínas exclusivas das células fúngicas presentes em sua superfície, responsáveis por sua interação com o meio ambiente, adesão ao substrato e hidrofobicidade, que também são cruciais na interação com o hospedeiro (Valsecchi *et al.*, 2017). SRT reprimiu o gene que codifica a hidrofobina (TERG_04234). Em um estudo anterior, o *T. rubrum* foi exposto a doses subletais de ácido undecanóico (UDA), onde esse gene também foi reprimido (Mendes *et al.*, 2018; Martins *et al.*, 2019).

Genes associados à biossíntese de ergosterol foram reprimidos após 12 h de exposição à SRT, revelando que o antidepressivo afeta as propriedades da membrana plasmática. Além disso, SRT reduziu níveis de ergosterol em comparação com anfotericina B e cetoconazol, que foram usados como controles positivos (**Figura 10**). Anfotericina B interage diretamente com ergosterol enquanto o cetoconazol é um potente inibidor de sua biossíntese (Martinez-Rossi *et al.*, 2021). Ergosterol modula a fluidez e permeabilidade da membrana plasmática e é essencial para a atividade enzimática de proteínas estruturais, transportadores e âncoras lipídicas pelas quais as proteínas são acopladas à parede celular e à membrana. Alterações em sua estrutura interfere principalmente na penetração da água (Abe *et al.*, 2009). A alteração resultante na membrana plasmática, juntamente com a modulação diferencial de genes associados à parede celular, sugere a ocorrência de estresse osmótico com alterações na composição do ergosterol das bicamadas lipídicas, fornecendo informações sobre a atividade antifúngica da SRT contra *T. rubrum*. Em trabalho anterior de nosso grupo, UDA também atuou promovendo a redução do ergosterol na membrana fúngica, o que afetou indiretamente a estrutura de parede do *T. rubrum*, prejudicando sua estabilidade e forçando seu remodelamento (Mendes *et al.*, 2018; Martins *et al.*, 2019).

SRT, uma droga anfifílica catiônica (CAD), causa fosfolipidose induzida por drogas (DIP) durante o armazenamento excessivo de fosfolipídios nos lisossomos (Rainey *et al.*, 2010). A expressão dos genes que codificam a fosfolipase A2 e a esfingomielinase D foram diminuídas após 12 h de tratamento com SRT. Inibição da fosfolipase A2 lisossômica correlaciona-se fortemente com drogas causando fosfolipidose (Hinkovska-Galcheva *et al.*, 2021), enquanto a enzima ácida esfingomielinase foi investigada como um alvo potencial para ação antidepressiva (Rhein *et al.*, 2017). Por outro lado, a fosfolipase B é regulada positivamente na exposição inicial à SRT e a fosfolipase D é

regulada positivamente ao longo do tempo. A fosfolipase B tem atividade de hidrolase que cliva ácidos graxos de fosfolipídios e lisofosfolípidos (Ramrakhiani and Chand, 2011). A fosfolipase D compreende enzimas responsáveis por gerar ácido fosfatídico (PA), um mensageiro secundário implicado na regulação de tráfego vesicular (O'luanaigh *et al.*, 2002). A SRT também modulou genes envolvidos no tráfego vesicular, incluindo a indução de genes codificadores de V-SNARE (TERG_06294, TERG_07174) e a proteína da vesícula do retículo endoplasmático, TERG_00785, que teve sua expressão induzida aproximadamente 25.388 vezes após 3 h de desafio (log2= 8,6). O sistema secretório de *T. rubrum* é essencial para sua patogênese. Diversas enzimas queratinolíticas estão envolvidas na quebra de moléculas de queratina, auxiliadas pela secreção de amônia e ureia pelo fungo (Martins *et al.*, 2020). Além disso, as vesículas do dermatófito *Trichophyton interdigitale* modula a resposta imune do hospedeiro (Bitencourt *et al.*, 2018).

Além de modificar a parede celular e a membrana, houve a regulação positiva de genes que codificam o sistema glioxalase. Um sistema antioxidante altamente conservado, onipresente em todos os organismos vivos. Ele desintoxica as células na presença de metilglioxal, um subproduto da glicólise e gliconeogênese. A enzima glioxalase catalisa a conversão de metilglioxal com glutationa em S-D-lactoilglutationa (He *et al.*, 2020). Curiosamente, os genes que codificam enzimas desse sistema foram induzidos pela SRT (TERG_00233, TERG_06533, TERG_04907) e reprimidos quando o dermatófito foi cultivado em queratina como única fonte de carbono (Martins *et al.*, 2020).

7.4 SRT e os transportadores de *Trichophyton rubrum*

Além de afetar a estrutura e composição da parede celular, a análise transcricional global em resposta à SRT demonstrou a indução de genes de resistência a drogas,

principalmente os genes que codificam MFS, como uma resposta celular ao estresse. O MFS é um dos maiores grupos de transportadores ativos secundários e desempenha vários papéis no transporte de uma ampla gama de substratos, incluindo açúcares, aminoácidos e drogas (Quistgaard *et al.*, 2016). O perfil geral regulado positivamente sugere uma atividade de desintoxicação que aumenta com o tempo, uma vez que esta família de proteínas inclui aqueles que codificam transportadores de resistência a drogas. No entanto, após 12 horas na presença da SRT, a regulação negativa de genes específicos pode representar uma tentativa de reter fosfato (TERG_05891; transportador de fosfato MFS) ou monossacarídeos (TERG_12194, TERG_04308; transportador de açúcar MFS) com o objetivo de superar os efeitos tóxicos das drogas.

Além disto, vários genes que codificam bombas de efluxo do tipo MDR (resistência a múltiplas drogas) foram super expressos após 3 e 12 horas de exposição à SRT. Este é um dos principais mecanismos de resposta a fármacos nos organismos vivos e atua logo após o reconhecimento pela célula da presença de substâncias tóxicas.

7.5 SRT desequilibra a Resposta ao Estresse Oxidativo

Após 3 h de exposição à SRT, *T. rubrum* induziu a expressão de genes da glutationa S-transferase para superar seus efeitos tóxicos. GSTs são pequenas proteínas citosólicas que contêm um grupo sulfidrila redox-ativo e estão envolvidos na desintoxicação celular. Xenobióticos e produtos endógenos do estresse oxidativo são conjugados à glutationa (GSH) e secretados através de vacúolos (Sato *et al.*, 2009). Os metabólitos tóxicos endógenos são removidos por processos de desintoxicação GSH-dependente. Assim, confere proteção contra o formaldeído produzido por metabolismo do metanol ou contra o metilglioxal, um subproduto da glicólise (He *et al.*, 2020). Interações de fármacos com GSTs também facilitam sua desintoxicação através da conjugação de GSH (Missall and Lodge, 2005). No entanto, após 12 h de exposição à droga, a regulação negativa de dois

genes da glutationa transferase pode reduzir a eficiência da extrusão de xenobióticos. Simultaneamente, a SRT reprime os genes da Fe superóxido dismutase e catalase A, que neutralizam as espécies reativas de oxigênio (ROS).

Os genes que codificam tioredoxina e tioredoxina redutase foram modulados de forma oposta após 12 horas de exposição à SRT. O sistema tiorredoxina/tioredoxina redutase (Trx/TrxR) confere homeostase redox às células fúngicas (Pannala and Dash, 2015). Como a SRT diminui o TrxR, o controle do equilíbrio redox celular permanece comprometido. Em *A. fumigatus* e *C. neoformans*, o gene que codifica TrxR é essencial para o crescimento *in vitro* e mostra fraca homologia com seu ortólogo humano, tornando-o um potencial alvo antifúngico (Binder *et al.*, 2020).

Saccharomyces cerevisiae submetido ao estresse oxidativo induzido por H_2O_2 apresenta maior transcrição TRX; a melatonina, um agente antioxidante, atenua parcialmente o estresse oxidativo aumentando o acúmulo de mRNA de TRX em células expostas a H_2O_2 (Vázquez *et al.*, 2017). No presente trabalho, a regulação positiva dos genes que codificam as enzimas responsáveis pela conversão da melatonina em seus metabólitos indica uma diminuição na disponibilidade de melatonina (**Figura 11**), seguida da regulação positiva do gene Trx e a regulação negativa de TrxR. Esses dados dão suporte ao mecanismo que consiste na dependência entre Trx e disponibilidade de melatonina, sugerindo a expressão contrabalançada do sistema tiorredoxina/tioredoxina redutase.

Em humanos, o fármaco SRT aumenta os níveis de serotonina nas fendas sinápticas (Devane *et al.*, 2002). De acordo com os resultados obtidos, SRT aumentou os transcritos de *T. rubrum* do gene que codifica um L-aminoácido aromático descarboxilase (EC 4.1.1.28) ligeiramente abaixo do limiar de log2 FC (1,36 vezes) (**Figura 11**). Esta enzima catalisa a conversão de 5-hidroxitriptofano em serotonina (Muñiz-Calvo *et al.*, 2019;

Gallardo-Fernández *et al.*, 2022). Serotonina funciona como um antifúngico contra *Aspergillus* spp. *in vitro* (Perkhofer *et al.*, 2007).

7.6 SRT impõe modulação metabólica dinâmica

O perfil geral mostrou flexibilidade na modulação metabólica em resposta ao efeito toxico da SRT, ativando o metabolismo alternativo do carbono. Em geral, os microrganismos consomem os nutrientes preferenciais, como a glicose, ativando uma cascata regulatória que reprime o consumo de fontes alternativas de carbono, como maltose, galactose ou etanol (New *et al.*, 2014).

De acordo com as análises dos níveis de transcrição, embora a glicose esteja disponível (pelo menos através do metabolismo do glicogênio) e a enzima hexoquinase esteja induzida, ativando a etapa inicial da glicólise que é responsável pela fosforilação da glicose pelo ATP para glicose-6-P, os fluxos glicolíticos não são direcionados para a síntese de duas moléculas de 2-fosfoenolpiruvato. A expressão diferencial induzida pela SRT direciona o metabolismo do *T. rubrum* a uma estratégia diferente em resposta ao desafio, redirecionando os padrões de expressão gênica para ativação de genes responsáveis pelo catabolismo de fontes de carbono menos favoráveis.

O tratamento com SRT resultou na repressão de genes que codificam enzimas glicolíticas e um aumento nos níveis de transcrição de genes envolvidos na utilização de vias alternativas de carbono, como o ciclo do glioxilato. A indução de isocitrato liase (TERG_11639) e malato sintase, glioxissomal (TERG_01281) após 3 h, e ATP-citrato sintases (TERG_08288/7) após 12 h de exposição à SRT mostram que a repressão da via glicolítica pode estar relacionada à ativação do ciclo do glioxilato. A indução do gene que codifica para isocitrato liase (TERG_11639) ocorre em 48 e 96 h de incubação de *T. rubrum* em queratina como única fonte de carbono (Martins *et al.*, 2020), juntamente com a repressão de genes relacionados com a glicólise, sugerindo a promoção de uma resposta

de virulência em ambas as condições. Ativação do ciclo do glioxilato é importante para patogenicidade fúngica (Lorenz and Fink, 2001; Cruz *et al.*, 2022). Especificamente, a isocitrato liase é uma enzima chave no ciclo do glioxilato (Chew *et al.*, 2019). Nossos resultados sugerem que a flexibilidade metabólica observada em *T. rubrum in vitro* presumivelmente contribui para sua aptidão e patogenicidade *in vivo*.

O perfil transcricional sugere que o fármaco SRT induziu o metabolismo do etanol através da atividade da enzima álcool desidrogenase e metabolismo do glicerol através da modulação da enzima glicerol quinase. O acúmulo de transcritos da enzima piruvato descarboxilase (TERG_00758), um pouco abaixo do corte estabelecido para as análises de expressão diferencial, sugere a catálise enzimática do ácido pirúvico ao acetaldeído e a posterior produção de etanol. Piruvato descarboxilase é uma enzima chave na fermentação do etanol, catalisa a descarboxilação do piruvato em acetaldeído com a liberação de dióxido de carbono (Ishchuk *et al.*, 2008). Desta forma, a atividade metabólica do *T. rubrum* é direcionada a diferentes vias alternativas de carbono em resposta à exposição a SRT.

7.7 Eventos de SA em *T.rubrum* na presença da SRT

Genes que codificam para as mais variadas funções proteicas foram descritos em *T. rubrum*, e eventos de SA foram confirmados e associados a resistência a fármacos, adaptação e resposta a mudanças de pH, patogenicidade e virulência em modelo de infecção *in vitro* e *ex-vivo* (Persinoti *et al.*, 2014; Gomes *et al.*, 2018; Mendes *et al.*, 2018; Neves-Da-Rocha *et al.*, 2019; Lopes *et al.*, 2022; Martins-Santana *et al.*, 2022). Desta forma, é presumível que genes que sofrem *splicing* alternativo na presença da SRT também estariam envolvidos nos mecanismos de resistência, permanência e adaptação de *T.rubrum* ao hospedeiro.

Fármacos que interferem no mecanismo de *splicing* podem ser úteis para o tratamento das infecções fúngicas. Dados na literatura evidenciam que a quinase SRPK é alvo atraente para o desenvolvimento de fármacos, devido ao seu envolvimento no processamento de RNA através da fosforilação de proteínas SR (Tzelepis *et al.*, 2018; Li *et al.*, 2021). Os efeitos inibitórios da SRT em *T.rubrum* podem estar relacionados aos eventos de SA revelados pelo RNAseq. Em um trabalho anterior, SPHINX31, um forte inibidor de SRPK, levou à indução de isoforma BRD4 (*bromodomain containing* 4), em vez da inibição total da transcrição, e teve como consequência efeito antileucêmico (Tzelepis *et al.*, 2018). Nós mostramos que a SRT atua no balanço entre as isoformas SRPK em *T.rubrum* direcionando para abundância de transcritos com a retenção do íntron 3, gerando uma possível isoforma menor da proteína.

Em outro estudo, os efeitos da SRT foram relacionados ao SA quando houve indução de uma variante de HSC70 em ratos submetidos ao antidepressivo. Os autores identificaram a presença de um códon de parada causando a ruptura de domínios na estrutura da proteína, além do predomínio da expressão da isoforma convencional em comparação com a isoforma truncada (Yamada *et al.*, 1999). No entanto, nossos resultados evidenciam o aumento da isoforma truncada e diminuição da isoforma convencional do gene.

Com a análise da sequência de aminoácidos foi prevista a redução do tamanho da proteína SRPK, porém, os sítios catalíticos e de ligação ao ATP foram conservados, sugerindo possível funcionalidade de ambas isoformas. É descrito que a retenção de íntrons pode levar, em alguns casos, a um códon de parada prematuro gerando uma proteína truncada. Porém, um códon de parada pode ser vantajoso para o fungo, pela exposição de um novo códon de início, possibilitando a tradução de uma isoforma alternativa como ocorrido para PAKA (Gomes *et al.*, 2018).

Como observado nos resultados do RNA-seq e confirmados por RT-qPCR, a retenção do intron 3 no gene TERG_07061 foi induzida na presença da SRT em 12h de exposição, apesar deste gene ter sido reprimido em ambos os tempos de exposição à SRT (**Tabela 7**), sugerimos que é provável a existência de uma funcionalidade da isoforma do gene com a retenção do íntron 3 como ocorrido para HSC70 (Yamada *et al.*, 1999).

Esses eventos de retenção podem estar associados à tentativa de neutralizar os efeitos tóxicos do antidepressivo na célula fúngica. Neste caso, podemos sugerir que a isoforma alternativa desta quinase seria produzida em maior quantidade que a isoforma convencional para compensar a repressão do próprio gene. Observamos que ocorre maior repressão do gene ao longo do tempo de exposição à SRT enquanto a sua isoforma alternativa é induzida. Vem sendo relatado que os eventos de SA podem ocorrer concomitantemente com a modulação gênica como um mecanismo de resistência e adaptação (Sieber *et al.*, 2018; Muzafar *et al.*, 2020), atuando cooperativamente para manter a homeostase celular. Porém, uma outra hipótese é que a SRT altere sítios de *splicing* reorganizando a paisagem transcricional de *T.rubrum* e bloqueando eventos fisiológicos significativos para a sobrevivência do fungo.

Conclusão

8. Conclusão

Com os resultados obtidos é possível concluir que:

- O antidepressivo teve como alvo eventos moleculares e vias metabólicas importantes para adaptação e virulência do dermatófito.
- SRT afeta a estrutura da membrana e da parede celular e inibe significativamente a síntese do ergoterol.
- SRT alterou a expressão de genes envolvidos no metabolismo energético, detoxificação celular e defesa contra o estresse oxidativo.
- SRT afeta a sinalização celular e a virulência de *T. rubrum*.
- SRT aumentou a expressão de vários genes responsáveis pelo efluxo celular sugerindo que *T. rubrum* atua em várias frentes para excluir o fármaco de suas células.
- Eventos de SA em um gene codificador da quinase CMGC/SRPK, TERG_07061 na presença da SRT sugere que a isoforma alternativa pode compensar a repressão da expressão do gene provocada pelo fármaco.
- O reposicionamento da SRT pode ser vantajoso para o combate de infecções causadas pelo dermatófito *T.rubrum*.

Referências Bibliográficas

Referências

ABE, F.; USUI, K.; HIRAKI, T. Fluconazole modulates membrane rigidity, heterogeneity, and water penetration into the plasma membrane in *Saccharomyces cerevisiae*. **Biochemistry,** v. 48, n. 36, p. 8494-504, Sep 15 2009. ISSN 0006-2960.

ARTHINGTON-SKAGGS, B. A. et al. Quantitation of ergosterol content: novel method for determination of fluconazole susceptibility of *Candida albicans*. **Journal of Clinical Microbiology,** v. 37, n. 10, p. 3332-3337, 1999. ISSN 1098-660X.

ASHBURN, T. T.; THOR, K. B. Drug repositioning: identifying and developing new uses for existing drugs. **Nature reviews Drug discovery,** v. 3, n. 8, p. 673-683, 2004. ISSN 1474-1784.

AYAZ, M. et al. Sertraline enhances the activity of antimicrobial agents against pathogens of clinical relevance. **J Biol Res (Thessalon),** v. 22, n. 1, p. 4, Dec 2015. ISSN 1790-045X

BAÚ-CARNEIRO, J. L. et al. Sertraline repositioning: an overview of its potential use as a chemotherapeutic agent after four decades of tumor reversal studies. **Transl Oncol,** v. 16, p. 101303, Feb 2022. ISSN 1936-5233

BENJAMINI, Y.; HOCHBERG, Y. Controlling the False Discovery Rate: A Practical and Powerful Approach to Multiple Testing. **Journal of the Royal Statistical Society: Series B (Methodological),** v. 57, n. 1, p. 289-300, 1995/01/01 1995. ISSN 0035-9246.

BINDER, J. et al. The Essential Thioredoxin Reductase of the Human Pathogenic Mold *Aspergillus fumigatus* Is a Promising Antifungal Target. **Front Microbiol,** v. 11, p. 1383, 2020. ISSN 1664-302X

BITENCOURT, T. A. et al. HacA governs virulence traits and adaptive stress responses in *Trichophyton rubrum*. **Frontiers in microbiology,** v. 11, p. 193, 2020. ISSN 1664-302X.

BITENCOURT, T. A. et al. StuA-regulated processes in the dermatophyte *Trichophyton rubrum*: Transcription profile, cell-cell adhesion, and immunomodulation. **Frontiers in cellular and infection microbiology,** v. 11, 2021.

BITENCOURT, T. A. et al. Extracellular vesicles from the dermatophyte *Trichophyton interdigitale* modulate macrophage and keratinocyte functions. **Frontiers in immunology,** v. 9, p. 2343, 2018. ISSN 1664-3224.

BOLGER, A. M.; LOHSE, M.; USADEL, B. Trimmomatic: a flexible trimmer for Illumina sequence data. **Bioinformatics,** v. 30, n. 15, p. 2114-20, Aug 1 2014. ISSN 1367-4811.

BRADLEY, R. K.; ANCZUKÓW, O. RNA splicing dysregulation and the hallmarks of cancer. **Nat Rev Cancer,** v. 23, n. 3, p. 135-155, Mar 2023. ISSN 1474-175X.

BREUER, M. R. et al. The Antidepressant Sertraline Induces the Formation of Supersized Lipid Droplets in the Human Pathogen *Cryptococcus neoformans*. **J Fungi (Basel),** v. 8, n. 6, Jun 17 2022. ISSN 2309-608x.

CHEW, S. Y. et al. Glyoxylate cycle gene ICL1 is essential for the metabolic flexibility and virulence of *Candida glabrata*. **Sci Rep,** v. 9, n. 1, p. 2843, Feb 26 2019. ISSN 2045-2322.

CHOUDHARY, C. et al. The growing landscape of lysine acetylation links metabolism and cell signalling. **Nat Rev Mol Cell Biol,** v. 15, n. 8, p. 536-50, Aug 2014. ISSN 1471-0072.

CLSI. **Reference method for broth dilution antifungal susceptibility testing of filamentous fungi**: Clinical Laboratory Standards Institute. 2nd ed. 2008.

CONG, L. et al. *In vitro* antifungal activity of sertraline and synergistic effects in combination with antifungal drugs against planktonic forms and biofilms of clinical *Trichosporon asahii* isolates. **PloS one,** v. 11, n. 12, p. e0167903, 2016. ISSN 1932-6203.

CRUZ, A. H. S. et al. Relevance of Nutrient-Sensing in the Pathogenesis of *Trichophyton rubrum* and *Trichophyton interdigitale*. **Frontiers in Fungal Biology,** v. 3, 2022. ISSN 2673-6128.

DEVANE, C. L.; LISTON, H. L.; MARKOWITZ, J. S. Clinical pharmacokinetics of sertraline. **Clin Pharmacokinet,** v. 41, n. 15, p. 1247-66, 2002.

DOBIN, A. et al. STAR: ultrafast universal RNA-seq aligner. **Bioinformatics,** v. 29, n. 1, p. 15-21, Jan 1 2013. ISSN 1367-4803.

FERREIRA, D. D. et al. Efficacy of sertraline against *Trypanosoma cruzi*: an *in vitro* and *in silico* study. **J Venom Anim Toxins Incl Trop Dis,** v. 24, p. 30, 2018. ISSN 1678-9199.

GALLARDO-FERNÁNDEZ, M. et al. Isotopic labelling-based analysis elucidates biosynthesis pathways in *Saccharomyces cerevisiae* for Melatonin, Serotonin and

Hydroxytyrosol formation. **Food Chem,** v. 374, p. 131742, Apr 16 2022. ISSN 0308-8146.

GOMES, E. V. et al. STE20/PAKA Protein Kinase Gene Releases an Autoinhibitory Domain through Pre-mRNA Alternative Splicing in the Dermatophyte *Trichophyton rubrum*. **Int J Mol Sci,** v. 19, n. 11, Nov 20 2018. ISSN 1422-0067.

GUPTA, A. K.; VENKATARAMAN, M. Antifungal resistance in superficial mycoses. **Journal of Dermatological Treatment,** v. 33, n. 4, p. 1888-1895, 2022/05/19 2022. ISSN 0954-6634.

HAVLICKOVA, B.; CZAIKA, V. A.; FRIEDRICH, M. Epidemiological trends in skin mycoses worldwide. **Mycoses,** v. 51 Suppl 4, p. 2-15, Sep 2008. ISSN 1439-0507.

HE, Y. et al. Glyoxalase system: A systematic review of its biological activity, related-diseases, screening methods and small molecule regulators. **Biomed Pharmacother,** v. 131, p. 110663, Nov 2020. ISSN 0753-3322.

HELLER, I. et al. Serotonin (5-HT) enhances the activity of amphotericin B against *Aspergillus fumigatus in vitro*. **Int J Antimicrob Agents,** v. 24, n. 4, p. 401-4, Oct 2004. ISSN 0924-8579.

HINKOVSKA-GALCHEVA, V. et al. Inhibition of lysosomal phospholipase A2 predicts drug-induced phospholipidosis. **J Lipid Res,** v. 62, p. 100089, 2021. ISSN 0022-2275.

HOKKEN, M. W. J. et al. Facilitators of adaptation and antifungal resistance mechanisms in clinically relevant fungi. **Fungal Genet Biol,** v. 132, p. 103254, Nov 2019. ISSN 1087-1845.

ISHCHUK, O. P. et al. Overexpression of pyruvate decarboxylase in the yeast Hansenula polymorpha results in increased ethanol yield in high-temperature fermentation of xylose. **FEMS Yeast Res,** v. 8, n. 7, p. 1164-74, Nov 2008. ISSN 1567-1356.

JACOB, T. R. et al. rpb2 is a reliable reference gene for quantitative gene expression analysis in the dermatophyte *Trichophyton rubrum*. **Med Mycol,** v. 50, n. 4, p. 368-77, May 2012. ISSN 1369-3786.

KANEHISA, M. et al. KEGG as a reference resource for gene and protein annotation. **Nucleic Acids Res,** v. 44, n. D1, p. D457-62, Jan 4 2016. ISSN 0305-1048.

KRETOVA, M. et al. Regulation of Pre-mRNA Splicing: Indispensable Role of Post-Translational Modifications of Splicing Factors. **Life (Basel),** v. 13, n. 3, Feb 21 2023. ISSN 2075-1729.

LANG, E. A. S. et al. The stuA gene controls development, adaptation, stress tolerance, and virulence of the dermatophyte *Trichophyton rubrum*. **Microbiol Res,** v. 241, p. 126592, Dec 2020. ISSN 0944-5013.

LASS-FLÖRL, C. et al. Antifungal activity against *Candida* species of the selective serotonin-reuptake inhibitor, sertraline. **Clin Infect Dis,** v. 33, n. 12, p. E135-6, Dec 15 2001. ISSN 1058-4838.

LASS-FLÖRL, C. et al. Interaction of sertraline with *Candida* species selectively attenuates fungal virulence in vitro. **FEMS Immunol Med Microbiol,** v. 35, n. 1, p. 11-5, Jan 21 2003. ISSN 0928-8244.

LI, Q. et al. Protein-Protein Interaction Inhibitor of SRPKs Alters the Splicing Isoforms of VEGF and Inhibits Angiogenesis. **iScience,** v. 24, n. 5, p. 102423, May 21 2021. ISSN 2589-0042.

LIMA, M. L. et al. Molecular Basis of the Leishmanicidal Activity of the Antidepressant Sertraline as a Drug Repurposing Candidate. **Antimicrob Agents Chemother,** v. 62, n. 12, Dec 2018. ISSN 1098-6596.

LOPES, M. E. R. et al. Alternative Splicing in *Trichophyton rubrum* Occurs in Efflux Pump Transcripts in Response to Antifungal Drugs. **J Fungi (Basel),** v. 8, n. 8, Aug 20 2022. ISSN 2309-608x.

LORENZ, M. C.; FINK, G. R. The glyoxylate cycle is required for fungal virulence. **Nature,** v. 412, n. 6842, p. 83-6, Jul 5 2001. ISSN 0028-0836.

LOVE, M. I.; HUBER, W.; ANDERS, S. Moderated estimation of fold change and dispersion for RNA-seq data with DESeq2. **Genome Biol,** v. 15, n. 12, p. 550, 2014. ISSN 1465-6906.

MANCINI, E. et al. Corrigendum to: ASpli: Integrative analysis of splicing landscapes through RNA-Seq assays. In: (Ed.). **Bioinformatics**. England, v.37, 2021. p.1783. ISBN 1367-4811.

MARTINEZ, D. A. et al. Comparative genome analysis of *Trichophyton rubrum* and related dermatophytes reveals candidate genes involved in infection. **mBio,** v. 3, n. 5, p. e00259-12, 2012.

MARTINEZ-ROSSI, N. M. et al. Dermatophyte Resistance to Antifungal Drugs: Mechanisms and Prospectus. **Front Microbiol,** v. 9, p. 1108, 2018. ISSN 1664-302X.

MARTINEZ-ROSSI, N. M. et al. State-of-the-Art Dermatophyte Infections: Epidemiology Aspects, Pathophysiology, and Resistance Mechanisms. **J Fungi (Basel),** v. 7, n. 8, Aug 3 2021. ISSN 2309-608x.

MARTINS, M. P. et al. Comprehensive analysis of the dermatophyte *Trichophyton rubrum* transcriptional profile reveals dynamic metabolic modulation. **Biochem J,** v. 477, n. 5, p. 873-885, Mar 13 2020. ISSN 0264-6021.

MARTINS, M. P. et al. Global Analysis of Cell Wall Genes Revealed Putative Virulence Factors in the Dermatophyte *Trichophyton rubrum*. **Frontiers in Microbiology,** v. 10, 2019-September-19 2019. ISSN 1664-302X.

MARTINS-SANTANA, L. et al. Peptidase Regulation in *Trichophyton rubrum* Is Mediated by the Synergism Between Alternative Splicing and StuA-Dependent Transcriptional Mechanisms. **Front Microbiol,** v. 13, p. 930398, 2022. ISSN 1664-302X.

MENDES, N. S. et al. Transcriptome-wide survey of gene expression changes and alternative splicing in *Trichophyton rubrum* in response to undecanoic acid. **Sci Rep,** v. 8, n. 1, p. 2520, Feb 6 2018. ISSN 2045-2322.

MENDES, N. S. et al. Pre-mRNA splicing is modulated by antifungal drugs in the filamentous fungus *Neurospora crassa*. **FEBS Open Bio,** v. 6, n. 4, p. 358-68, Apr 2016. ISSN 2211-5463 .

MISSALL, T. A.; LODGE, J. K. Function of the thioredoxin proteins in *Cryptococcus neoformans* during stress or virulence and regulation by putative transcriptional modulators. **Mol Microbiol,** v. 57, n. 3, p. 847-58, Aug 2005. ISSN 0950-382X.

MUTHU, D. et al. Repurposing of antidepression drug sertraline for antimicrobial activity against *Staphylococcus aureus*: a potential approach for the treatment of osteomyelitis. **New Journal of Chemistry,** v. 43, n. 14, p. 5315-5324, 2019. ISSN 1144-0546.

MUZAFAR, S. et al. Intron distribution and emerging role of alternative splicing in fungi. **FEMS Microbiol Lett,** v. 368, n. 19, Oct 26 2021. ISSN 0378-1097.

MUZAFAR, S. et al. Identification of Genomewide Alternative Splicing Events in Sequential, Isogenic Clinical Isolates of *Candida albicans* Reveals a Novel Mechanism of Drug Resistance and Tolerance to Cellular Stresses. **mSphere,** v. 5, n. 4, Aug 12 2020. ISSN 2379-5042.

MUÑIZ-CALVO, S. et al. Deciphering the melatonin metabolism in *Saccharomyces cerevisiae* by the bioconversion of related metabolites. **J Pineal Res,** v. 66, n. 3, p. e12554, Apr 2019. ISSN 0742-3098.

NEVES-DA-ROCHA, J. et al. Alternative Splicing in Heat Shock Protein Transcripts as a Mechanism of Cell Adaptation in *Trichophyton rubrum*. **Cells,** v. 8, n. 10, Oct 5 2019. ISSN 2073-4409.

NEW, A. M. et al. Different levels of catabolite repression optimize growth in stable and variable environments. **PLoS Biol,** v. 12, n. 1, p. e1001764, Jan 2014. ISSN 1544-9173.

O'LUANAIGH, N. et al. Continual production of phosphatidic acid by phospholipase D is essential for antigen-stimulated membrane ruffling in cultured mast cells. **Mol Biol Cell,** v. 13, n. 10, p. 3730-46, Oct 2002. ISSN 1059-1524.

OSSET-TRÉNOR, P.; PASCUAL-AHUIR, A.; PROFT, M. Fungal Drug Response and Antimicrobial Resistance. **J Fungi (Basel),** v. 9, n. 5, May 12 2023. ISSN 2309-608x.

PALIT, P.; ALI, N. Oral therapy with sertraline, a selective serotonin reuptake inhibitor, shows activity against *Leishmania donovani*. **J Antimicrob Chemother,** v. 61, n. 5, p. 1120-4, May 2008. ISSN 1460-2091.

PANNALA, V. R.; DASH, R. K. Mechanistic characterization of the thioredoxin system in the removal of hydrogen peroxide. **Free Radic Biol Med,** v. 78, p. 42-55, Jan 2015. ISSN 0891-5849 .

PERES, N. T. A. et al. The bZIP Ap1 transcription factor is a negative regulator of virulence attributes of the anthropophilic dermatophyte *Trichophyton rubrum*. **Curr Res Microb Sci,** v. 3, p. 100132, 2022. ISSN 2666-5174.

PERKHOFER, S. et al. Interaction of 5-hydroxytryptamine (serotonin) against *Aspergillus* spp. in vitro. **Int J Antimicrob Agents,** v. 29, n. 4, p. 424-9, Apr 2007. ISSN 0924-8579..

PERSINOTI, G. F. et al. RNA-sequencing analysis of *Trichophyton rubrum* transcriptome in response to sublethal doses of acriflavine. **BMC Genomics,** v. 15 Suppl 7, p. S1, 2014. ISSN 1471-2164.

PIAZZI, M. et al. Signal Transduction in Ribosome Biogenesis: A Recipe to Avoid Disaster. **Int J Mol Sci,** v. 20, n. 11, Jun 3 2019. ISSN 1422-0067.

QUISTGAARD, E. M. et al. Understanding transport by the major facilitator superfamily (MFS): structures pave the way. In: (Ed.). **Nat Rev Mol Cell Biol**. England, v.17, 2016. p.123-32. ISBN 1471-0080.

RAINEY, M. M. et al. The antidepressant sertraline targets intracellular vesiculogenic membranes in yeast. **Genetics,** v. 185, n. 4, p. 1221-33, Aug 2010. ISSN 1943-2631.

RAMRAKHIANI, L.; CHAND, S. Recent progress on phospholipases: different sources, assay methods, industrial potential and pathogenicity. **Appl Biochem Biotechnol,** v. 164, n. 7, p. 991-1022, Aug 2011. ISSN 0273-2289.

RHEIN, C. et al. Alternative splicing of SMPD1 coding for acid sphingomyelinase in major depression. **J Affect Disord,** v. 209, p. 10-15, Feb 2017. ISSN 0165-0327.

ROBINSON, J. T. et al. Integrative genomics viewer. **Nature Biotechnology,** v. 29, n. 1, p. 24-26, Jan 2011. ISSN 1087-0156.

ROCHA, C. H. L. et al. Synergism between the Antidepressant Sertraline and Caspofungin as an Approach to Minimise the Virulence and Resistance in the Dermatophyte *Trichophyton rubrum*. **J Fungi (Basel),** v. 8, n. 8, Aug 3 2022. ISSN 2309-608x.

RONCERO, C.; VÁZQUEZ DE ALDANA, C. R. Glucanases and Chitinases. **Curr Top Microbiol Immunol,** v. 425, p. 131-166, 2020. ISSN 0070-217X.

SATO, I. et al. The glutathione system of *Aspergillus nidulans* involves a fungus-specific glutathione S-transferase. **J Biol Chem,** v. 284, n. 12, p. 8042-53, Mar 20 2009. ISSN 0021-9258.

SIEBER, P. et al. Comparative Study on Alternative Splicing in Human Fungal Pathogens Suggests Its Involvement During Host Invasion. **Front Microbiol,** v. 9, p. 2313, 2018. ISSN 1664-302X.

SINGH, P.; AHI, E. P. The importance of alternative splicing in adaptive evolution. **Mol Ecol,** v. 31, n. 7, p. 1928-1938, Apr 2022. ISSN 0962-1083.

THORVALDSDOTTIR, H.; ROBINSON, J. T.; MESIROV, J. P. Integrative Genomics Viewer (IGV): high-performance genomics data visualization and exploration. **Brief Bioinform,** v. 14, n. 2, p. 178-92, Mar 2012. ISSN 1477-4054.

TREVINO-RANGEL, R. J. et al. In vivo evaluation of the antifungal activity of sertraline against *Aspergillus fumigatus*. **J Antimicrob Chemother,** v. 74, n. 3, p. 663-666, Mar 1 2019. ISSN 1460-2091.

TZELEPIS, K. et al. SRPK1 maintains acute myeloid leukemia through effects on isoform usage of epigenetic regulators including BRD4. **Nat Commun,** v. 9, n. 1, p. 5378, Dec 19 2018. ISSN 2041-1723.

VALSECCHI, I. et al. Role of Hydrophobins in *Aspergillus fumigatus*. **J Fungi (Basel),** v. 4, n. 1, Dec 24 2017. ISSN 2309-608x.

VILLANUEVA-LOZANO, H. et al. In vitro inhibitory activity of sertraline against clinical isolates of *Sporothrix schenckii*. **Rev Iberoam Micol,** v. 36, n. 3, p. 139-141, Jul-Sep 2019. ISSN 1130-1406.

VÁZQUEZ, J. et al. Melatonin Reduces Oxidative Stress Damage Induced by Hydrogen Peroxide in *Saccharomyces cerevisiae*. **Front Microbiol,** v. 8, p. 1066, 2017. ISSN 1664-302X.

VÊNCIO, R. Z. et al. BayGO: Bayesian analysis of ontology term enrichment in microarray data. **BMC Bioinformatics,** v. 7, p. 86, Feb 23 2006. ISSN 1471-2105.

WANG, Z.; GERSTEIN, M.; SNYDER, M. RNA-Seq: a revolutionary tool for transcriptomics. **Nat Rev Genet,** v. 10, n. 1, p. 57-63, Jan 2009. ISSN 1471-0056.

WATSON, N. A. et al. Kinase inhibition profiles as a tool to identify kinases for specific phosphorylation sites. **Nat Commun,** v. 11, n. 1, p. 1684, Apr 3 2020. ISSN 2041-1723.

WHITE, T. C. et al. Fungi on the skin: dermatophytes and *Malassezia*. **Cold Spring Harb Perspect Med,** v. 4, n. 8, Aug 1 2014. ISSN 2157-1422.

YAMADA, M. et al. Identification of a novel splice variant of heat shock cognate protein 70 after chronic antidepressant treatment in rat frontal cortex. **Biochem Biophys Res Commun,** v. 261, n. 2, p. 541-5, Aug 2 1999. ISSN 0006-291X.

ZHAI, B. et al. The antidepressant sertraline provides a promising therapeutic option for neurotropic cryptococcal infections. **Antimicrob Agents Chemother,** v. 56, n. 7, p. 3758-66, Jul 2012. ISSN 1098-6596.

ZHOU, Z.; FU, X. D. Regulation of splicing by SR proteins and SR protein-specific kinases. **Chromosoma,** v. 122, n. 3, p. 191-207, Jun 2013. ISSN 0009-5915.

Anexos de publicação

Anexo A

Journal of *Fungi*

MDPI

Article

The Antidepressant Sertraline Affects Cell Signaling and Metabolism in *Trichophyton rubrum*

Flaviane M. Galvão-Rocha [1], Carlos H. L. Rocha [1], Maíra P. Martins [1], Pablo R. Sanches [1], Tamires A. Bitencourt [1], Matthew S. Sachs [2], Nilce M. Martinez-Rossi [1] and Antonio Rossi [1,*]

[1] Department of Genetics, Ribeirao Preto Medical School, University of São Paulo, USP, Ribeirao Preto 14049-900, SP, Brazil
[2] Department of Biology, Texas A&M University, College Station, TX 77843-3258, USA
* Correspondence: anrossi@usp.br

Abstract: The dermatophyte *Trichophyton rubrum* is responsible for most human cutaneous infections. Its treatment is complex, mainly because there are only a few structural classes of fungal inhibitors. Therefore, new strategies addressing these problems are essential. The development of new drugs is time-consuming and expensive. The repositioning of drugs already used in medical practice has emerged as an alternative to discovering new drugs. The antidepressant sertraline (SRT) kills several important fungal pathogens. Accordingly, we investigated the inhibitory mechanism of SRT in *T. rubrum* to broaden the knowledge of its impact on eukaryotic microorganisms and to assess its potential for future use in dermatophytosis treatments. We performed next-generation sequencing (RNA-seq) to identify the genes responding to SRT at the transcript level. We identified that a major effect of SRT was to alter expression for genes involved in maintaining fungal cell wall and plasma membrane stability, including ergosterol biosynthetic genes. SRT also altered the expression of genes encoding enzymes related to fungal energy metabolism, cellular detoxification, and defense against oxidative stress. Our findings provide insights into a specific molecular network interaction that maintains metabolic stability and is perturbed by SRT, showing potential targets for its strategic use in dermatophytosis.

Keywords: RNA-seq; drug repositioning; dermatophyte; membrane damage; oxidative stress; ergosterol; sertraline; *Trichophyton rubrum*

Citation: Galvão-Rocha, F.M.; Rocha, C.H.L.; Martins, M.P.; Sanches, P.R.; Bitencourt, T.A.; Sachs, M.S.; Martinez-Rossi, N.M.; Rossi, A. The Antidepressant Sertraline Affects Cell Signaling and Metabolism in *Trichophyton rubrum*. *J. Fungi* **2023**, *9*, 275. https://doi.org/10.3390/jof9020275

Academic Editor: David S. Perlin

Received: 17 December 2022
Revised: 24 January 2023
Accepted: 8 February 2023
Published: 20 February 2023

1. Introduction

Dermatophytoses are skin infections caused by fungi. These dermatophytes are associated with keratinized tissues, such as skin, hair, and nails. Although dermatophytes do not usually cause deep lesions, the disease can progress to severe acute illness in hosts with poor immune protection [1]. *Trichophyton rubrum* is responsible for most onychomycosis cases in humans worldwide [2].

The number of antifungal agents available for the treatment of dermatophyte infections is limited. The most used drugs converge to a similar mechanism of action in fungal cells, targeting ergosterol biosynthesis. Consequently, intense selective pressure is exerted on clinical isolates, leading to the emergence of strains that are resistant to available drugs [3,4].

The development of new antifungal drugs is limited by the similarities between fungal and host cells, which restrict the number of cellular targets [4]. Furthermore, the time-consuming efforts and elevated costs required to achieve effective drugs engender the need to exploit alternatives for the management of fungal infections [4,5]. One approach is to evaluate the potential use of non-antifungal drugs as antifungals [6].

Numerous drugs used to treat non-infectious conditions such as inflammation, cardiovascular diseases, or depression are known to exhibit antimicrobial activities. The selective serotonin reuptake inhibitor (SSRI) sertraline (SRT), commonly used as an antidepressant, was revealed to have antifungal activity [7–10]. Furthermore, this drug interacts

synergistically in vitro with antifungals such as azoles, caspofungin, and amphotericin B, indicating its potential use as an adjuvant in treating fungal infections [11–15]. This synergistic association could decrease drug dosages and emerging drug resistance rates [6].

In the mammalian nervous system, SRT inhibits serotonin (5-hydroxytryptamine, 5-HT) reuptake, releasing serotonin into the synaptic cleft [16]. In addition, the drug enhances 5-HT synthesis by increasing the expression of tryptophan hydroxylase, the enzyme responsible for converting L-tryptophan to 5-HT [17]. SRT targets the serotonin transporter (5-HTT) responsible for 5-HT reuptake into presynaptic neurons in human cells. Interestingly, there is no conserved homolog of the 5-HT transporter in fungi, highlighting the occurrence of secondary targets for this drug [11]. However, the mechanisms underlying the antifungal activity of SRT remain unclear. It has been proposed that SRT intercalates into the phospholipid membranes of V-ATPase-acidified organelles [18]. Moreover, it is possible that the potent antifungal activity against *Cryptococcus neoformans* could also be driven by the inhibition of protein synthesis and/or other actions interfering with lipid metabolism [10,11].

Here, we evaluated the effects of sub-lethal doses of SRT against the dermatophyte *T. rubrum* through RNA-seq analysis. Our findings revealed changes in the comprehensive induction of the cellular antioxidant system, membrane transport-associated genes, and biosynthetic genes, resulting in changes in the cell membrane.

2. Materials and Methods

2.1. Strain and Culture Conditions for RNA-Seq Analysis

T. rubrum strain CBS118892 from the Westerdijk Fungal Biodiversity Institute (formerly CBS-KNAW Collections), The Netherlands, was maintained on malt extract agar (2% glucose, 2% malt extract, 0.1% peptone (*w/v*), pH 5.7). Conidial suspensions were obtained by flooding 21-day-old plates with sterile 0.9% NaCl, recovering the liquid, mixing by vortexing, and filtering through glass wool. We estimated the conidial concentration by counting in a Neubauer chamber. Approximately 1×10^6 conidia were inoculated into 100 mL Sabouraud dextrose broth (SDB; 2% (*w/v*) glucose, 1% (*w/v*) peptone) and incubated with agitation (120 rpm) at 28 °C for 96 h. Next, we aseptically transferred mycelia into new flasks containing 100 mL SDB media with 70 µg/mL of SRT hydrochloride (Cayman Chemical Co., Ann Arbor, MI, USA), corresponding to 70% of the minimal inhibitory concentration (MIC) [15], and in the absence of drugs (control). After 3 or 12 h of incubation at 28 °C with agitation, the resultant mycelia were collected, quick-frozen, and stored at −80 °C until RNA isolation.

2.2. RNA Isolation and cDNA Library Construction

Total RNA was isolated from ~100 mg mycelia using the Illustra RNAspin mini RNA isolation kit (GE Healthcare, Chicago, IL, USA). RNA concentrations were determined using a NanoDrop ND-1000 spectrophotometer (Thermo Fisher Scientific, Waltham, MA, USA). RNA quality was verified by agarose electrophoresis and an Agilent 2100 Bioanalyzer (Agilent Technologies, Santa Clara, CA, USA). Equal amounts of RNA from three independent biological replicates at each time point (3 and 12 h) were used for cDNA synthesis using the TruSeq RNA library kit (Illumina, San Diego, CA, USA) and sequenced using Illumina technology (HiSeq 2000 sequencer) according to the manufacturer's instructions. Paired-end reads were 150 bp in size.

2.3. Transcriptome Analysis

Raw read data obtained were filtered for quality control using the FastQC tool and trimmed using Trimmomatic [19] to remove adapters and Illumina-specific sequences. Trimmed paired-end reads from each sample were aligned to the reference genome using the STAR aligner [20]. We inspected the average coverage of transcripts and alignments using the Interactive Genomics Viewer (IGV) software [21]. We generated gene-level read

counts by STAR using the quantModeGeneCounts option. Differential expression was analyzed using the DESeq2 Bioconductor package [22].

After the above, the Benjamini–Hochberg correction was applied ($p < 0.05$) [23], and a cutoff threshold of ± 1.5 log2 fold change was set to reveal statistically significant expression differences (genes surpassing these thresholds are referred to as differentially expressed genes (DEG)) [24]. We functionally categorized them using Gene Ontology (GO) terms assigned by the Blast2GO algorithm. Highly represented categories were determined by enrichment analysis using the BayGO algorithm [25].

2.4. Data Analysis and Gene Selection

We predicted transporter-associated domain-containing proteins in the *T. rubrum* CBS 118892 genome sequence using the HMMER v3.1 b2 pipeline [26]. We built the hidden Markov model (HMM) utilizing a Pfam [27] multiple alignment-based search of 55 sequences corresponding to the ABC domain-containing proteins and another Pfam multiple alignment-based search of 192 sequences corresponding to the MFS (major facilitator superfamily) domain-containing proteins, both from different organisms (https://pfam.xfam.org/family/PF00005 and https://pfam.xfam.org/family/PF07690, respectively—accessed on 10 June 2022). The resulting models with epitopes of the consensus sequences of transporter-associated domain-containing proteins were used to search for homologs in *T. rubrum* protein sequences. In addition, we identified proteins using the keywords "transporter", "transcription factor", and "kinase" in Ensembl Fungi (https://fungi.ensembl.org). We compared the gene codes for specific proteins with the DEGs identified in RNA-seq.

2.5. cDNA Synthesis and RT-qPCR Analysis

We treated total RNA with DNase I (Sigma-Aldrich, Milwaukee, WI, USA) to remove residual genomic DNA and generate complementary DNA (cDNA) using a High-Capacity cDNA Synthesis Kit (Applied Biosystems, Foster City, CA, USA). We performed RT-qPCR with a StepOnePlus Real-Time PCR system (Applied Biosystems). Reactions were run in 12.5 µL with Power SYBR Green PCR Master Mix (Applied Biosystems), 70 ng template cDNA, and forward and reverse primers (Table S1). We used glyceraldehyde-3-phosphate dehydrogenase (*gapdh*) and DNA-dependent RNA polymerase II (*rpb2*) as internal controls [28]. Thermocycler conditions included an initial PCR step at 95 °C for 10 min, followed by 40 cycles at 95 °C for 15 s and 60 °C for 1 min. Data were obtained from three independent replicates. The $2^{-\Delta\Delta ct}$ relative expression quantification method was used to calculate gene responsiveness [29]. For RNA-seq validation, we used 3 h and 12 h without SRT as the reference samples. Statistical analyses were performed using a *t*-test followed by Tukey's post-hoc test using GraphPad Prism v. 5.1 software (GraphPad, La Jolla, CA, USA). A significance level of 95% was considered; therefore, the measures were statistically different at $p < 0.05$.

2.6. Quantitation of Ergosterol Content

The *T. rubrum* strain CBS118892 was cultivated on Sabouraud dextrose agar (SDA) for 17 days at 28 °C. The mycelia were transferred to 50 mL of SDB for 24 h at 28 °C with agitation (200 rpm). After this period, the mycelium was recovered, inoculated in 20 mL of SDA containing a sub-inhibitory concentration of SRT (6.25 µg/mL), ketoconazole (KTC, 4 µg/mL; Sigma-Aldrich), or amphotericin B (AMB, 1.25 µg/mL; Sigma-Aldrich), and incubated for 48 h at 28 °C, 200 rpm. Mycelia were also inoculated in SDA without drugs (control). The resulting mycelia were filtered, the dry weight was measured, and the ergosterol content was determined following the protocol described by Arthington-Skaggs et al. [30], with modifications [31]. Briefly, 3 mL of 25% alcoholic potassium hydroxide solution was added to the dried mycelia and mixed by vortexing for 5 min. We incubated the mycelium at 85 °C for 1 h. The tubes were cooled to room temperature and sterile distilled water (1 mL) and 3 mL of *n*-heptane were added, followed by vigorous vortex mixing for 5 min. The heptane layer was transferred to a clean polystyrene tube, and a 20 µL aliquot

was diluted five-fold in 100% ethanol and scanned in a spectrophotometer between 230 and 300 nm. All assays were performed in triplicate. Both 24(28)-dehydroergosterol (a sterol pathway intermediate) and ergosterol absorb at 281.5 nm, but 24(28)-dehydroergosterol also absorbs at 230 nm, which was subtracted from the absorbance obtained at 281.5 nm [31]. We calculated the reduction in ergosterol content as the difference in the treatments compared to the growth control samples based on a standard curve of various concentrations of standard ergosterol (Sigma-Aldrich). The results are expressed as a percentage of ergosterol content compared with the growth control. One-way ANOVA was used to determine the amount of ergosterol in the control with the treatments, followed by Tukey's post-hoc test. Statistical significance was set at $p < 0.05$, and Prism v. 5.1 software was used to generate graphs and perform statistical analyses.

3. Results

3.1. Transcriptional Profiling of Trichophyton rubrum Challenged by SRT

We used next-generation sequencing to comprehensively analyze the *T. rubrum* global transcriptome in response to sub-lethal doses of the antidepressant SRT at two different time points. Approximately 535.5 million high-quality reads of 150-bp paired-end sequences were obtained (Table S2). In response to SRT exposure, 169 and 1197 genes were modulated at 3 and 12 h, respectively, when compared to the expression levels of the control. Three hundred seventy-two genes were modulated at both time points, totaling 1738 genes that were responsive to SRT (Figure 1A). SRT differentially upregulates more genes than it represses after 3 h of treatment. This profile was inverted at 12 h exposure with a less expressive difference between up- and downregulated genes compared to the 3 h time point (Figure 1B). We list the products of all genes modulated in response to SRT for each drug exposure time in Table S3 and present the most significantly up- and downregulated genes in Table 1.

A

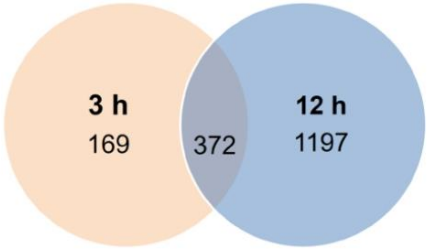

B

Condition	Total genes	Up-regulated	Down-regulated
3 h	541	452	89
12 h	1569	768	801

Figure 1. SRT-induced differential gene expression. (**A**) Venn diagram presenting the time-dependent differential expression of 1738 genes after exposure to sub-lethal dose of SRT for 3 h and 12 h compared to the control samples without SRT. (**B**) Total up- and downregulated genes in each experimental condition.

Table 1. The most significantly up- or downregulated genes.

Upregulated		log_2 (Fold Change)	
ID	**Gene Product Name**	**3 h**	**12 h**
TERG_06548	hypothetical protein (oxidoreductase, *M. canis*)	10.86	11.80
TERG_00785	endoplasmic reticulum vesicle protein 25	8.60	
TERG_01782	hypothetical protein	8.34	9.02
TERG_00010	amidase family protein (*T. verrucosum*)		8.72
TERG_03829	FAD binding domain-containing protein (*T. equinum*)		6.92
TERG_04952	multidrug resistance protein (*T. equinum*)	6.87	7.69
TERG_08954	hypothetical protein	6.61	
TERG_06106	sulfate permease 2 (*T. tonsurans*)		6.45
TERG_08751	ABC multidrug transporter, putative (*A. benhamiae*)	5.82	6.33
TERG_01543	S-adenosylmethionine (SAM)-dependent methyltransferase (*M. gypseum*)	5.42	7.48
TERG_08041	aminotransferase, putative (*A. benhamiae*)	5.42	
TERG_04937	alpha/beta hydrolase (*T. equinum*)	5.41	6.40
TERG_07830	hypothetical protein	5.41	8.22
Downregulated		**log_2 (Fold Change)**	
ID	**Gene Product Name**	**3 h**	**12 h**
TERG_02653	hypothetical protein	−6.21	
TERG_02652	O-methyltransferase, putative (*T. verrucosum*)	−4.91	
TERG_04066	filamentation protein (Rhf1), putative (*T. verrucosum*)	−4.67	
TERG_02959	hypothetical protein	−4.16	
TERG_05816	hypothetical protein	−3.74	
TERG_02650	NmrA family protein (*T. equinum*)	−3.56	
TERG_12339	hypothetical protein	−3.31	
TERG_01619	toxin biosynthesis protein (Tri7), putative (*T. verrucosum*)	−3.20	
TERG_00490	erythromycin esterase (*T. tonsurans*)	−3.13	
TERG_03826	hypothetical protein	−2.77	
TERG_02959	hypothetical protein		−5.90
TERG_11536	hypothetical protein		−5.69
TERG_11771	hypothetical protein		−5.51
TERG_04742	hypothetical protein		−5.29
TERG_01148	hypothetical protein		−5.26
TERG_00490	erythromycin esterase (*T. tonsurans*)		−5.24
TERG_03919	phytoene dehydrogenase (*T. equinum*)		−5.20
TERG_01599	hypothetical protein		−4.95
TERG_12035	NB-ARC and TPR domain protein (*A. benhamiae*)		−4.87
TERG_11963	hypothetical protein		−4.79

The functional categorization of the modulated genes was performed using Blast2Go, which revealed the molecular mechanisms by which *T. rubrum* senses and responds to the challenge of SRT presence (Figure 2). Gene function analysis using GO enriched mainly molecular function terms after 3 h of treatment. Genes associated with catalytic and hydrolase activities and those related to transmembrane transport were upregulated. The oxidoreductase activity induces or represses many genes after 3 h of drug exposure (Figure 2A). The upregulated membrane-associated genes and downregulated genes associated with the oxidation–reduction process increased at 12 h compared to those after 3 h of treatment. The terms related to translation were all inhibited at the 12 h time point. The number of genes associated with hydrolase activity and transmembrane transport increased compared to those in the 3 h condition, remaining induced in response to 12 h of SRT exposure (Figure 2B).

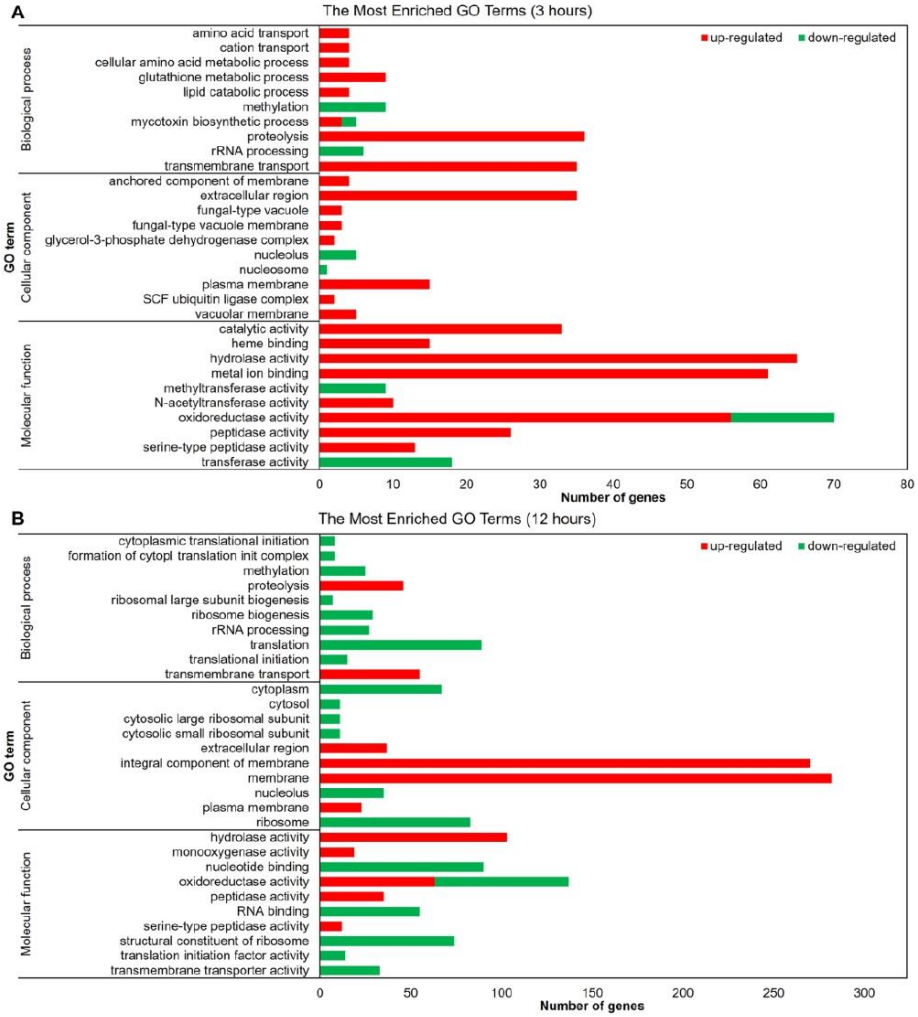

Figure 2. Gene ontology-based functional categorization of the most representative differentially expressed genes. The red and green bars indicate the number of up- and downregulated genes modulated by *T. rubrum* in response to SRT ($p < 0.05$). Results show genes after (**A**) 3 h and (**B**) 12 h drug exposure compared to the control without SRT.

To validate the RNA-seq results, we randomly selected 15 genes from the differentially expressed genes related to processes such as catalytic activity, transferase activity, and transmembrane transport (Figure 3). The RT-qPCR data and corresponding RNA-seq values obtained from biological replicates (Table 2) confirmed the reliability of the results (Pearson's correlation, $r > 0.92$, $p < 0.001$).

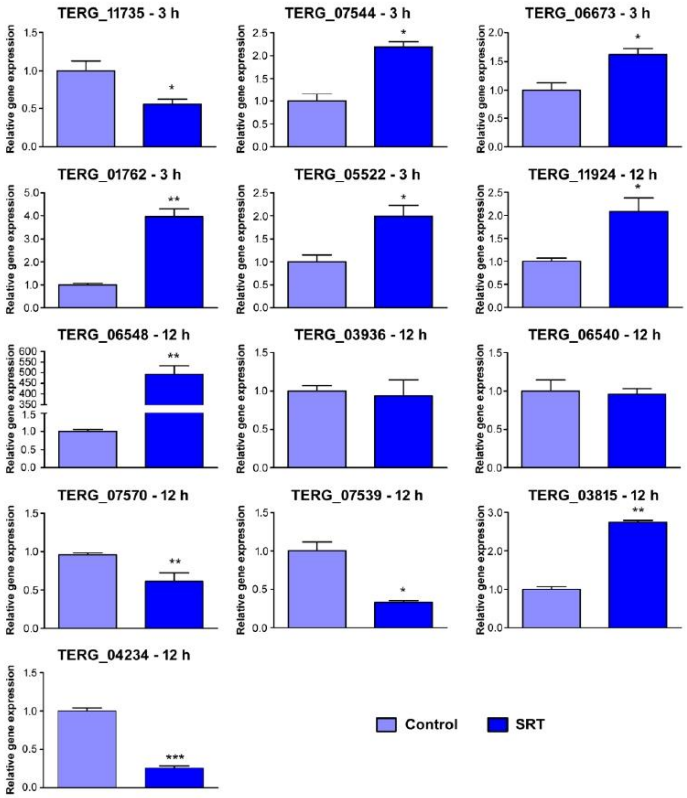

Figure 3. Validation by RT-qPCR of 15 genes differentially expressed in response to SRT exposure. Log2 fold change at each time point represents gene expression level changes at each time point. Expression levels are relative to the control without SRT. Asterisks indicate the statistical significance determined by the *t*-test followed by Tukey's post-hoc test (* $p < 0.05$; ** $p < 0.01$; *** $p < 0.001$). The identification of each gene is listed in Table 2.

Table 2. Comparison of the gene expression levels assayed by RNA sequencing and RT-qPCR.

ID	Condition	Gene Product Name	RNA-seq	RT-qPCR
TERG_11735	3 h	microtubule-associated protein (*T. tonsurans*)	−2.4	−1.41
TERG_07544	3 h	lipase (*T. tonsurans*)	2.02	1.13
TERG_06673	3 h	pachytene checkpoint component Pch2 (*T. tonsurans*)	2.0	0.70
TERG_01762	3 h	sulfite reductase (NADPH) hemoprotein beta-component	2.14	1.99
TERG_05522	3 h	lysophospholipase (*T. equinum*)	1.55	0.97
TERG_11924	12 h	ankyrin repeat protein (*T. tonsurans*)	3.85	1.06
TERG_06548	12 h	hypothetical protein (oxidoreductase, *M. canis*)	11.8	8.63
TERG_03936	12 h	CAMK protein kinase	−4.19	−0.09
TERG_06540	12 h	glutathione S-transferase (*T. tonsurans*)	−3.44	−0.07
TERG_07570	12 h	G-protein signaling regulator putative (*T. verrucosum*)	−3.47	−0.70
TERG_04234	12 h	hydrophobin putative (*T. verrucosum*)	−3.41	−1.98
TERG_07539	12 h	multidrug resistance protein (*T. tonsurans*)	−1.72	−1.61
TERG_03815	12 h	subtilisin-like protease 3	1.78	1.46

3.2. SRT Interferes with T. rubrum Signaling and Regulation

Few kinase- and transcription factor-coding genes were modulated in response to SRT. The *T. rubrum* kinome (protein kinase superfamily members) is predicted to comprise 170 coding genes [32]. In our results, 81 kinases were modulated (Figure S1), coding chiefly for serine/threonine–protein kinases and kinases belonging to the CMGC (cyclin-dependent kinases (CDKs)) group. Among the 15 serine/threonine–protein kinase genes modulated, only TERG_07509 was repressed after 12 h of treatment. Among the eight CMGC-type kinases modulated by SRT exposure, TERG_12259 (CMGC/CLK protein kinase), TERG_05893 (CMGC protein kinase), and TERG_07061 (CMGC/SRPK protein kinase) were repressed. The latter two belong to the SRPK family and are active in the regulation of splicing by phosphorylation [33]. SRPKs act synergistically with CLK protein kinases, a family of Cdc2-like kinases that can auto-phosphorylate tyrosine residues, but phosphorylate their substrates exclusively on serine/threonine residues. The associated activity of SRPKs and CLK proteins phosphorylates SR (serine/arginine-rich) proteins, which mediate the phosphorylation of SR proteins and direct pre-mRNA splicing [34].

The comparative evaluation between anthropophilic and zoophilic dermatophytes revealed that only kinases and transcription factor Interpro (IPR) domain families were enriched in anthropophilic dermatophytes, suggesting that the modulation of signaling pathways and transcriptional regulation are key factors in host specificity [32]. Here, the reduced number of transcription factors modulated in response to SRT challenge (Figure S2) suggests the restrained infective potential of *T. rubrum* under SRT exposure. Most modulated transcription factors code for zinc finger domain-containing proteins and are preferentially repressed, mainly after 12 h of SRT exposure (including TERG_02532, TERG_01042, and TERG_05497), for which transcript accumulation increased over time.

3.3. Cell Wall and Membrane Structure Are Affected by SRT

SRT modulates the expression of genes associated with the formation of glucans and chitins, which are important structural polysaccharides in the fungal cell wall. These genes include endoglucanases (TERG_08178, TERG_03353, TERG_06189, and TERG_04268), chitinases (TERG_05626 and TERG_05625), and chitin synthases (TERG_12318 and TERG_12319). While glucan-related genes were predominantly induced after 12 h of treatment, chitin-associated genes were repressed after 12 h of SRT challenge. The hydrophobin-coding gene (TERG_04234) was repressed after only 12 h of SRT exposure.

Furthermore, SRT was found to downregulate the expression of genes encoding components of the ergosterol biosynthetic pathway in *T. rubrum*. After 12 h, the genes that code for diphosphomevalonate decarboxylase (*erg*19; TERG_07616), C-8 sterol isomerase (*erg*1; TERG_06755), c-14 sterol reductase (*erg*24; TERG_04382), C-4 methylsterol oxidase (*erg*25; TERG_08545), ergosterol biosynthesis protein *erg*28 (TERG_04740), and sterol 24-C-methyltransferase/Delta (24(24[1]))-sterol reductase (*erg*4; TERG_06528/TERG_03102) were downregulated. The squalene epoxidase-coding gene (*erg*1; TERG_05717) was repressed after 3 and 12 h. The ergosterol dosage confirmed the inhibition of the biosynthetic pathway activity (Figure 4).

SRT, a cationic amphiphilic drug (CAD), causes drug-induced phospholipidosis (DIP) during excessive phospholipid storage within the lysosomes [18]. We observed the modulation of sphingomyelinase D (TERG_01406), lysosomal phospholipase A2 (TERG_03747), B (TERG_05522), and D (TERG_05303), and upregulation of secretory phospholipase A2 (TERG_00127).

Exposure to SRT led to the accumulation of transcripts of genes related to membrane transport. The number of modulated genes increased over time. Most downregulated genes at both time points are MFS transporters (3 of the 4 downregulated genes after 3 h, and 25 genes among the 38 downregulated genes after 12 h of SRT challenge). Among the upregulated genes, 23 remained upregulated after 3 and 12 h of drug challenge (Figure S3).

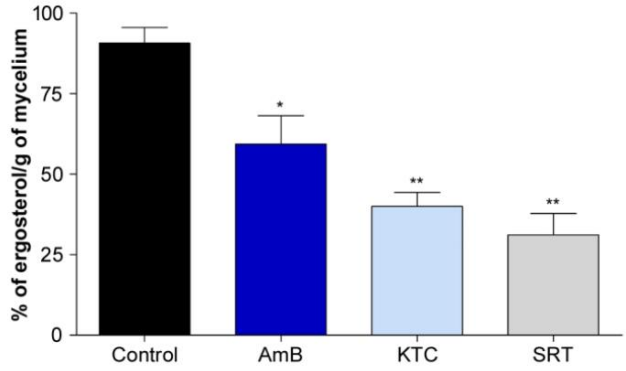

Figure 4. Effect of SRT on ergosterol content as a percentage of the wet weight of *T. rubrum*. Absence (negative control) and presence of amphotericin B (AMB, 1.25 µg/mL), ketoconazole (KTC, 4 µg/mL) (positive controls), and SRT (6.25 µg/mL). We tested the antifungals AMB and KTC at the minimal inhibitory concentration and the antidepressant SRT at a sub-inhibitory concentration. Asterisks represent statistical difference * $p < 0.05$ and ** $p < 0.01$ related to the control.

3.4. SRT Affects the Transcription of Oxidative Stress Genes in T. rubrum

Through upregulating the glutathione S-transferase (GST) genes (TERG 03390, TERG 04960, TERG 01405, TERG 07326, TERG 02041, TERG 00579, TERG 08208, and TERG 05135), *T. rubrum* could have an altered oxidative stress response when exposed to SRT. These genes participate in the sequestration of endogenous or xenobiotic compounds [35]. In the presence of SRT, two other GST genes (TERG_06540 and TERG_06578), as well as genes encoding catalase A (TERG_01252) and Fe-superoxide dismutase (TERG_04819), were downregulated. Additionally, SRT upregulated the gene encoding thioredoxin reductase (TERG_08849) and downregulated the thioredoxin gene (TERG_05849). Thioredoxins (TRX) are small ubiquitous redox proteins that play key roles in redox signaling and oxidative stress responses. The genes responsible for the conversion of melatonin into two metabolites, 6-hydroxymelatonin and N-acetyl-N-formyl-5-methoxykynuramine, were also upregulated by SRT (Figure 5). Finally, the most induced gene at both time points (TERG_06548) was an oxidoreductase ortholog identified in *Microsporum canis*.

3.5. Effect of SRT on T. rubrum Metabolism

SRT apparently interferes with the primary metabolism of *T. rubrum*. While genes involved in glycolysis are repressed, the genes involved in the glyoxylate cycle, ethanol and glycerol biosynthesis, and glycogen debranching are induced. The drug makes *T. rubrum* deviate from standard carbon metabolism to alternative pathways based on gene expression patterns (Figure 6). This repressive effect on glycolysis pathway genes counteracts the initial step performed by hexokinase (TERG_03229), which is induced. Metabolic reprogramming induced the expression of glyoxylate cycle-associated genes (TERG_11639, TERG_01281, TERG_08288, and TERG_08287) and glycerol biosynthesis genes (TERG_07273, TERG_12172, and TERG_12173). Additionally, SRT modulated ethanol- and glycerol-catabolism-related genes and induced a debranching enzyme (TERG_06681). This enzyme facilitates the breakdown of glycogen, which serves as a store of glucose.

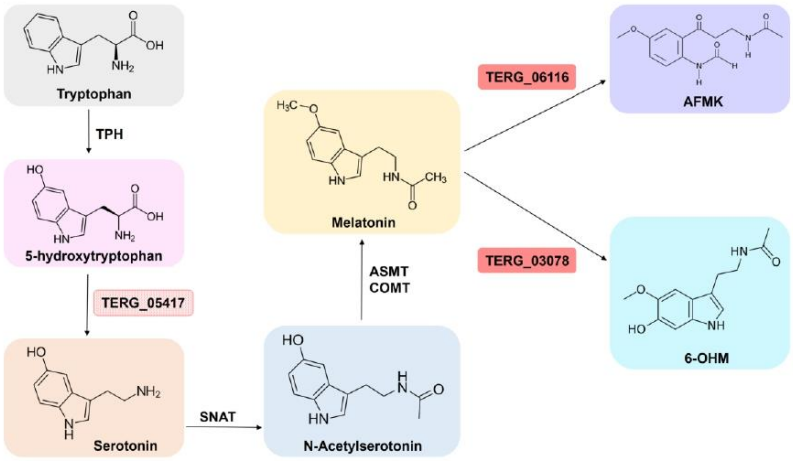

Figure 5. The biosynthetic pathway involved in synthesis of melatonin from tryptophan. Enzymatic steps from tryptophan to melatonin and the correlated metabolites. TPH: tryptophan hydroxylase; SNAT: serotonin N-acetyltransferase; ASMT: acetylserotonin O-methyltransferase; COMT: caffeic acid 3-O-methyltransferase; AFMK: N-acetyl-N-formyl-5-methoxykynuramine; 6-OHM: 6-hydroxymelatonin. The red genes are upregulated by *T. rubrum* in response to SRT. In pink, transcript accumulation is slightly below the log2 fold threshold (corresponding to 1.36 fold). Figure adapted from [36,37].

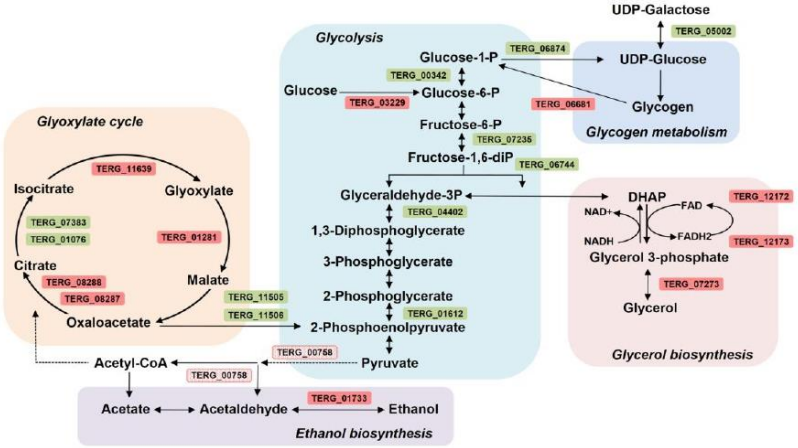

Figure 6. Schematic overview of the effect of SRT on the metabolism of *Trichophyton rubrum*. Genes induced (red) or repressed (green) considering log2 fold threshold ± 1.5. In pink, transcript accumulation is slightly below the log2 fold threshold (corresponding to 1.47 fold). UDP-galactose: uridine diphosphate galactose; UDP-glucose: uridine diphosphate glucose; DHAP: dihydroxyacetone phosphate.

4. Discussion

In addition to its use as an antidepressant, SRT has also been explored for other therapeutic applications. In vitro and in vivo studies have demonstrated its potential application in treating osteomyelitis infection [38] and cancer [39]. Furthermore, SRT presents antiparasitic [40], antibacterial [41], and antifungal activities against various pathogenic fungi, including *C. neoformans* [10,11], *Aspergillus fumigatus* [7], *Trichosporon asahii* [12], *Sporothrix schenckii* [9], and *T. rubrum* [15]. Through a drug repurposing approach, novel therapeutic options can rapidly enter clinical practice, as their safety and pharmacokinetics have been validated previously in patients. SRT is also effective alone or as an adjuvant therapeutic agent against fungal biofilm formation in vitro [15]. The synergistic effects of SRT combined with antifungals such as amphotericin B, caspofungin, or fluconazole have been documented in vitro [11–13,15]. Despite the potential therapeutic use of SRT in association with these drugs to control fungal infections, some are preferentially used intravenously.

4.1. SRT Affects Cell Signaling and Transcription in T. rubrum

Enrichment of the serine/threonine protein kinase domain (IPR002290), the catalytic domain of the protein kinase tyrosine, and the Zn(2)- C(6) fungal-like DNA-binding domain (IPR001138) has been reported in fungal anthropophilic organisms [32]. The transcriptional profile of *T. rubrum* after being challenged with SRT provided evidence that both kinases and transcriptional regulation-associated genes, when modulated, were preferentially induced, mainly at 12 h.

Phosphorylation by protein kinases is a critical mechanism that tunes cell activities, such as proliferation, metabolism, apoptosis, and gene expression. Cells possess thousands of kinases that phosphorylate specific sites in response to precise and controlled interactions [42]. The observed induced kinase modulation resulting from SRT exposure suggests the activation of specific signaling pathways. Our results indicate the activation of splicing events through the reversible phosphorylation of SR proteins. These phosphorylation events are dependent on both the SRPK and CLK families. The SRPK family of kinases phosphorylates SR proteins, promoting the nuclear import of SR proteins. Once in the nucleus, SR proteins may be further phosphorylated by the CLK family of kinases, which comprises a sequence of events essential for pre-mRNA splicing [33].

Conversely, the restricted number of protein kinase-coding genes modulated, considering the predicted whole kinome, implies the putative deactivation of other pathways. This deactivation strategy may represent a demand for energy conservation supported by, for example, the downregulation of ribosome biogenesis (Figure 2). Ribosome biogenesis is energetically expensive for cells. Consequently, unfavorable environmental conditions inhibit such processes [43].

Transcription factors are also associated with host specificity in dermatophytes [32]. We observed that a small number of transcriptional regulators were modulated, most of which had a zinc finger structural motif. Cells use transcription factors to dictate gene expression rates and regulate transcriptional networks [44]. Considering the relevance of transcription factor regulation and its key role in anthropophilic dermatophyte pathogenesis, we assume that drug challenge directly regulates transcription, possibly limiting energy expenditure under unfavorable conditions.

4.2. SRT Disturbs T. rubrum Cell Wall and Membrane

The fungal cell wall is a rigid layer with high plasticity that is essential for maintaining intracellular osmotic pressure [45]. β-1,3-glucan, chitin, and glycoproteins are primarily responsible for interactions between the cell and the environment. This wall is associated with a cell membrane that is predominantly composed of glycerophospholipids, sterols, and sphingolipids. Several molecules that form cell walls and membranes are exclusive to fungi and constitute suitable targets for antifungal development [45–47]. SRT exposure affects the expression of hydrolytic enzyme-coding genes in *T. rubrum*, which may contribute to changes in the cell wall structure.

Additionally, the repression of a beta-1,6 glucan synthetase that acts as a glycosidic linker suggests an imposed instability in cell wall assembly [48]. The overall repressive effects of SRT on the transcript levels for chitin synthases and chitinases may function as a compensatory mechanism to maintain cell wall integrity. This modulatory profile is similar to the effects of echinocandin antifungal agents on fungal cells. Echinocandins target the β-1,3-glucan synthase gene, deplete the glucan content of the cell wall, and increase chitin content.

Genes associated with ergosterol biosynthesis were downregulated after 12 h exposure to SRT, revealing that SRT affects plasma membrane properties. Moreover, SRT reduced ergosterol levels compared with amphotericin B and ketoconazole, which were used as positive controls (Figure 4). Amphotericin B complexes with ergosterol [49], whereas ketoconazole is a potent inhibitor of ergosterol biosynthesis [3]. Ergosterol modulates fluidity and permeability, interfering with water penetration [50]. The resultant alteration in the plasma membrane, together with the differential modulation of cell-wall-associated genes, suggests the occurrence of osmotic stress with alterations in the ergosterol composition of lipid bilayers, providing insights into the antifungal activity of SRT against *T. rubrum*.

Phospholipase A_2 and sphingomyelinase D activities are downregulated after 12 h treatment with SRT. Lysosomal phospholipase A_2 inhibition robustly correlates with drugs causing phospholipidosis [51], whereas the enzyme acid sphingomyelinase has been investigated as a potential target for antidepressant action [52]. Conversely, phospholipase B is upregulated at the initial SRT exposure, and phospholipase D is upregulated over time. Phospholipase B has hydrolase activity that cleaves fatty acids from phospholipids and lysophospholipids [53]. Phospholipase D comprises enzymes responsible for generating phosphatidic acid (PA), a putative secondary messenger implicated in the regulation of vesicular trafficking [54]. We observed that SRT also modulated genes involved in vesicular trafficking, including the induction of V-SNARE-coding genes (TERG_06294, TERG_07174) and the endoplasmic reticulum vesicle protein (TERG_00785) 25,388-fold induced after 3 h (log2 = 8.6). The secretory system of *T. rubrum* is essential for pathogenesis. Several keratinolytic enzymes are involved in the breakdown of keratin molecules, which may be assisted by ammonia and urea secretion [55]. The extra-vesicular content of *T. rubrum* is still not well understood. However, the vesicles of the dermatophyte *Trichophyton interdigitale* modulate the host immune response [56].

Besides affecting the cell wall structure and composition, global transcriptional analysis in response to SRT demonstrated the induction of drug resistance genes, mainly of the MFS genes, as a cellular stress response. The MFS is one of the largest groups of secondary active transporters and plays multiple roles in transporting a broad range of substrates, including sugars, amino acids, and drugs. The overall upregulated profile suggests a detoxification activity that increases with time since this family of proteins includes those encoding drug resistance transporters. However, at the 12 h time point, the downregulation of specific genes could represent an attempt to retain molecules such as phosphate (TERG_05891; MFS phosphate transporter) or monosaccharides (TERG_12194, TERG_04308; MFS sugar transporter), aiming to overcome the toxic drug effects.

4.3. SRT Overbalances Oxidative Stress Response

After 3 h of exposure to SRT, *T. rubrum* induced the expression of glutathione S-transferase genes to overcome its toxic effects. GSTs are small cytosolic proteins that contain a redox-active sulfhydryl group and are involved in cellular detoxification. Xenobiotics and endogenous products of oxidative stress are conjugated to glutathione (GSH) and secreted through vacuoles [57]. Endogenous toxic metabolites are removed through GSH-dependent detoxification processes. Thus, it confers protection against formaldehyde produced by methanol metabolism or against methylglyoxal, a byproduct of glycolysis [58,59]. Drug interactions with GSTs also facilitate their detoxification through GSH conjugation [60].

However, after 12 h of drug exposure, the downregulation of two glutathione transferase genes may reduce the efficiency of xenobiotic extrusion. Simultaneously, SRT down-

regulates Fe superoxide dismutase and catalase A genes, which neutralize reactive oxygen species (ROS).

The genes encoding thioredoxin and thioredoxin reductase were oppositely modulated after 12 h of SRT exposure. The thioredoxin/thioredoxin reductase system (Trx/TrxR) confers redox homeostasis to fungal cells [61]. Because SRT downregulates TrxR, the control of the cellular redox balance remains compromised. In *A. fumigatus* and *C. neoformans*, the TrxR-encoding gene is essential for growth under in vitro conditions and shows weak homology to its human ortholog, making it a potential antifungal target [60,62].

Saccharomyces cerevisiae subjected to oxidative stress induced by H_2O_2 shows increased *TRX* transcription; melatonin, an antioxidant agent, partially mitigates oxidative stress by enhancing *TRX* mRNA accumulation in cells exposed to H_2O_2 [63]. Here, the upregulation of the genes encoding the enzymes responsible for the conversion of melatonin into its metabolites indicates a decrease in melatonin availability (Figure 5), followed by the upregulation of the *Trx* gene and the downregulation of *TrxR*. These data support the speculated dependency between *Trx* and melatonin availability, suggesting the counterbalanced expression of the thioredoxin/thioredoxin reductase system under experimental conditions.

In humans, SSRI drugs increase serotonin levels in synaptic spaces. Based on our data, SRT increased in *T. rubrum* transcripts of the gene encoding an aromatic-L-amino acid decarboxylase (EC 4.1.1.28) slightly below the log2 fold threshold (1.36 fold) (Figure 5). This enzyme catalyzes the conversion of 5-hydroxytryptophan to serotonin [36,37]. In *Aspergillus* spp., serotonin can directly kill fungi in vitro [64].

4.4. SRT Imposes Dynamic Metabolic Modulation

The overall profile showed flexibility in metabolic modulation in response to the toxic effect of SRT, activating alternative carbon metabolism. In general, microorganisms deplete preferred nutrients such as glucose by activating a regulatory cascade that represses the consumption of alternative carbon sources such as maltose, galactose, or ethanol [65]. The induction of a glycogen debranching enzyme and sugar transporters indicates the cellular effort to release glucose through glycogen degradation in response to energy deficiency. In our results based on analyses of transcript levels, although glucose is available (at least through glycogen metabolism) and the enzyme hexokinase is induced, activating the initial step of glycolysis that is responsible for the phosphorylation of glucose by ATP to glucose-6-P, the glycolytic fluxes are not directed downward toward the synthesis of two 2-phosphoenolpyruvate molecules. Carbon catabolite repression (CCR) is a mechanism that handles the utilization of an energy-efficient and readily available carbon source preferentially over a relatively less easily degradable carbon source. This mechanism helps microorganisms to obtain the maximum amount of glucose to provide carbon for biosynthetic processes [66]. We hypothesize that *T. rubrum* triggers a different strategy in response to SRT challenge, overcoming CCR and redirecting gene expression patterns, activating genes responsible for the catabolism of less favored carbon sources. A glucose reservoir may, somehow, counteract the harmful effects caused by SRT exposure.

SRT treatment resulted in the repression of genes encoding glycolytic enzymes and an increase in the transcript levels of genes involved in alternative carbon utilization pathways, including the glyoxylate cycle. The induction of isocitrate lyase (TERG_11639) and malate synthase, glyoxysomal (TERG_01281) at the 3 h time point, and ATP-citrate synthases (TERG_08288/7) after 12 h drug exposure show the anabolic activity of the glyoxylate cycle counterbalancing glycolysis downregulation. The induction of the same isocitrate lyase (TERG_11639) at 48 and 96 h of *T. rubrum* incubation in keratin as the sole carbon source [55], coupled with the repression of genes related to glycolysis, suggests the promotion of a virulence response under both conditions. Glyoxylate cycle activation is directly associated with fungal pathogenicity [67,68]. Specifically, isocitrate lyase is a key enzyme in the glyoxylate cycle [69]. Our results suggest that the metabolic flexibility

observed in *T. rubrum* in vitro presumably contributes to its fitness and pathogenicity in vivo.

Based on transcriptional profiling, we hypothesize that SRT induced ethanol metabolism via alcohol dehydrogenase activity, and glycerol metabolism via glycerol kinase modulation. Transcript accumulation of pyruvate decarboxylase (TERG_00758) slightly below the log2 fold threshold (corresponding to 1.47 fold) suggests the enzymatic catalysis of pyruvic acid to acetaldehyde and the subsequent ethanol production. Pyruvate decarboxylase catalyzes the decarboxylation of pyruvate to acetaldehyde with the release of carbon dioxide and is a key enzyme in ethanol fermentation [70]; thus, it directs the metabolic activity of *T. rubrum* to different alternative carbon pathways in response to SRT exposure.

5. Concluding Remarks, Challenges, and Perspectives

The limited number of antifungals available in the market and the increase in antifungal resistance highlight the urgent need for new antifungals with new targets. This approach requires detailed knowledge of the basic biology of the organism and intracellular processes essential for its growth and survival in the human host. Here, we assessed the transcriptional profile of the dermatophyte *T. rubrum*, focusing on the mechanisms activated to counteract the antifungal activity of SRT. The repositioning of SRT as an antifungal drug seems to be reliable from a molecular perspective. This drug targets important molecular events and metabolic pathways. With our results, it was possible to perceive the depth of the complexity of the regulatory systems that operate to restore damage but that can be useful to direct innovative strategies focusing on the weaknesses of dermatophytes, taking advantage of well-tolerated drugs for human use. SRT challenge analysis provided clues to understand the response and adaptive mechanisms of *T. rubrum* to drug exposure. Although its clinical use as an antifungal agent is promising, further studies are needed to validate our findings.

Supplementary Materials: The following supporting information can be downloaded at: https://www.mdpi.com/article/10.3390/jof9020275/s1, Supplementary Figure S1. Kinase-related genes modulated in response to SRT. Supplementary Figure S2. Transcription-factor-related genes modulated in response to SRT. Supplementary Figure S3. *Trichophyton rubrum* membrane transporter genes modulated in response to SRT. Supplementary Table S1. List of primers used in RT-qPCR assays. Supplementary Table S2. General features of RNA-seq reads mapped to the *Trichophyton rubrum* reference genome. Supplementary Table S3. *Trichophyton rubrum* genes modulated in response to SRT exposure at each time point.

Author Contributions: N.M.M.-R. and A.R. designed the project. F.M.G.-R. and C.H.L.R. performed the laboratory experiments. T.A.B. and M.P.M. helped with some laboratory experiments and assisted in RNA-seq construction. P.R.S. performed the bioinformatics analyses. F.M.G.-R., C.H.L.R., P.R.S. and M.P.M. composed the figures. F.M.G.-R., M.P.M. and A.R. wrote the manuscript. N.M.M.-R. and A.R. provided funds, supervised the study, and edited the manuscript. M.S.S. discussed the results and edited the manuscript. All authors have read and agreed to the published version of the manuscript.

Funding: This work was supported by research grants from the following Brazilian funding agencies: São Paulo Research Foundation (FAPESP; Grant No. 2019/22596-9, and Fellowships No. 2018/11319-1 to M.M. and No. 2015/23435-8 to T.B.), National Council for Scientific and Technological Development (CNPq; Grant Nos. 307871/2021-5 and 307876/2021-7), Coordenação de Aperfeiçoamento de Pessoal de Nível Superior (CAPES; Finance Code 001), and Fundação de Apoio ao Ensino, Pesquisa e Assistência (FAEPA).

Institutional Review Board Statement: The Ethics Committee of the University Hospital of Ribeirão Preto Medical School, USP, Brazil (HCFMRP-USP) (Protocol No. 4.278.367/2020), approved this study.

Informed Consent Statement: Not applicable.

Data Availability Statement: We deposited RNA-sequencing (RNA-seq) data in the Gene Expression Omnibus (GEO) database under accession number GSE218521.

Acknowledgments: We thank V. M. de Oliveira, M. Mazucato, and M. D. Martins for the technical assistance.

Conflicts of Interest: The authors declare no conflict of interest.

References

1. Rouzaud, C.; Hay, R.; Chosidow, O.; Dupin, N.; Puel, A.; Lortholary, O.; Lanternier, F. Severe Dermatophytosis and Acquired or Innate Immunodeficiency: A Review. *J. Fungi* **2015**, *2*, 4. [CrossRef] [PubMed]
2. Piraccini, B.M.; Alessandrini, A. Onychomycosis: A Review. *J. Fungi* **2015**, *1*, 30–43. [CrossRef] [PubMed]
3. Martinez-Rossi, N.M.; Peres, N.T.; Bitencourt, T.A.; Martins, M.P.; Rossi, A. State-of-the-art Dermatophyte infections: Epidemiology aspects, pathophysiology, and resistance mechanisms. *J. Fungi* **2021**, *7*, 629. [CrossRef] [PubMed]
4. Martinez-Rossi, N.M.; Bitencourt, T.A.; Peres, N.T.A.; Lang, E.A.S.; Gomes, E.V.; Quaresemin, N.R.; Martins, M.P.; Lopes, L.; Rossi, A. Dermatophyte Resistance to Antifungal Drugs: Mechanisms and Prospectus. *Front. Microbiol.* **2018**, *9*, 1108. [CrossRef]
5. Rossi, A.; Martins, M.r.P.; Bitencourt, T.A.; Peres, N.T.A.; Rocha, C.H.L.; Rocha, F.M.G.; Neves-da-Rocha, J.o.; Lopes, M.E.R.; Sanches, P.R.; Bortolossi, J.C. Reassessing the use of undecanoic acid as a therapeutic strategy for treating fungal infections. *Mycopathologia* **2021**, *186*, 327–340. [CrossRef]
6. Zhang, Q.; Liu, F.; Zeng, M.; Mao, Y.; Song, Z. Drug repurposing strategies in the development of potential antifungal agents. *Appl. Microbiol. Biotechnol.* **2021**, *105*, 5259–5279. [CrossRef]
7. Lass-Flörl, C.; Dierich, M.; Fuchs, D.; Semenitz, E.; Jenewein, I.; Ledochowski, M. Antifungal properties of selective serotonin reuptake inhibitors against *Aspergillus* species in vitro. *J. Antimicrob. Chemother.* **2001**, *48*, 775–779. [CrossRef]
8. Ayaz, M.; Subhan, F.; Ahmed, J.; Khan, A.U.; Ullah, F.; Ullah, I.; Ali, G.; Syed, N.I.; Hussain, S. Sertraline enhances the activity of antimicrobial agents against pathogens of clinical relevance. *J. Biol. Res.* **2015**, *22*, 4. [CrossRef]
9. Villanueva-Lozano, H.; Treviño-Rangel, R.J.; Téllez-Marroquín, R.; Bonifaz, A.; Rojas, O.C.; Hernández-Rodríguez, P.A.; González, G.M. In vitro inhibitory activity of sertraline against clinical isolates of *Sporothrix schenckii*. *Rev. Iberoam. Micol.* **2019**, *36*, 139–141. [CrossRef]
10. Breuer, M.R.; Dasgupta, A.; Vasselli, J.G.; Lin, X.; Shaw, B.D.; Sachs, M.S. The Antidepressant Sertraline Induces the Formation of Supersized Lipid Droplets in the Human Pathogen *Cryptococcus neoformans*. *J. Fungi* **2022**, *8*, 642. [CrossRef]
11. Zhai, B.; Wu, C.; Wang, L.; Sachs, M.S.; Lin, X. The antidepressant sertraline provides a promising therapeutic option for neurotropic cryptococcal infections. *Antimicrob. Agents Chemother.* **2012**, *56*, 3758–3766. [CrossRef]
12. Cong, L.; Liao, Y.; Yang, S.; Yang, R. *In vitro* antifungal activity of sertraline and synergistic effects in combination with antifungal drugs against planktonic forms and biofilms of clinical *Trichosporon asahii* isolates. *PLoS ONE* **2016**, *11*, e0167903. [CrossRef]
13. Rossato, L.; Loreto, É.S.; Zanette, R.A.; Chassot, F.; Santurio, J.M.; Alves, S.H. *In vitro* synergistic effects of chlorpromazine and sertraline in combination with amphotericin B against *Cryptococcus neoformans* var. grubii. *Folia Microbiol.* **2016**, *61*, 399–403. [CrossRef]
14. Villanueva-Lozano, H.; González, G.M.; Espinosa-Mora, J.E.; Bodden-Mendoza, B.A.; Andrade, A.; Martínez-Reséndez, M.F.; Treviño-Rangel, R.J. Evaluation of the expanding spectrum of sertraline against uncommon fungal pathogens. *J. Infect. Chemother.* **2020**, *26*, 309–311. [CrossRef]
15. Rocha, C.H.L.; Rocha, F.M.G.; Bitencourt, T.A.; Martins, M.P.; Sanches, P.R.; Rossi, A.; Martinez-Rossi, N.M. Synergism between the Antidepressant Sertraline and Caspofungin as an Approach to Minimise the Virulence and Resistance in the Dermatophyte *Trichophyton rubrum*. *J. Fungi* **2022**, *8*, 815. [CrossRef]
16. Sangkuhl, K.; Klein, T.E.; Altman, R.B. Selective serotonin reuptake inhibitors pathway. *Pharm. Genom.* **2009**, *19*, 907–909. [CrossRef]
17. Kim, S.W.; Park, S.Y.; Hwang, O. Up-regulation of tryptophan hydroxylase expression and serotonin synthesis by sertraline. *Mol. Pharmacol.* **2002**, *61*, 778–785. [CrossRef]
18. Rainey, M.M.; Korostyshevsky, D.; Lee, S.; Perlstein, E.O. The antidepressant sertraline targets intracellular vesiculogenic membranes in yeast. *Genetics* **2010**, *185*, 1221–1233. [CrossRef]
19. Bolger, A.M.; Lohse, M.; Usadel, B. Trimmomatic: A flexible trimmer for Illumina sequence data. *Bioinformatics* **2014**, *30*, 2114–2120. [CrossRef]
20. Dobin, A.; Davis, C.A.; Schlesinger, F.; Drenkow, J.; Zaleski, C.; Jha, S.; Batut, P.; Chaisson, M.; Gingeras, T.R. STAR: Ultrafast universal RNA-seq aligner. *Bioinformatics* **2013**, *29*, 15–21. [CrossRef]
21. Thorvaldsdóttir, H.; Robinson, J.T.; Mesirov, J.P. Integrative Genomics Viewer (IGV): High-performance genomics data visualization and exploration. *Brief. Bioinform.* **2013**, *14*, 178–192. [CrossRef] [PubMed]
22. Love, M.I.; Huber, W.; Anders, S. Moderated estimation of fold change and dispersion for RNA-seq data with DESeq2. *Genome Biol.* **2014**, *15*, 550. [CrossRef] [PubMed]
23. Benjamini, Y.; Hochberg, Y. Controlling the False Discovery Rate: A Practical and Powerful Approach to Multiple Testing. *J. R. Stat. Soc. Ser. B Methodol.* **1995**, *57*, 289–300. [CrossRef]
24. Persinoti, G.F.; de Aguiar Peres, N.T.; Jacob, T.R.; Rossi, A.; Vêncio, R.Z.; Martinez-Rossi, N.M. RNA-sequencing analysis of *Trichophyton rubrum* transcriptome in response to sublethal doses of acriflavine. *BMC Genom.* **2014**, *15* (Suppl 7), S1. [CrossRef] [PubMed]

25. Vencio, R.Z.; Koide, T.; Gomes, S.L.; Pereira, C.A. BayGO: Bayesian analysis of ontology term enrichment in microarray data. *BMC Bioinform.* **2006**, *7*, 86. [CrossRef]
26. Finn, R.D.; Clements, J.; Eddy, S.R. HMMER web server: Interactive sequence similarity searching. *Nucleic Acids Res.* **2011**, *39*, W29–W37. [CrossRef]
27. Finn, R.D.; Bateman, A.; Clements, J.; Coggill, P.; Eberhardt, R.Y.; Eddy, S.R.; Heger, A.; Hetherington, K.; Holm, L.; Mistry, J.; et al. Pfam: The protein families database. *Nucleic Acids Res.* **2014**, *42*, D222–D230. [CrossRef]
28. Jacob, T.R.; Peres, N.T.A.; Persinoti, G.F.; Silva, L.G.; Mazucato, M.; Rossi, A.; Martinez-Rossi, N.M. *rpb2* is a reliable reference gene for quantitative gene expression analysis in the dermatophyte *Trichophyton rubrum*. *Med. Mycol.* **2012**, *50*, 368–377. [CrossRef]
29. Livak, K.J.; Schmittgen, T.D. Analysis of relative gene expression data using real-time quantitative PCR and the $2^{-\Delta\Delta CT}$ method. *Methods* **2001**, *25*, 402–408. [CrossRef]
30. Arthington-Skaggs, B.A.; Jradi, H.; Desai, T.; Morrison, C.J. Quantitation of ergosterol content: Novel method for determination of fluconazole susceptibility of *Candida albicans*. *J. Clin. Microbiol.* **1999**, *37*, 3332–3337. [CrossRef]
31. Mendes, N.S.; Bitencourt, T.A.; Sanches, P.R.; Silva-Rocha, R.; Martinez-Rossi, N.M.; Rossi, A. Transcriptome-wide survey of gene expression changes and alternative splicing in *Trichophyton rubrum* in response to undecanoic acid. *Sci. Rep.* **2018**, *8*, 14. [CrossRef]
32. Martinez, D.A.; Oliver, B.G.; Graser, Y.; Goldberg, J.M.; Li, W.; Martinez-Rossi, N.M.; Monod, M.; Shelest, E.; Barton, R.C.; Birch, E.; et al. Comparative Genome Analysis of *Trichophyton rubrum* and Related Dermatophytes Reveals Candidate Genes Involved in Infection. *MBio* **2012**, *3*, e00259-12. [CrossRef]
33. Zhou, Z.; Fu, X.D. Regulation of splicing by SR proteins and SR protein-specific kinases. *Chromosoma* **2013**, *122*, 191–207. [CrossRef]
34. Bullock, A.N.; Das, S.; Debreczeni, J.E.; Rellos, P.; Fedorov, O.; Niesen, F.H.; Guo, K.; Papagrigoriou, E.; Amos, A.L.; Cho, S.; et al. Kinase domain insertions define distinct roles of CLK kinases in SR protein phosphorylation. *Structure* **2009**, *17*, 352–362. [CrossRef]
35. Hayes, J.D.; Strange, R.C. Glutathione S-transferase polymorphisms and their biological consequences. *Pharmacology* **2000**, *61*, 154–166. [CrossRef]
36. Muñiz-Calvo, S.; Bisquert, R.; Fernández-Cruz, E.; García-Parrilla, M.C.; Guillamón, J.M. Deciphering the melatonin metabolism in *Saccharomyces cerevisiae* by the bioconversion of related metabolites. *J. Pineal Res.* **2019**, *66*, e12554. [CrossRef]
37. Gallardo-Fernández, M.; Valls-Fonayet, J.; Valero, E.; Hornedo-Ortega, R.; Richard, T.; Troncoso, A.M.; Garcia-Parrilla, M.C. Isotopic labelling-based analysis elucidates biosynthesis pathways in *Saccharomyces cerevisiae* for Melatonin, Serotonin and Hydroxytyrosol formation. *Food Chem.* **2022**, *374*, 131742. [CrossRef]
38. Muthu, D.; Gowri, M.; Suresh Kumar, G.; Kattimani, V.S.; Girija, E.K. Repurposing of antidepression drug sertraline for antimicrobial activity against *Staphylococcus aureus*: A potential approach for the treatment of osteomyelitis. *New J. Chem.* **2019**, *43*, 5315–5324. [CrossRef]
39. Baú-Carneiro, J.L.; Akemi Guirao Sumida, I.; Gallon, M.; Zaleski, T.; Boia-Ferreira, M.; Bridi Cavassin, F. Sertraline repositioning: An overview of its potential use as a chemotherapeutic agent after four decades of tumor reversal studies. *Transl. Oncol.* **2022**, *16*, 101303. [CrossRef]
40. Ferreira, D.D.; Mesquita, J.T.; da Costa Silva, T.A.; Romanelli, M.M.; da Gama Jaen Batista, D.; da Silva, C.F.; da Gama, A.N.S.; Neves, B.J.; Melo-Filho, C.C.; Correia Soeiro, M.N.; et al. Efficacy of sertraline against *Trypanosoma cruzi*: An in vitro and in silico study. *J. Venom. Anim. Toxins Incl. Trop. Dis.* **2018**, *24*, 30. [CrossRef]
41. Krzyżek, P.; Franiczek, R.; Krzyżanowska, B.; Laczmański, L.; Migdal, P.; Gościniak, G. In Vitro Activity of Sertraline, an Antidepressant, Against Antibiotic-Susceptible and Antibiotic-Resistant *Helicobacter pylori* Strains. *Pathogens* **2019**, *8*, 228. [CrossRef] [PubMed]
42. Watson, N.A.; Cartwright, T.N.; Lawless, C.; Cámara-Donoso, M.; Sen, O.; Sako, K.; Hirota, T.; Kimura, H.; Higgins, J.M.G. Kinase inhibition profiles as a tool to identify kinases for specific phosphorylation sites. *Nat. Commun.* **2020**, *11*, 1684. [CrossRef] [PubMed]
43. Piazzi, M.; Bavelloni, A.; Gallo, A.; Faenza, I.; Blalock, W.L. Signal Transduction in Ribosome Biogenesis: A Recipe to Avoid Disaster. *Int. J. Mol. Sci.* **2019**, *20*, 2718. [CrossRef] [PubMed]
44. Shelest, E. Transcription factors in fungi. *FEMS Microbiol. Lett.* **2008**, *286*, 145–151. [CrossRef]
45. Beauvais, A.; Latgé, J.-P. Special Issue: Fungal Cell Wall. *J. Fungi* **2018**, *4*, 91. [CrossRef]
46. Martins, M.P.; Silva, L.G.; Rossi, A.; Sanches, P.R.; Souza, L.D.R.; Martinez-Rossi, N.M. Global Analysis of Cell Wall Genes Revealed Putative Virulence Factors in the Dermatophyte *Trichophyton rubrum*. *Front. Microbiol.* **2019**, *10*, 2168. [CrossRef]
47. Ibe, C.; Munro, C.A. Fungal cell wall: An underexploited target for antifungal therapies. *PLoS Pathog.* **2021**, *17*, e1009470. [CrossRef]
48. Roncero, C.; Vázquez de Aldana, C.R. Glucanases and Chitinases. *Curr. Top. Microbiol. Immunol.* **2020**, *425*, 131–166.
49. Yamamoto, T.; Umegawa, Y.; Tsuchikawa, H.; Hanashima, S.; Matsumori, N.; Funahashi, K.; Seo, S.; Shinoda, W.; Murata, M. The Amphotericin B-Ergosterol Complex Spans a Lipid Bilayer as a Single-Length Assembly. *Biochemistry* **2019**, *58*, 5188–5196. [CrossRef]
50. Abe, F.; Usui, K.; Hiraki, T. Fluconazole modulates membrane rigidity, heterogeneity, and water penetration into the plasma membrane in *Saccharomyces cerevisiae*. *Biochemistry* **2009**, *48*, 8494–8504. [CrossRef]

51. Hinkovska-Galcheva, V.; Treadwell, T.; Shillingford, J.M.; Lee, A.; Abe, A.; Tesmer, J.J.G.; Shayman, J.A. Inhibition of lysosomal phospholipase A2 predicts drug-induced phospholipidosis. *J. Lipid Res.* **2021**, *62*, 100089. [CrossRef]
52. Rhein, C.; Reichel, M.; Kramer, M.; Rotter, A.; Lenz, B.; Mühle, C.; Gulbins, E.; Kornhuber, J. Alternative *splicing* of SMPD1 coding for acid sphingomyelinase in major depression. *J. Affect. Disord.* **2017**, *209*, 10–15. [CrossRef]
53. Ramrakhiani, L.; Chand, S. Recent progress on phospholipases: Different sources, assay methods, industrial potential and pathogenicity. *Appl. Biochem. Biotechnol.* **2011**, *164*, 991–1022. [CrossRef]
54. O'Luanaigh, N.; Pardo, R.; Fensome, A.; Allen-Baume, V.; Jones, D.; Holt, M.R.; Cockcroft, S. Continual production of phosphatidic acid by phospholipase D is essential for antigen-stimulated membrane ruffling in cultured mast cells. *Mol. Biol. Cell* **2002**, *13*, 3730–3746. [CrossRef]
55. Martins, M.P.; Rossi, A.; Sanches, P.R.; Bortolossi, J.C.; Martinez-Rossi, N.M. Comprehensive analysis of the dermatophyte *Trichophyton rubrum* transcriptional profile reveals dynamic metabolic modulation. *Biochem. J.* **2020**, *477*, 873–885. [CrossRef]
56. Bitencourt, T.A.; Rezende, C.P.; Quaresemin, N.R.; Moreno, P.; Hatanaka, O.; Rossi, A.; Martinez-Rossi, N.M.; Almeida, F. Extracellular Vesicles From the Dermatophyte *Trichophyton interdigitale* Modulate Macrophage and Keratinocyte Functions. *Front. Immunol.* **2018**, *9*, 2343. [CrossRef]
57. Sato, I.; Shimizu, M.; Hoshino, T.; Takaya, N. The glutathione system of *Aspergillus nidulans* involves a fungus-specific glutathione S-transferase. *J. Biol. Chem.* **2009**, *284*, 8042–8053. [CrossRef]
58. Pócsi, I.; Prade, R.A.; Penninckx, M.J. Glutathione, altruistic metabolite in fungi. *Adv. Microb. Physiol.* **2004**, *49*, 1–76.
59. He, Y.; Zhou, C.; Huang, M.; Tang, C.; Liu, X.; Yue, Y.; Diao, Q.; Zheng, Z.; Liu, D. Glyoxalase system: A systematic review of its biological activity, related-diseases, screening methods and small molecule regulators. *Biomed. Pharmacother.* **2020**, *131*, 110663. [CrossRef]
60. Missall, T.A.; Lodge, J.K. Function of the thioredoxin proteins in *Cryptococcus neoformans* during stress or virulence and regulation by putative transcriptional modulators. *Mol. Microbiol.* **2005**, *57*, 847–858. [CrossRef]
61. Pannala, V.R.; Dash, R.K. Mechanistic characterization of the thioredoxin system in the removal of hydrogen peroxide. *Free Radic. Biol. Med.* **2015**, *78*, 42–55. [CrossRef] [PubMed]
62. Binder, J.; Shadkchan, Y.; Osherov, N.; Krappmann, S. The Essential Thioredoxin Reductase of the Human Pathogenic Mold *Aspergillus fumigatus* Is a Promising Antifungal Target. *Front. Microbiol.* **2020**, *11*, 1383. [CrossRef] [PubMed]
63. Vázquez, J.; González, B.; Sempere, V.; Mas, A.; Torija, M.J.; Beltran, G. Melatonin Reduces Oxidative Stress Damage Induced by Hydrogen Peroxide in *Saccharomyces cerevisiae*. *Front. Microbiol.* **2017**, *8*, 1066. [CrossRef] [PubMed]
64. Perkhofer, S.; Niederegger, H.; Blum, G.; Burgstaller, W.; Ledochowski, M.; Dierich, M.P.; Lass-Flörl, C. Interaction of 5-hydroxytryptamine (serotonin) against *Aspergillus* spp. in vitro. *Int. J. Antimicrob. Agents* **2007**, *29*, 424–429. [CrossRef]
65. New, A.M.; Cerulus, B.; Govers, S.K.; Perez-Samper, G.; Zhu, B.; Boogmans, S.; Xavier, J.B.; Verstrepen, K.J. Different levels of catabolite repression optimize growth in stable and variable environments. *PLoS Biol.* **2014**, *12*, e1001764. [CrossRef]
66. Adnan, M.; Zheng, W.; Islam, W.; Arif, M.; Abubakar, Y.S.; Wang, Z.; Lu, G. Carbon Catabolite Repression in Filamentous Fungi. *Int. J. Mol. Sci.* **2017**, *19*, 48. [CrossRef]
67. Lorenz, M.C.; Fink, G.R. The glyoxylate cycle is required for fungal virulence. *Nature* **2001**, *412*, 83–86. [CrossRef]
68. Cruz, A.H.S.; Santos, R.S.; Martins, M.P.; Peres, N.T.A.; Trevisan, G.L.; Mendes, N.S.; Martinez-Rossi, N.M.; Rossi, A. Relevance of Nutrient-Sensing in the Pathogenesis of *Trichophyton rubrum* and *Trichophyton interdigitale*. *Front. Fungal Biol.* **2022**, *3*. [CrossRef]
69. Chew, S.Y.; Ho, K.L.; Cheah, Y.K.; Ng, T.S.; Sandai, D.; Brown, A.J.P.; Than, L.T.L. Glyoxylate cycle gene ICL1 is essential for the metabolic flexibility and virulence of Candida glabrata. *Sci. Rep.* **2019**, *9*, 2843. [CrossRef]
70. Ishchuk, O.P.; Voronovsky, A.Y.; Stasyk, O.V.; Gayda, G.Z.; Gonchar, M.V.; Abbas, C.A.; Sibirny, A.A. Overexpression of pyruvate decarboxylase in the yeast Hansenula polymorpha results in increased ethanol yield in high-temperature fermentation of xylose. *FEMS Yeast Res.* **2008**, *8*, 1164–1174. [CrossRef]

Anexo B

Journal of *Fungi*

MDPI

Article

Synergism between the Antidepressant Sertraline and Caspofungin as an Approach to Minimise the Virulence and Resistance in the Dermatophyte *Trichophyton rubrum*

Carlos H. Lopes Rocha, Flaviane M. Galvão Rocha, Tamires A. Bitencourt, Maíra P. Martins, Pablo R. Sanches, Antonio Rossi and Nilce M. Martinez-Rossi *

Department of Genetics, Ribeirão Preto Medical School, University of São Paulo, USP, Ribeirao Preto 14049-900, SP, Brazil; henriqueclr16@usp.br (C.H.L.R.); flavianerocha@usp.br (F.M.G.R.); tabitencourt@yahoo.com.br (T.A.B.); mairapompeu@hotmail.com (M.P.M.); psanches@usp.br (P.R.S.); anrossi@usp.br (A.R.)

* Correspondence: nmmrossi@usp.br

Abstract: *Trichophyton rubrum* is responsible for several superficial human mycoses. Novel strategies aimed at controlling this pathogen are being investigated. The objective of this study was to evaluate the antifungal activity of the antidepressant sertraline (SRT), either alone or in combination with caspofungin (CASP). We calculated the minimum inhibitory concentrations of SRT and CASP against *T. rubrum*. Interactions between SRT and CASP were evaluated using a broth microdilution chequerboard. We assessed the differential expression of *T. rubrum* cultivated in the presence of SRT or combinations of SRT and CASP. We used MTT and violet crystal assays to compare the effect of SRT alone on *T. rubrum* biofilms with that of the synergistic combination of SRT and CASP. A human nail infection assay was performed. SRT alone, or in combination with CASP, exhibited antifungal activity against *T. rubrum*. SRT targets genes involved in the biosyntheses of cell wall and ergosterol. Furthermore, the metabolic activity of the *T. rubrum* biofilm and its biomass were affected by SRT and the combination of SRT and CASP. SRT alone, or in combination, shows potential as an approach to minimise resistance and reduce virulence.

Keywords: *Trichophyton rubrum*; dermatophyte; synergistic combinations; antifungal resistance; sertraline; caspofungin and biofilm

check for updates

Citation: Rocha, C.H.L.; Rocha, F.M.G.; Bitencourt, T.A.; Martins, M.P.; Sanches, P.R.; Rossi, A.; Martinez-Rossi, N.M. Synergism between the Antidepressant Sertraline and Caspofungin as an Approach to Minimise the Virulence and Resistance in the Dermatophyte *Trichophyton rubrum*. *J. Fungi* **2022**, *8*, 815. https://doi.org/10.3390/jof8080815

Academic Editors: Aditya K. Gupta and Bianca Maria Piraccini

Received: 5 July 2022
Accepted: 29 July 2022
Published: 3 August 2022

Publisher's Note: MDPI stays neutral with regard to jurisdictional claims in published maps and institutional affiliations.

1. Introduction

Dermatophytosis is a common fungal infection caused by dermatophytes, a class of non-opportunistic pathogens that obtain nutrients from keratinised tissues such as hair, skin, and nails. *Trichophyton rubrum* is a cosmopolitan species often isolated from cutaneous infections and immunocompromised human hosts worldwide, resulting in severe conditions that may lead to public health issues [1]. It is estimates that dermatophytes affect approximately 25% of the world population, wherein 30–70% of adults act as carriers who do not present with clinical manifestations [2]. The damp climate and elevated temperatures of tropical and subtropical regions contribute to the high rate of dermatophytosis [1].

Treating *T. rubrum* infections is challenging because only a few therapeutic options, such as azoles and allylamines that interfere with the ergosterol biosynthesis pathway, are available. Furthermore, in addition to lengthy and costly treatments, several antifungal resistance cases have been reported [3]. Primary defence mechanisms of the host include skin peeling, decreased humidity, skin pH, elevated temperature, and fatty acids. In contrast, fungi develop adaptive responses to overcome these challenges [4]. Fungi trigger several mechanisms that overexpress drug efflux pumps, detoxify enzymes, and modify drug targets, all of which are aimed at tolerating or resisting the effects of antifungals [3,5].

Additionally, surface-based cell population complexes, termed biofilms, contribute to drug resistance, mainly by resisting penetration. These complex structures manifest in the form of an extracellular matrix, characterised by metabolic heterogeneity and upregulated efflux pump-related genes [6,7]; thus, the tracking and identification of compounds with antifungal activity are urgently required [8,9]. In this regard, drug repositioning appears to be an exciting alternative. When repurposing an existing drug for a newer use, drug characteristics, such as toxicity and pharmacokinetics, must already be established [10].

Combining sertraline (SRT), one of the most prescribed antidepressants explored for its antifungal properties, with commercial antifungals represents a promising therapeutic approach that would enhance the therapeutic efficacy [11,12]. SRT significantly reduced the pulmonary fungal burden associated with *Aspergillus fumigatus* infection in a murine aspergillosis model. The same study reported that SRT ensured the survival of 25% of infected larvae of a *Galleria mellonella* aspergillosis model, compared to the high mortality rates observed in infected and untreated larvae [13].

In mammals, SRT selectively inhibits serotonin reuptake by locking the 5-hydroxytryptamine (5-HT) transporter [14]. In yeast cells, SRT targets the phospholipid membranes of acidic organelles, which are part of an intracellular vesicle transport system [15]. SRT also exerts antifungal effects by disrupting translation, thereby inhibiting protein synthesis [11].

A synergistic combination of SRT and amphotericin B improves inhibitory activity against *A. fumigatus*. Notably, combining SRT with itraconazole was also synergistic [16]. Essays on *Cryptococcus neoformans* evidenced the antifungal activity of SRT, either in monotherapy or in synergic combination with fluconazole [16,17]. In addition, SRT exhibited synergistic effects against *Trichosporon asahii* planktonic cells with caspofungin (CASP) [18].

The activity of CASP against dermatophytes is not well defined. Pioneering works have demonstrated that CASP shows excellent activity against the dermatophytes *T. rubrum, Trichophyton interdigitale,* and *Microscoporum canis* [19,20]. Another study showed that CASP promotes several morphological changes, including shortening and induction of aberrant hyphae growth; however, it has reduced efficacy and incompletely inhibited in vitro growth [21].

There are few studies demonstrating the CASP effect with other antifungal agents. In most cases, the combination therapy of CASP with another agent is used for treating infections caused by the genus *Candida* [22,23]. In association with farnesol, CASP significantly inhibited the metabolic activity of *Candida parapsilosis* cells [24]. CASP, with fluconazole and posaconazole, is an effective strategy against *Candida glabrata* [22]. CASP belongs to a class of antifungal agents known as echinocandins, which inhibit the synthesis of the fungal cell wall component, beta-(1,3)-D-glucan.

Thus, owing to the necessity of expanding the range of therapeutics available against dermatophytosis, we hypothesised that SRT combined with CASP might help minimise drug resistance. Furthermore, we evaluated the expression of genes associated with the resistance of *T. rubrum* to SRT alone and its combination with CASP.

2. Materials and Methods

2.1. Strain and Growth Conditions

The *T. rubrum* strain, CBS118892 (Westerdijk Fungal Biodiversity Institute, Utrecht, Netherlands), obtained from a patient with onychomycosis, was cultivated on malt extract agar (Becton Dickinson, Franklin Lakes, NJ, USA) for 35 days at 28 °C, as previously described [25], for total RNA extraction. The fungal suspension was prepared in 0.9% NaCl, following which the conidia concentration was estimated using a Newbauer chamber. Approximately 1×10^6 conidia were added to 100 mL of liquid Sabouraud (SB) at pH 5.7 supplemented with 2% glucose and 1% peptone (Becton Dickinson, Franklin Lakes, NJ, USA), followed by incubation at 28 °C for 96 h under continuous shaking. The resulting mycelia were then transferred to 100 mL of SB in the presence of a sublethal dose (70 mg/L) of SRT (Cayman Chemical, Ann Arbor, MI, USA), in the presence of a sublethal

combination (sc) of 0.273 mg/L SRT + 10.93 mg/L CASP (Merck Sharp & Dohme, São Paulo, SP, Brazil), 0.273 mg/L SRT, 10.93 mg/L CASP, and in the absence of drugs (control), followed by incubation at 28 °C with shaking (120 rpm) for 3 h and 12 h.

2.2. Minimum Inhibitory Concentration (MIC) and Interaction between SRT and CASP

MICs were obtained according to the M38-A reference method recommended by the Clinical and Laboratory Standards Institute (CLSI) [26], with the following modification: 100 µL of the conidial suspension, amounting to 6×10^4 conidia/mL, was added to each well in the 96-well microtitre plate. The final conidial concentration was adjusted to approximately 3×10^4 conidia per well in RPMI 1640 (Sigma-Aldrich, St Louis, MO, USA) or SB medium. RPMI was buffered with 0.165 M morpholinepropanesulfonic acid (MOPS) (Sigma-Aldrich), and the pH was adjusted to 7.0. SRT and CASP were prepared as stock solutions in dimethyl sulfoxide (DMSO, Sigma-Aldrich): SRT (50,000 mg/L); and CASP (5000 mg/L). Serial dilutions of SRT and CASP were performed in RPMI medium, buffered with 0.165 M morpholinepropanesulfonic acid (MOPS), or SB medium. The final concentrations of SRT ranged between 0.78–200 mg/L, whereas those of CASP ranged between 0.98–250 mg/L. Interactions between SRT and CASP were evaluated using a broth microdilution chequerboard and quantified using the fractional inhibitory concentration index (FICI): FICI $\leq$ 0.5, FICI > 0.5 to $\leq$ 4.0, and FICI > 4.0 were categorised as synergism, indifference, and antagonism, respectively [27]. FICIs were calculated for all possible combinations of different concentrations. The results were expressed as the mean of FICIs. Assay plates were used to determine MICs, and the broth microdilution chequerboard was incubated at 28 °C for seven days. Growth controls were performed in wells containing only the fungal suspension and medium. Individual and combined MICs were defined by comparison with growth controls performed in wells containing only fungal suspension and media, with complete growth inhibition. All experiments were performed in triplicate.

2.3. Total RNA Extraction and cDNA Synthesis

Total RNA was extracted from *T. rubrum*, cultivated in the presence of SRT alone and SRT combined with CASP, using an Illustra RNAspin mini-isolation kit (GE Healthcare, Chicago, IL, USA). Mycelia were ground via mechanical pulverisation using a mortar and pestle in liquid nitrogen, and RNA samples were treated with RNase-free DNase I (Sigma-Aldrich). Complementary DNA (cDNA) was synthesised from each condition containing 1000 ng of total RNA in a 20 µL reaction volume using a High-Capacity cDNA Synthesis kit (Applied Biosystems, Waltham, MA, USA). Equal amounts of RNA from three independent biological replicates were used to synthesise cDNA.

2.4. RT-qPCR Analysis

Gene expression was quantified via qPCR using a StepOnePlus Real-Time PCR system (Applied Biosystems). PCR reactions were performed with specific primer pairs designed using Prime3Plus software (https://www.bioinformatics.nl/cgi-bin/primer3plus/primer3plus.cgi (accessed on 4 July 2022)) and specificity (Table S1). Each qPCR reaction was performed using a final volume of 12.5 µL: 0.5 µL primer, 6.25 µL SYBR Green PCR Master Mix (Applied Biosystem, Waltham, MA, USA), and 70 ng cDNA. The thermocycler conditions for RT-qPCR were 95 °C for 10 min, followed by 40 cycles of 95 °C for 15 s and 60 °C for 1 min. We selected genes encoding the enzymes glyceraldehyde 3 phosphate dehydrogenase (*gapdh*) and DNA-dependent RNA polymerase II (*rpb2*) as endogenous controls. Data were derived from three independent replicates, and the $2^{-\Delta\Delta ct}$ method was used to assess the relative quantification of responsive genes [28].

2.5. In Vitro Biofilm Formation

T. rubrum biofilms were formed according to a previously described method [29], with some modifications. *T. rubrum* CBS118892 was grown on malt extract agar for 15 days at 28 °C. The fungal suspension was prepared in 0.9% NaCl, and the conidial concentration

was adjusted to approximately 1×10^6 conidia/mL. The plates were initially incubated at 37 °C for 4 h without agitation for pre-adhesion.

2.6. Metabolic Activity of the Biofilm by MTT Assay

Following pre-adhesion, treatments consisting of 200 µL each of SRT (12.5 mg/L, and 3.12 mg/L), CASP (15.62 mg/L, and 1.95 mg/L), and SRT + CASP (3.12 mg/L + 1.95 mg/L respectively) prepared in RPMI 1640 medium, supplemented with 2% of glucose, were added into the wells. Biofilms were prepared at different time points (0, 24, 48, 72, and 96 h). Following each incubation, 2 µL of menadione (Sigma-Aldrich) and 20 µL of MTT (Sigma-Aldrich) at 5000 mg/L were added to each well. The plates were incubated at 37 °C for 4 h. Colorimetric changes were measured using an ELISA reader (Thermo Fisher Scientific, Waltham, MA, USA) at 550 nm. A control was prepared by adding 200 µL of untreated conidial suspension to each well.

2.7. Quantification of In Vitro Biofilm by Crystal Violet

Following pre-adhesion, the supernatant was removed from the wells and washed thrice with 0.9% sterile saline, after which 200 µL RPMI 1640 medium supplemented with 2% glucose was added to each well. Three independent biological replicates were incubated at 37 °C for 72 h for biofilm maturation. Following biofilm formation, culture medium was removed and treatments comprising 200 µL each of SRT 25 mg/L, SRT 6.25 mg/L, CASP 62.50 mg/L, CASP 1.95 mg/L, and SRT 6.25 mg/L + CASP 1.95 mg/L were added to wells. The treatments were prepared in RPMI 1640 medium supplemented with 2% glucose. Replicates were incubated at 37 °C for 3–7 days. Next, the drugs were removed, and each well was washed thrice with 0.01 M PBS (pH 7.2), following which 100 µL of crystal violet solution was added to each well to quantify biomass. Then, each well was washed twice with sterile water, treated with 100 µL of 95% ethanol and carefully homogenised. The resulting solution was transferred to a new 96-well plate and read using an ELISA reader at a wavelength of 550 nm. A control consisting of 200 µL of untreated conidial suspension was added to each well.

2.8. Assessment of Biofilms in Human Nails

The human nail infection assay was performed as previously described [29], with some modifications. Human nail fragments (1 mm^2) obtained from healthy donors were initially sterilised by autoclaving and transferred to water agar-containing 24-well plates. The fragments were infected with 2 mL suspension prepared in sterile saline 0.9% (NaCl), and conidia concentration was adjusted to approximately 3×10^4 conidia per well. After 4 h of pre-adhesion at 37 °C, the suspension was removed, and each well was washed thrice with 0.9% sterile saline. Next, 2 mL of 0.9% sterile saline was added to each well, following which the plates were incubated for 20 days at 28 °C. Then, 2 mL each of SRT 50 mg/L, SRT 12.5 mg/L, CASP 62.50 mg/L, CASP 3.90 mg/L, and SRT 12.5 mg/L + CASP 3.90 mg/L prepared in 0.9% sterile saline were added to wells daily for seven days. After seven days, the biofilms were analysed using scanning electron microscopy. The assay was conducted according to the Medical School Ethics Committee and approved per protocol number 4.304.317/2020.

2.9. Scanning Electron Microscopy

The samples were initially fixed using 3% glutaraldehyde in 0.1% phosphate buffer (*v*/*v*) (pH 7.2) at 4 °C for 24 h and rinsed with 0.1% phosphate buffer (pH 7.2). Osmium tetroxide (1%) was used during the post-fixation step. Subsequently, the samples were dehydrated in an increasing ethanol gradient involving successive baths of increasing ethanol concentrations. Gold was then spray-coated on these samples to visualise biofilms formed in human nails. A JEOL JSM-6610 LV scanning electron microscope at an acceleration voltage of 25 kV was used for visualisation.

2.10. Statistical Analysis

We calculated the gene expression using the comparative $2^{-\Delta\Delta CT}$ method. The paired Student's *t*-test was used to compare gene expression between treatment and control conditions at each time point. The results are reported as the mean ± standard deviation of three independent biological replicas. For comparing the biofilm's metabolic activity and quantification biomass, one-way ANOVA was used, followed by Tukey's post hoc test. For all tests, statistical significance was adopted at $p < 0.05$. Prism v. 5.1 (GraphPad Software, San Diego, CA, USA) was used to generate the graphs and statistical analyses.

3. Results

3.1. Antifungal Susceptibility and Interaction between SRT and CASP

SRT alone and in combination with CASP exhibited antifungal activity against *T. rubrum* free-flowing planktonic cells. The MIC of SRT required to inhibit *T. rubrum* in RPMI medium was 25 mg/L, whereas that of CASP was 31.25 mg/L. The MICs of SRT and CASP increased considerably when the assay was performed in the SB medium. In this medium, SRT showed a MIC of 100 mg/L, whereas CASP showed a MIC of 62.50 mg/L. The interactions between SRT/CASP in both culture media (RPMI or SB) could be considered synergistic (FICI $\leq$ 0.5). Assays performed in both media indicated that the FICIs corresponding to the SRT/CASP combination ranged between 0.1–0.5. The mean FICIs in the RPMI and SB medium were 0.28 and 0.25, respectively (Table 1). The combined MIC values associated with synergism between SRT and CASP are displayed (Table 2).

Table 1. MICs of sertraline (SRT) and caspofungin (CASP) against planktonic forms of *T. rubrum*. FICI and the mean of FICI of interactions between SRT and CASP.

Medium	MIC_{100}-mg/L		FICI Range	FICI (Mean)
	SRT	CASP	SRT/CASP	SRT/CASP
SB	100	62.50	0.1–0.50	0.25
RPMI	25	31.25	0.1–0.50	0.28

FICI $\leq$ 0.5, FICI > 0.5 to $\leq$4.0, and FICI > 4.0 were categorised as synergism, indifference, and antagonism, respectively.

Table 2. MICcb (combined MICs) values for analysis of synergism between sertraline (SRT) and caspofungin (CASP) in assays performed in RPMI medium and Sabouraud (SB) medium.

Medium	Drug	Concentrations Ranged of the SRT (mg/L)								
		200	100	50	25	12.5	6.25	3.12	1.56	0.78
SB	CASP	0	0	1.95	1.95	1.95	1.95	7.81	15.62	15.62
RPMI	(mg/mL)	0	0	0	0	0.98	0.98	1.95	1.95	3.90

3.2. RT-qPCR

RT-qPCR-based gene expression analysis revealed that an SRT concentration amounting to 70% of its MIC induced a gene encoding a transporter (*TERG_00162*) belonging to the major facilitator superfamily (MFS) at 3 and 12 h. In contrast, exposure to SRT for 3 and 12 h downregulated *TERG_12319*, a critical chitin synthase-associated gene linked to fungal virulence and cell wall remodelling. Furthermore, *TERG_04234*, encoding hydrophobin, a putative protein essential for fungal pathogenesis, and *TERG_06755*, encoding a c-8 sterol isomerase protein, required for the ergosterol pathway, were downregulated at 3 and 12 h, respectively (Figure 1).

Gene expression analysis using RT-qPCR was extended to examine *T. rubrum* growth in the presence of the SRT + antifungal CASP combination. SRT + CASP exposure downregulated gene transcription of the MFS multidrug transporter, *TERG_00162*, at 3 and 12 h, in contrast to the induction caused by the SRT alone. In contrast, SRT + CASP downregulated *TERG_04234* and *TERG_06755*, as well as the gene encoding the enzyme chitin synthase, *TERG_12319*, which was similar to that observed under conditions involving the use of SRT alone (Figure 2).

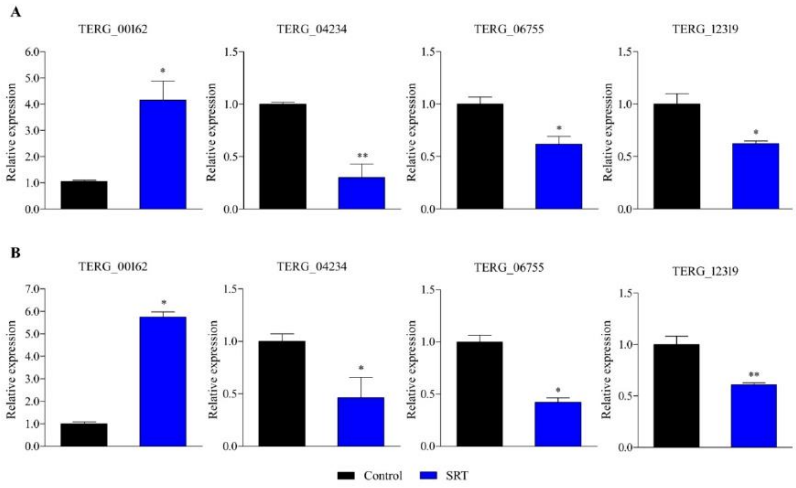

Figure 1. Differentially expressed genes in response to SRT, identified using RT-qPCR analysis. The relative expression of genes *TERG_00162* (MFS multidrug transporter), *TERG_04234* (Hydrophobin), *TERG_06755* (C-8 sterol isomerase), and *TERG_12319* (Chitin synthase 2) at 3 h (**A**) and 12 h (**B**) are represented. Asterisks indicate the statistical significance of the *t*-test compared to the control (SB drug absence). * $p < 0.05$; and ** $p < 0.01$.

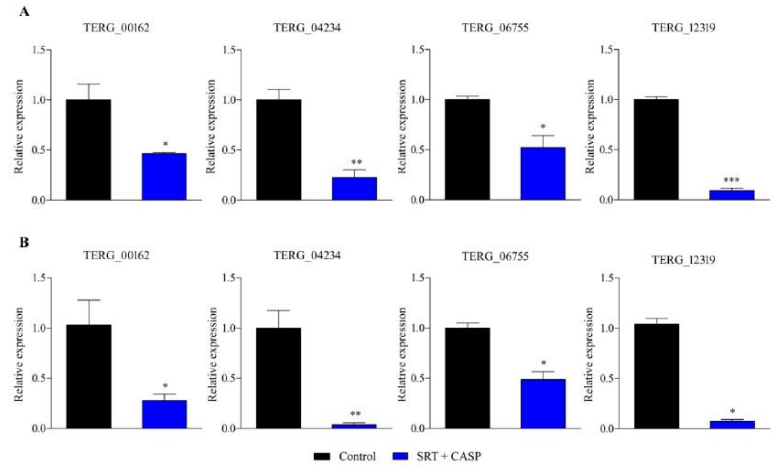

Figure 2. Genes encoding *TERG_00162* (MFS multidrug transporter), *TERG_04234* (Hydrophobin), *TERG_06755* (C-8 sterol isomerase), and *TERG_12319* (Chitin synthase 2) are differentially expressed in response to combinations of SRT with CASP. Asterisks indicate statistical significance determined by *t*-test as compared to the control (SB absence drug) at 3 h (**A**) and 12 h (**B**); * $p < 0.05$; ** $p < 0.01$; *** $p < 0.001$.

The effects of low concentrations of CASP and SRT on the expression levels of these genes in *T. rubrum* cultured in the presence of CASPsc or SRTsc were analysed. The results showed that SRTsc maintained the expression level of *TERG_00162*, which encodes

a multidrug transporter, at a level similar to that observed in the control at 3 h; in contrast, the expression of *TERG_00162* increased at 12 h. Moreover, a significant difference existed between the expression levels shown under these conditions and that of the control ($p < 0.05$). *TERG_06755* expression was downregulated at 3 h, but its expression at 12 h was similar to that of the control. *TERG_04234* and *TERG_12319* maintained their expression under both conditions (control and SRTsc) at 3 h and 12 h (Figure S1).

Exposure of *T. rubrum* to CASPsc resulted in *TERG_00162*, *TERG_04234*, *TERG_06755*, and *TERG_12319* presenting similar expression levels at 3 h or 12 h, compared to that of the untreated control. Therefore, no statistically significant differences existed between these treatment conditions (Figure S2).

3.3. Effects of SRT and Its Combination with CASP on the Activity of T. rubrum Biofilm

Metabolic activity in the biofilm was measured every 24 h. A significant increase in metabolic activity was observed up to 72 h, following which the activity stabilised. Therefore, 72 h was considered ideal for biofilm formation. The MTT assay results indicated that 12.5 mg/L SRT alone and of 15.62 mg/L CASP alone, as well as low concentrations of SRT + CASP (3.12 mg/L SRT+ 1.95 mg/L CASP), interfered significantly with the metabolic activities of the biofilm. Treatment with SRTsc or CASPsc did not reduce the metabolic activity of *T. rubrum* biofilms (Figure 3).

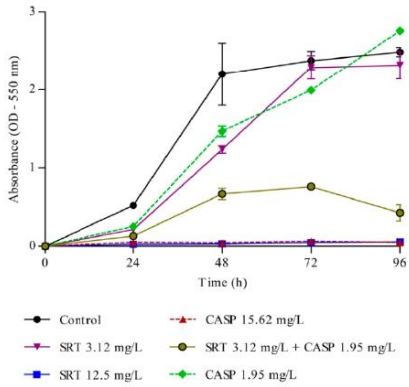

Figure 3. Metabolism of *T. rubrum* biofilm. Effects of sertraline (SRT), caspofungin (CASP), and SRT + CASP on the metabolic activity of *T. rubrum* biofilm.

The biomass of the biofilm was also affected by SRT, CASP, and SRT + CASP treatments. Three days after the biofilm was treated with 62.50 mg/L CASP, a significant reduction was observed in the biomass compared with that of the control ($p < 0.01$). Treatment with 25 mg/L SRT as well as 6.25 mg/L SRT + 1.95 mg/L CASP significantly reduced biomass. By contrast, 6.25 mg/L SRT or 1.95 mg/L CASP did not reduce biomass but instead increased production in a manner similar to that of the control (Figure 4).

After the biofilm matured for seven days, the 25 mg/L SRT, 62.50 mg/L CASP, or 6.25 mg/L SRT + 1.95 mg/L CASP treatments significantly reduced biomass when compared with the control ($p < 0.001$). However, treatment with 6.25 mg/L SRT or 1.95 mg/L CASP did not reduce the biomass of biofilm that had matured for three days. The biomass produced by these treatments was similar to that observed in the absence of drugs (Figure 5).

The results of the human nail infection assay corroborated the reduction in biomass and metabolic activity of the biofilm, observed via the MTT and crystal violet assays. Scanning electron microscopy revealed that *T. rubrum* forms mature biofilms in human nail fragments after 20 d. Its growth on the substrate was characterised by infinite filaments,

which were denser, interconnected, and spread in all directions to form an actual network of connected hyphae. The high antifungal tolerance in *T. rubrum* may be attributed to this network of connected hyphae. Thus, biofilm maturation in human nail fragments was considerably affected by SRT.

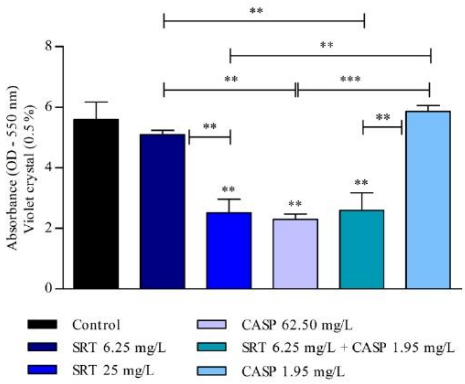

Figure 4. Evaluation of the effect of SRT, CASP, and the synergistic combination (SRT + CASP) on the biomass of *T. rubrum* biofilm stained with violet crystal. The treatments were performed 3 days after the biofilm matured. Statistical analyses showing significant differences ($p < 0.05$) between tested compounds and growth control were estimated using one-way ANOVA and Tukey's post hoc test; ** $p < 0.01$ and *** $p < 0.001$.

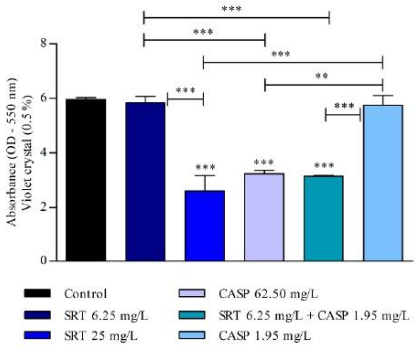

Figure 5. Effect of SRT, CASP, and SRT + CASP on the biomass of *T. rubrum* biofilm. Treatments were performed 7 days after the biofilm matured and stained with violet crystal. Significant differences between tested compounds and growth control were obtained using one-way ANOVA and Tukey's post hoc test. Asterisks indicate statistical significance: ** $p < 0.01$ and *** $p < 0.001$.

Filament density was significantly reduced by the treatments compared to that in the untreated control. A significant reduction in the thickness of filaments that formed the hyphal network was observed. Additionally, most hyphae could not complete their development to a level that enabled them to create a more uniform biofilm. In this context, the highest activity was observed after *T. rubrum* was treated with SRT and CASP at concentrations corresponding to 2 × MICs, which amounted to 50 mg/L, and 62.50 mg/L, respectively. Excellent biofilm reduction resulting from treatment with 12.5 mg/L SRT + 3.90 mg/L CASP

must be highlighted. However, we did not verify the reduction in filament density and the alterations mentioned earlier under isolated, uncombined conditions (Figure 6).

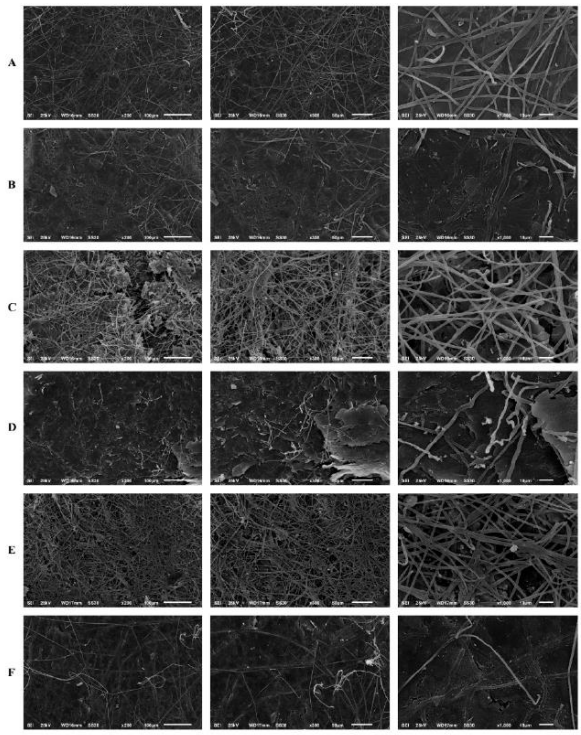

Figure 6. Scanning electron microscopy of the *T. rubrum* biofilm on a human nail. *T. rubrum* strain growth on nail fragments in the absence of drugs (**A**). Treatment with SRT 50 mg/L (**B**), SRT 12.5 mg/L (**C**), CASP 62.50 mg/L (**D**), CASP 3.90 mg/L (**E**) and SRT 12.5 mg/L + CASP 3.90 mg/L (**F**), 20 days of after biofilm matured.

4. Discussion

The human antidepressant, SRT, exhibited antifungal activity against planktonic forms of *T. rubrum* (100 mg/L SB and 25 mg/L RPMI media). When combined with CASP, SRT showed excellent synergistic effects by inhibiting *T. rubrum* in vitro. Interaction results showed that the combination of SRT and CASP decreased the concentration of antifungals required to inhibit the fungus by up to 30 times compared to antifungals used individually. These results suggest that repositioning SRT and combining it with CASP constitutes a promising therapy against *T. rubrum*. Several reports have demonstrated SRT activity against pathogenic fungi in vitro and in vivo, with particular reference to *Cryptococcus*, *Candida*, and *Aspergillus* [30–33]. To the best of our knowledge, we are the first to demonstrate its effect alone and in combination with CASP against the dermatophyte, *T. rubrum*, though a previous study has discussed the advantages of using a combination of SRT and CASP against *Trichosporon asahii* [18]. Moreover, the SRT concentration in the skin is much higher than that in blood; thus, the usefulness of SRT as a treatment against dermatophytosis appears to be promising [34].

We observed that an SRT concentration of 70% of its MIC induced a gene that encodes a transmembrane transporter (*TERG_00162*) belonging to the major facilitator superfamily (MFS). These transporters mediate increased drug efflux, the primary resistance mechanism in dermatophytes [35–37]. In this context, the combination of SRT and CASP reduced the transcript levels of the *TERG_00162* gene. Furthermore, exposure of *T. rubrum* to SRTsc or CASPsc (0.273 mg/L SRT or 10.93 mg/L CASP) showed that the expression level of the gene *TERG_00162* was associated with the amount of SRT in the cell and with the activity of the combination.

Fungi may evolve several adaptation mechanisms in response to environmental changes. The fungal cell wall, which enables fungi to interact dynamically with the ambient environment, constitutes a promising antifungal target. Furthermore, its structural integrity, which is actively modulated in response to stress conditions, plays a role in adhesion, signalling, and colonisation, making it essential for the survival of the pathogen [38,39]. Accordingly, other promising antifungal targets were revealed by the treatments, SRT alone and SRT + CASP, which downregulated critical genes that encode chitin synthase (*TERG_12319*) and hydrophobin (*TERG_04234*). However, the expression of these genes did not change when *T. rubrum* was cultured with SRTsc or CASPsc compared to that with the control. This suggested that the efficacy of activity against TERG_04234 and TERG_12319 is due exclusively to the combination of drugs and not to each drug used alone. Chitin, a linear protein that provides strength and protection to many eukaryotes, is vital for cell wall morphogenesis. Chitin is absent in mammalian cells; thus, its metabolism is an attractive target for highly specific antifungal agents [39]. Usually, upregulation of chitin synthesis-related genes is the primary response to cell wall stress [40,41]. The chitin synthase is essential for synthesising chitin in the primary septa of fungi [42]. Hydrophobin, a cysteine-rich protein secreted only by filamentous fungi, lowers the surface tension of water. Identifying drugs that downregulate the genes encoding hydrophobin may help develop novel strategies to treat infections caused by *T. rubrum*. This protein regulates water flux across the fungal cell wall and mediates the attachment of infective structures associated with fungal pathogenesis. Thus, its downregulation is associated with decreased fungal virulence [39,43].

We also identified the effects of SRT and SRT + CASP on the ergosterol pathway. SRT alone at a 70% of its MIC and low concentrations of SRT + CASP downregulated the *TERG_06755* gene, which encodes a c-8 sterol isomerase. This enzyme is involved in the ergosterol biosynthesis cascade [44].The relevance of drugs that target genes or proteins involved in ergosterol biosynthesis has been reported [45].

Our assays demonstrated the impact of SRT and its synergic combination on the metabolism and biomass of *T. rubrum* biofilms. We demonstrated that even low concentrations of SRT, when combined with CASP, are effective against *T. rubrum* biofilms; scanning electron microscopy results substantiated this inhibitory effect. Thus, our results indicate that SRT activity at high concentrations, as well as in combination with CASP, downregulate essential genes related to the formation and constitution of the cell wall, and a gene associated with the ergosterol pathway.

Despite the mechanisms that underlie the effects of CASP on the cell wall of yeasts being known [46], we excluded the possibility that alterations in the expression levels of genes involved in biofilms could be caused by this drug at low concentrations. Our studies indicated that CASP alone or in SC concentrations did not alter the expression of genes involved in cell wall constitution. It did not significantly affect *T. rubrum* biofilms in any of the aspects studied.

Although we used a single reference strain from the *T. rubrum* species, our findings indicate an alternative treatment for dermatophytosis caused by this fungus. SRT combined with CASP minimises fungal resistance and virulence in vitro. However, in vivo studies must also validate our findings and define their clinical utility.

Structural modifications of SRT and CASP molecules would also increase their spectrum of action as antifungal agents, thereby optimising their usefulness against other pathogenic fungi.

Supplementary Materials: The following supporting information can be downloaded at: https://www.mdpi.com/article/10.3390/jof8080815/s1, Table S1. Primer sets used for real-time quantitative reverse transcription polymerase chain reaction (RT-qPCR). Figure S1. Expression of *TERG_00162* (MFS multidrug transporter), *TERG_04234* (Hydrophobin), *TERG_06755* (C-8 sterol isomerase), and *TERG_12319* (Chitin synthase 2) following SRTsc exposure. Asterisks indicate statistical significance determined by the *t*-test, compared to the control (SB absence drug) at 3 h (A) and 12 h (B); * $p < 0.05$. Figure S2. Differentially expressed genes, *TERG_00162* (MFS multidrug transporter), *TERG_04234* (Hydrophobin), *TERG_06755* (C-8 sterol isomerase), and *TERG_12319* (Chitin synthase 2), following exposure to CASPsc compared to the control (SB absence drug) at 3 h (A) and 12 h (B).

Author Contributions: C.H.L.R. thoroughly reviewed the literature and wrote the manuscript. C.H.L.R. and F.M.G.R. performed the laboratory experiments. C.H.L.R., F.M.G.R. and P.R.S. were responsible for the illustrations. T.A.B. and M.P.M. helped with the laboratory experiments. N.M.M.-R. has supervised the investigation. N.M.M.-R. and A.R. obtained the resources, reviewed, and edited the manuscript. All authors have read and agreed to the published version of the manuscript.

Funding: This work was supported by grants from the Brazilian Agencies: São Paulo Research Foundation-FAPESP [proc. No. 2019/22596-9, and Fellowships No. 2015/23435-8 to T.A.B. and No. 2018/11319-1 to M.P.M.]; National Council for Scientific and Technological Development–CNPq [Grants Nos. 307871/2021-5 and 307876/2021-7], Coordenação de Aperfeiçoamento de Pessoal de Nível Superior (CAPES)-Finance Code 001; and Fundação de Apoio ao Ensino, Pesquisa e Assistência-FAEPA.

Institutional Review Board Statement: The Ethics Committee of the University Hospital of Ribeirão Preto Medical School, USP, Brazil (HCFMRP-USP) (Protocol No. 4.304.317/2020), approved this study.

Informed Consent Statement: Not applicable.

Data Availability Statement: The data presented in this study are available in this article and the accompanying Supplementary Data.

Acknowledgments: We thank V. M. Oliveira, M. Mazucato, and M. D. Martins for technical support.

Conflicts of Interest: The authors declare no conflict of interest.

References

1. Martinez-Rossi, N.M.; Peres, N.T.; Bitencourt, T.A.; Martins, M.P.; Rossi, A. State-of-the-art Dermatophyte infections: Epidemiology aspects, pathophysiology, and resistance mechanisms. *J. Fungi* **2021**, *7*, 629. [CrossRef] [PubMed]
2. De Hoog, S.; Monod, M.; Dawson, T.; Boekhout, T.; Mayser, P.; Gräser, Y. Skin Fungi from Colonization to Infection. *Microbiol. Spectr.* **2017**, *5*, 4. [CrossRef]
3. Martinez-Rossi, N.M.; Bitencourt, T.A.; Peres, N.T.; Lang, E.A.; Gomes, E.V.; Quaresemin, N.R.; Martins, M.P.; Lopes, L.; Rossi, A. Dermatophyte resistance to antifungal drugs: Mechanisms and prospectus. *Front. Microbiol.* **2018**, *9*, 1108. [CrossRef] [PubMed]
4. Mendes, N.S.; Bitencourt, T.A.; Sanches, P.R.; Silva-Rocha, R.; Martinez-Rossi, N.M.; Rossi, A. Transcriptome-wide survey of gene expression changes and alternative splicing in *Trichophyton rubrum* in response to undecanoic acid. *Sci. Rep.* **2018**, *8*, 2520. [CrossRef] [PubMed]
5. Yamada, T.; Yaguchi, T.; Tamura, T.; Pich, C.; Salamin, K.; Feuermann, M.; Monod, M. Itraconazole resistance of *Trichophyton rubrum* mediated by the ABC transporter TruMDR2. *Mycoses* **2021**, *64*, 936–946. [CrossRef] [PubMed]
6. Robbins, N.; Caplan, T.; Cowen, L.E. Molecular Evolution of Antifungal Drug Resistance. *Annu. Rev. Microbiol.* **2017**, *71*, 753–775. [CrossRef] [PubMed]
7. Brilhante, R.S.N.; Aguiar, L.; Sales, J.A.; Araújo, G.D.S.; Pereira, V.S.; Pereira-Neto, W.A.; Pinheiro, A.Q.; Paixão, G.C.; Cordeiro, R.A.; Sidrim, J.J.C.; et al. Ex vivo biofilm-forming ability of der-matophytes using dog and cat hair: An ethically viable approach for an infection model. *Biofouling* **2019**, *35*, 392–400. [CrossRef]
8. Zhai, B.; Zhou, H.; Yang, L.; Zhang, J.; Jung, K.; Giam, C.-Z.; Xiang, X.; Lin, X. Polymyxin B, in combination with fluconazole, exerts a potent fungicidal effect. *J. Antimicrob. Chemother.* **2010**, *65*, 931–938. [CrossRef]
9. Wang, Y.; Lu, C.; Zhao, X.; Wang, D.; Liu, Y.; Sun, S. Antifungal activity and potential mechanism of Asiatic acid alone and in combination with fluconazole against *Candida albicans*. *Biomed. Pharmacother.* **2021**, *139*, 111568. [CrossRef]
10. Ashburn, T.T.; Thor, K.B. Drug repositioning: Identifying and developing new uses for existing drugs. *Nat. Rev. Drug Discov.* **2004**, *3*, 673–683. [CrossRef]

11. Zhai, B.; Wu, C.; Wang, L.; Sachs, M.S.; Lin, X. The antidepressant sertraline provides a promising therapeutic option for neurotropic cryptococcal infections. *Antimicrob. Agents Chemother.* **2012**, *56*, 3758–3766. [CrossRef]
12. Katende, A.; Mbwanji, G.; Faini, D.; Nyuri, A.; Kalinjuma, A.V.; Mnzava, D.; Hullsiek, K.H.; Rhein, J.; Weisser, M.; Meya, D.B.; et al. Short-course amphotericin B in addition to sertraline and fluconazole for treatment of HIV-associated cryptococcal meningitis in rural Tanzania. *Mycoses* **2019**, *62*, 1127–1132. [CrossRef]
13. Treviño-Rangel, R.d.J.; Villanueva-Lozano, H.; Méndez-Galomo, K.S.; Solís-Villegas, E.M.; Becerril-García, M.A.; Montoya, A.M.; Robledo-Leal, E.R.; González, G.M. In vivo evaluation of the antifungal activity of sertraline against *Aspergillus fumigatus*. *J. Antimicrob. Chemother.* **2019**, *74*, 663–666. [CrossRef]
14. De Vane, C.L.; Liston, H.L.; Markowitz, J.S. Clinical pharmacokinetics of sertraline. *Clin. Pharmacokinet.* **2002**, *41*, 1247–1266. [CrossRef]
15. Rainey, M.M.; Korostyshevsky, D.; Lee, S.; Perlstein, E.O. The antidepressant sertraline targets intracellular vesiculogenic membranes in yeast. *Genetics* **2010**, *185*, 1221–1233. [CrossRef]
16. Heller, I.; Leitner, S.; Dierich, M.; Lass-Flörl, C. Serotonin (5-HT) enhances the activity of amphotericin B against *Aspergillus fumigatus* in vitro. *Int. J. Antimicrob. Agents* **2004**, *24*, 401–404. [CrossRef]
17. Breuer, M.R.; Dasgupta, A.; Vasselli, J.G.; Lin, X.; Shaw, B.D.; Sachs, M.S. The Antidepressant Sertraline Induces the For-mation of Supersized Lipid Droplets in the Human Pathogen *Cryptococcus neoformans*. *J. Fungi* **2022**, *8*, 642. [CrossRef]
18. Cong, L.; Liao, Y.; Yang, S.; Yang, R. In vitro antifungal activity of sertraline and synergistic effects in combination with antifungal drugs against planktonic forms and biofilms of clinical *Trichosporon asahii* isolates. *PLoS ONE* **2016**, *11*, e0167903. [CrossRef]
19. Badali, H.; Mohammadi, R.; Mashedi, O.; de Hoog, G.S.; Meis, J.F. In vitro susceptibility patterns of clinically important *Trichophyton* and *Epidermophyton* species against nine antifungal drugs. *Mycoses* **2015**, *58*, 303–307. [CrossRef]
20. Baghi, N.; Shokohi, T.; Badali, H.; Makimura, K.; Rezaei-Matehkolaei, A.; Abdollahi, M.; Didehdar, M.; Haghani, I.; Abasta-bar, M. In vitro activity of new azoles luliconazole and lanoconazole compared with ten other antifungal drugs against clinical dermatophyte isolates. *Med. Mycol.* **2016**, *54*, 757–763. [CrossRef]
21. Bao, Y.Q.; Wan, Z.; Li, R.Y. In vitro antifungal activity of micafungin and caspofungin against dermatophytes isolated from China. *Mycopathologia* **2013**, *175*, 141–145. [CrossRef]
22. Su, S.; Yan, H.; Min, L.; Wang, H.; Chen, X.; Shi, J.; Sun, S. The antifungal activity of caspofungin in combination with antifungals or non-antifungals against *Candida* species in vitro and in clinical therapy. *J. Fungi* **2021**, *20*, 161–178. [CrossRef]
23. Caballero, U.; Eraso, E.; Quindós, G.; Jauregizar, N. In vitro interaction and killing-kinetics of amphotericin B combined with anidulafungin or caspofungin against *Candida auris*. *Pharmaceutics* **2021**, *13*, 1333. [CrossRef]
24. Kovács, R.; Bozó, A.; Gesztelyi, R.; Domán, M.; Kardos, G.; Nagy, F.; Majoros, L. Effect of caspofungin and micafungin in combination with farnesol against *Candida parapsilosis* biofilms. *Int. J. Antimicrob. Agents* **2016**, *47*, 304–310. [CrossRef]
25. Peres, N.T.d.A.; Silva, L.G.d.; Santos, R.d.S.; Jacob, T.R.; Persinoti, G.F.; Rocha, L.B.; Falcao, J.P.; Rossi, A.; Martinez-Rossi, N.M. In vitro and ex vivo infection models help assess the molecular aspects of the interaction of *Trichophyton rubrum* with the host milieu. *Sabouraudia* **2016**, *54*, 420–427. [CrossRef] [PubMed]
26. *M38-A2*; Reference Method for Broth Dilution Antifungal Susceptibility Testing of Filamentous Fungi—Second Edition. Clinical and Laboratory Standards Institute: Wayne, PA, USA, 2008.
27. Gómez-López, A.; Cuenca-Estrella, M.; Mellado, E.; Rodríguez-Tudela, J.L. In vitro evaluation of combination of terbinafine with itraconazole or amphotericin B against Zygomycota. *Diagn. Microbiol. Infect. Dis.* **2003**, *45*, 199–202. [CrossRef]
28. Livak, K.J.; Schmittgen, T.D. Analysis of relative gene expression data using real-time quantitative PCR and the $2^{-\Delta\Delta CT}$ method. *Methods* **2001**, *25*, 402–408. [CrossRef] [PubMed]
29. Costa-Orlandi, C.; Sardi, J.; Santos, C.; Fusco-Almeida, A.; Mendes-Giannini, M.J.S. In vitro characterization of *Trichophyton rubrum* and *T. mentagrophytes* biofilms. *Biofouling* **2014**, *30*, 719–727. [CrossRef] [PubMed]
30. Lass-Flörl, C.; Dierich, M.; Fuchs, D.; Semenitz, E.; Jenewein, I.; Ledochowski, M. Antifungal properties of selective serotonin reuptake inhibitors against *Aspergillus* species in vitro. *J. Antimicrob. Chemother.* **2001**, *48*, 775–779. [CrossRef]
31. Liu, S.; Hou, Y.; Chen, X.; Gao, Y.; Li, H.; Sun, S. Combination of fluconazole with non-antifungal agents: A promising approach to cope with resistant *Candida albicans* infections and insight into new antifungal agent discovery. *Int. J. Antimicrob. Agents* **2014**, *43*, 395–402. [CrossRef]
32. Gowri, M.; Jayashree, B.; Jeyakanthan, J.; Girija, E.K. Sertraline as a promising antifungal agent: Inhibition of growth and biofilm of *Candida auris* with special focus on the mechanism of action in vitro. *J. Appl. Microbiol.* **2020**, *128*, 426–437. [CrossRef]
33. Villanueva-Lozano, H.; González, G.M.; Espinosa-Mora, J.E.; Bodden-Mendoza, B.A.; Andrade, A.; Martínez-Reséndez, M.F.; Treviño-Rangel, R.J. Evaluation of the expanding spectrum of sertraline against uncommon fungal pathogens. *J. Infect. Chemother.* **2020**, *26*, 309–311. [CrossRef]
34. Tremaine, L.M.; Welch, W.M.; Ronfeld, R.A. Metabolism and disposition of the 5-hydroxytryptamine uptake blocker sertraline in the rat and dog. *Drug Metab. Dispos.* **1989**, *17*, 542–550.
35. Scorzoni, L.; de Paula e Silva, A.C.; Marcos, C.M.; Assato, P.A.; de Melo, W.C.; de Oliveira, H.C.; Costa-Orlandi, C.B.; Mendes-Giannini, M.J.; Fusco-Almeida, A.M. Antifungal therapy: New advances in the understanding and treatment of mycosis. *Front. Microbiol.* **2017**, *8*, 36. [CrossRef]
36. Yamada, T.; Yaguchi, T.; Salamin, K.; Guenova, E.; Feuermann, M.; Monod, M. MFS1, a Pleiotropic Transporter in Derma-tophytes That Plays a Key Role in Their Intrinsic Resistance to Chloramphenicol and Fluconazole. *J. Fungi* **2021**, *7*, 542. [CrossRef]

37. Monod, M.; Feuermann, M.; Salamin, K.; Fratti, M.; Makino, M.; Alshahni, M.M.; Makimura, K.; Yamada, T. *Trichophyton rubrum* Azole Resistance Mediated by a New ABC Transporter, TruMDR3. *Antimicrob. Agents Chemother.* **2019**, *63*, e00863-19. [CrossRef]
38. Cowen, L.E.; Sanglard, D.; Howard, S.J.; Rogers, P.D.; Perlin, D.S. Mechanisms of antifungal drug resistance. *Cold Spring Harb. Perspect. Med.* **2015**, *5*, a019752. [CrossRef]
39. Martins, M.P.; Silva, L.G.; Rossi, A.; Sanches, P.R.; Souza, L.D.R.; Martinez-Rossi, N.M. Global Analysis of Cell Wall Genes Revealed Putative Virulence Factors in the Dermatophyte *Trichophyton rubrum*. *Front. Microbiol.* **2019**, *10*, 2168. [CrossRef]
40. Walker, L.A.; Munro, C.A.; De Bruijn, I.; Lenardon, M.D.; McKinnon, A.; Gow, N.A. Stimulation of chitin synthesis rescues *Candida albicans* from echinocandins. *PLoS Pathog.* **2008**, *4*, e1000040. [CrossRef]
41. Fortwendel, J.R.; Juvvadi, P.R.; Pinchai, N.; Perfect, B.Z.; Alspaugh, J.A.; Perfect, J.R.; Steinbach, W.J. Differential effects of inhibiting chitin and 1, 3-β-D-glucan synthesis in ras and calcineurin mutants of *Aspergillus Fumigatus*. *Antimicrob. Agents Chemother.* **2009**, *53*, 476–482. [CrossRef]
42. Silverman, S.J.; Sburlati, A.; Slater, M.L.; Cabib, E. Chitin synthase 2 is essential for septum formation and cell division in *Saccharomyces cerevisiae*. *Proc. Natl. Acad. Sci. USA* **1988**, *85*, 4735–4739. [CrossRef]
43. Lang, E.A.S.; Bitencourt, T.A.; Peres, N.T.A.; Lopes, L.; Silva, L.G.; Cazzaniga, R.A.; Rossi, A.; Martinez-Rossi, N.M. The stuA gene controls development, adaptation, stress tolerance, and virulence of the dermatophyte *Trichophyton rubrum*. *Microbiol. Res.* **2020**, *241*, 126592. [CrossRef]
44. Petrucelli, M.F.; Matsuda, J.B.; Peroni, K.; Sanches, P.R.; Silva, W.A.; Beleboni, R.O., Jr.; Martinez-Rossi, N.M.; Marins, M.; Fachin, A.L. The Transcriptional Profile of *Trichophyton rubrum* Co-Cultured with Human Keratinocytes Shows New In-sights about Gene Modulation by Terbinafine. *Pathogens* **2019**, *8*, 274. [CrossRef]
45. Zhang, W.; Yu, L.; Yang, J.; Wang, L.; Peng, J.; Jin, Q. Transcriptional profiles of response to terbinafine in *Trichophyton Rubrum*. *Appl. Microbiol. Biotechnol.* **2009**, *82*, 1123–1130. [CrossRef] [PubMed]
46. Odds, F.C.; Brown, A.J.; Gow, N.A. Antifungal agents: Mechanisms of action. *Trends Microbiol.* **2003**, *11*, 272–279. [CrossRef]

Anexo C

Mycopathologia
https://doi.org/10.1007/s11046-021-00550-4

REVIEW

Reassessing the Use of Undecanoic Acid as a Therapeutic Strategy for Treating Fungal Infections

Antonio Rossi · Maíra P. Martins · Tamires A. Bitencourt · Nalu T. A. Peres · Carlos H. L. Rocha · Flaviane M. G. Rocha · João Neves-da-Rocha · Marcos E. R. Lopes · Pablo R. Sanches · Júlio C. Bortolossi · Nilce M. Martinez-Rossi

Received: 11 December 2020 / Accepted: 21 March 2021

Abstract Treating fungal infections is challenging and frequently requires long-term courses of antifungal drugs. Considering the limited number of existing antifungal drugs, it is crucial to evaluate the possibility of repositioning drugs with antifungal properties and to revisit older antifungals for applications in combined therapy, which could widen the range of therapeutic possibilities. Undecanoic acid is a saturated medium-chain fatty acid with known antifungal effects; however, its antifungal properties have not been extensively explored. Recent advances indicate that the toxic effect of undecanoic acid involves modulation of fungal metabolism through its effects on the expression of fungal genes that are critical for virulence. Additionally, undecanoic acid is suitable for chemical modification and might be useful in synergic therapies. This review highlights the use of undecanoic acid in antifungal treatments, reinforcing its known activity against dermatophytes. Specifically, in *Trichophyton rubrum*, against which the activity of undecanoic acid has been most widely studied, undecanoic acid elicits profound effects on pivotal processes in the cell wall, membrane assembly, lipid metabolism, pathogenesis, and even mRNA processing. Considering the known antifungal activities and associated mechanisms of undecanoic acid, its potential use in combination therapy, and the ability to modify the parent compound structure, undecanoic acid shows promise as a novel therapeutic against fungal infections.

Keywords Fatty acid · Undecanoic acid · Dermatophyte · Antifungal resistance · Synergistic · Pre-mRNA processing

Handling Editor: Vishnu Chaturvedi.

A. Rossi · M. P. Martins · T. A. Bitencourt · C. H. L. Rocha · F. M. G. Rocha · J. Neves-da-Rocha · M. E. R. Lopes · P. R. Sanches · J. C. Bortolossi · N. M. Martinez-Rossi (✉)
Department of Genetics, Ribeirão Preto Medical School, University of São Paulo, USP, Ribeirão Preto, SP 14049-900, Brazil
e-mail: nmmrossi@usp.br

N. T. A. Peres
Department of Microbiology, Institute of Biological Sciences, Federal University of Minas Gerais, Belo Horizonte, MG, Brazil

Published online: 09 April 2021

Introduction

Antifungal therapy is based on drugs that block cellular processes, such as cell wall assembly, cell membrane biosynthesis and maintenance, microtubule formation, and nucleic acid biosynthesis. The limited arsenal of antifungal drugs, the increasing prevalence of fungal infections, and the isolation of strains resistant to current medicines have motivated researchers to search for new therapeutic strategies

to control these infections [1]. The search for new antifungal drugs has involved studies of compounds derived from plants and other microorganisms that display antifungal properties [2, 3]. Various approaches have been evaluated to improve the efficacies of antifungal treatments. For example, combination therapy involves the use of clinically approved medicines that act synergistically with low toxicity and enhanced effectiveness. Novel technologies have been developed, especially those using nanoparticles, which have enabled improved drug delivery and availability, and decreased toxicity [4].

The therapeutic use of fatty acids (FA) has been known for a long time, especially against fungal skin infections. Their presence in the human skin represents a chemical barrier against opportunistic and pathogenic bacteria and fungi and is essential in maintaining skin integrity. FAs are also produced by the hydrolysis of phospholipids in keratinocytes, sebaceous glands, or the stratum corneum. In addition to their antimicrobial activities, they also play essential roles in maintaining acidification in the stratum corneum, making the skin a hostile environment for most pathogenic microorganisms [5, 6].

The antimycotic properties of organic acids have been evaluated since the nineteenth century [7]. In the 1940s, ointments containing propionate and undecylenate were proposed for treating dermatophytosis [8]. In addition, using a preparation of zinc undecylenate ($C_{22}H_{38}O_4Zn$) and undecylenic acid ($C_{11}H_{20}O_2$) (Fig. 1) in a vanishing emulsion base led to a complete clinical cure in the great majority of tinea pedis and tinea cruris cases [9]. Furthermore, the superiority of the propionate-caprylate mixture was verified in vitro and in vivo against dermatophytes, demonstrating that this combination seemed to be more effective than any other fatty acids previously used to treat these diseases [10]. At that time, studies were aimed at evaluating the fungistatic or fungicidal effect of FAs, particularly those found in human sweat (such as propionic, caproic, and caprylic acid); perspiration was attributed a protective activity against fungal infections [10].

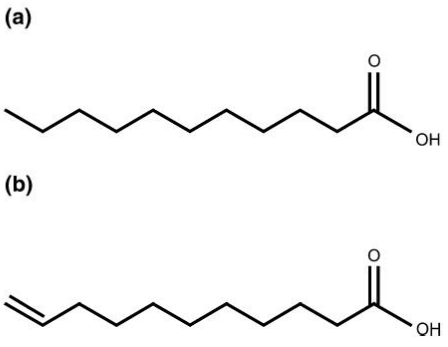

Fig. 1 Chemical structure of **a** undecanoic acid and **b** undecylenic acid

The antifungal activity of FAs was believed to be directly proportional to the number of carbon atoms in the molecule [11] or associated with the pH of the medium used in the assay. FAs with six or fewer carbon atoms exhibited higher antifungal activity in acidic medium, whereas FAs with more than seven carbons ($C_{7:0}$–$C_{12:0}$) exhibited higher activities at pH 7.0 or 8.0 [12]. The hypothesis of a relationship between antifungal activity and the number of carbon atoms in FA molecules was refuted when valeric acid, a FA with 5 carbon atoms, displayed the strongest fungicide activity of all the acids analyzed, including formic acid (1 carbon atom) to capric acid (10 carbon atoms), as well as the unsaturated undecylenic acid [13]. Further tests against dermatophytes demonstrated short-chain saturated FAs (C_7 to C_{11}) to be more toxic than long-chain molecules (> C_{12}), and undecanoic acid (UDA, a medium-chain saturated C_{11}) (Fig. 1) was the most toxic within the $C_{7:0}$-$C_{18:0}$ carbon atom series [14]. Interestingly, this FA is also found naturally in human sweat.

Studies on the activities of FAs in fungi have shown that they inhibit several biological processes, including respiration [15], cellular FA accumulation, and pigment formation in the dermatophyte *Trichophyton rubrum* [16]. FAs also reduced phosphate uptake and glucose fermentation in *Saccharomyces cerevisiae* [17]. UDA inhibited the growth of *T. rubrum*, conidia germination [18], phospholipid biosynthesis [19], and extracellular keratinase and lipase activities, but enhanced the activity of phospholipase A [20]. But, at low doses, UDA increased the lipid content [21]. Moreover, UDA-resistant strains have lowered virulence and important pathogenic traits are compromised by this FA [20, 22]. Recently, our group showed that UDA exposure affected the integrity, stability, and assembly of the cell wall and membrane of *T. rubrum*, and caused a decrease in the ergosterol level. These studies showed that UDA influenced the

expression of several genes involved in lipid metabolism, oxidative stress, cell wall and plasma membrane assembly, and pathogenesis [23, 24]. Furthermore, UDA affected the splicing of genes essential for cellular metabolism, intracellular signaling, and adaptation to stress [24–26].

Avrahami and Shai showed that UDA conjugation with antimicrobial lipopeptides can broaden their spectrum of actions, making them useful against several microorganisms [27]. These authors discussed the potential for increasing the activities of antimicrobial peptides by exploiting the property of synthetic lipopeptides in which they act directly on plasma membranes, thereby altering membrane permeability and facilitating drug uptake. UDA also causes damage to the cell wall and plasma membrane of fungi, suggesting it contributes to the synergistic effect of these two antimicrobial substances.

Combination treatment with UDA and quinic acid (QA), a compound derived from plants, synergistically inhibited the growth of *Candida albicans*, *Candida glabrata,* and *Candida tropicalis* by affecting several traits involved in virulence, such as biofilm formation and the production of proteases and phospholipases [28]. UDA was also effective inhibiting hyphal growth, a key step in *C. albicans* biofilm development, mimicking the quorum-sensing molecule farnesol that usually inhibits the yeast-to-hyphal transition [29]. In this review, we discuss recent findings highlighting the feasibility of using UDA as a cost-effective compound for antifungal treatment. We also discuss the suitability of UDA for chemical modification, conjugation with other molecules, and combination therapy.

Chemical Aspects, Molecule Modification, and Synergism

UDA, an 11-carbon, saturated medium-chain FA, is naturally present in the human skin and eliminated through sweat, and is industrially prepared from castor oil. UDA is a white crystalline solid, is insoluble in water, and is possibly involved in stimulating triacylglycerol synthesis [14, 30].

Although the therapeutic effectiveness of UDA against dermatophytes has been established for many years [14, 31], the enormous potential of this molecule remains poorly explored. Various studies demonstrated the therapeutic effectiveness of UDA when administered alone, enhanced activity when chemically modified, and synergistic activity when administered in combination with other compounds, such as antimicrobial peptides. The hydroxamate derivative of UDA, 10-undecanhydroxamic acid, functions as a novel antimicrobial agent with increased efficacy and a greater spectrum of activity by controlling the growth of clinically relevant microorganisms, including bacteria (such as *Escherichia coli* and *Enterococcus faecalis*) and fungi (*C. albicans* and *Aspergillus niger*). Its enhanced effectiveness is due to the introduction of an iron-chelating chemical group in the molecule, which interferes with iron homeostasis [31]. Disturbances in iron homeostasis have been associated with the effect of UDA against *T. rubrum*. Over time, UDA exposure accentuated the inhibitory effects on the expression of genes related to iron-binding activity [24]. The initial maintenance of the iron-acquisition system, with some upmodulated genes, occurs in response to UDA stress. After a 12-h UDA exposure, the repression of genes related to iron metabolism and many other categories is suggestive of widespread damage.

In another study, the activity of UDA was reduced by introducing acetylenic or ethylenic unsaturation into the UDA molecule in different positions from $C11\Delta^2$ to $C11\Delta^{10}$. These results established the saturated molecule as the most effective form of UDA. The effects of unsaturated UDA derivatives were evaluated against *Streptococcus pyogenes*. Comparatively, acetylenic compounds were slightly more active than the ethylenic isomers. The position of the ethylenic unsaturation site exerted minor effects against bacteria, whereas significant differences were observed with acetylenic derivatives, depending on the location of the unsaturated position [32].

Most antimicrobial peptides with high antibacterial activity are not active toward fungi. However, chemical modification of antimicrobial peptides can change this scenery. An antibacterial peptide, a magainin analog, exhibited antifungal activity when conjugated with lipophilic acids [33]. Also, conjugating UDA with this antibacterial lipopeptide resulted in high potency against some fungi [27]. These results led to the proposal of a new group of lipopeptide candidates with antifungal activity. Additionally, conjugating UDA to a weakly active diastereomeric lytic peptide containing Lys and Leu ([D]-K_5L_7) produced a highly potent lipopeptide. This compound was active against

gram-negative bacteria (*E. coli* and *Pseudomonas aeruginosa*), gram-positive bacteria (*Bacillus subtilis* and *Staphylococcus aureus*), yeasts (*C. albicans* and *Cryptococcus neoformans*), and the opportunistic fungus *Aspergillus fumigatus* [27].

Finally, the combined use of QA and UDA significantly repressed the major virulence genes of *C. albicans*. The synergistic interaction between these two compounds significantly inhibited important perpetuation-related aspects, such as biofilm formation and the filamentation capability [28]. The results obtained after combination therapy with UDA and other compounds with antifungal properties emphasized that such treatment represents a viable and promising alternative strategy.

In general, the use of UDA is mostly associated with antimycotic and antibacterial activity. However, the molecule also exhibits toxicity toward ticks and chiggers and displays repellent properties against fleas, house flies, *Anopheles quadrimaculatus*, and *Aedes aegypti* [34, 35]. It also inhibits oviposition in the phloem-feeding insect *Bemisia tabaci*, which is important for managing plant pests [36].

The well-known properties of UDA and its promising capacity for chemical modification and/or synergistic use highlight its potential importance in controlling fungal infections. The diverse strategies used to enhance its antimicrobial efficacy and its use in widespread applications, particularly its antifungal properties, establish UDA as a promising substance in the pharmaceutical field.

Impact of UDA on Fungal Metabolism

The antifungal activity of UDA has been demonstrated with various fungal species such as *Aspergillus nidulans* [37, 38], *Candida* spp. [28], *Trichophyton* spp. [14, 19], *Albifimbria verrucaria* (formerly *Myrothecium verrucaria*) [39], *S. cerevisiae* [40], and *Trichoderma viride* [39].

The possible mechanisms of action of medium-chain FAs, as previously described for *C. albicans*, include regulating cellular-membrane fluidity, mitochondrial activity changes, impaired formation of hyphae, and biofilm formation [41, 42]. Data from a recent study demonstrated that combination treatment with UDA and QA caused decreased secretion of aspartyl proteinases and lipase biosynthesis [28]. The same study showed a significant reduction in polysaccharide and lipid levels in the extracellular polymeric substance (EPS) of *Candida* spp. biofilm. Moreover, the inhibitory effect of QA-UDA combinations resulted in a prominent decrease in *C. albicans* filamentous growth [28]. UDA exhibited antibiofilm and anti-hyphal forming properties against *Candida* species [29], and antibiofilm activity against *Serratia marcescens* [43], suggesting UDA could be used to control the development of pathogenic biofilms.

A previous investigation of *S. cerevisiae* that assessed aspects of FA uptake and metabolism demonstrated the influence of the ergosterol pathway, specifically the *erg4* gene, in terms of the capacity of fungi to cope with exogenous FAs, such as UDA [40]. Several lines of evidence suggest that UDA is involved in FA and energy metabolism, as previously described for *Umbelopsis isabellina* (formerly *Mortierella isabellina*) [44]. UDA impacts the cellular lipid pattern of this fungus by inhibiting mitochondrial enzymes, blocking the elongation and acetylation of FAs, and making it difficult to incorporate these FAs into lipids in the cell. Moreover, data from a previous study demonstrated the effect of FAs on the growth of *Aspergillus flavus*, correlating with imbalanced peroxisome function, which ultimately resulted in aflatoxin production [45]. Also, *A. nidulans* exposed to sublethal doses of UDA led to decreased conidia germination [46], showed a significant decrease in extracellular lipase activity, and a reduction of approximately 70% in both intracellular and extracellular esterase activities [37].

Among studies exploring the antifungal properties of UDA, many were conducted against dermatophytes, mostly *T. rubrum*. Das and colleagues exploited the toxic effects of UDA against *T. rubrum* and confirmed the growth-inhibitory activity against this fungus [18–21]. UDA changed the lipid composition by lowering the synthesis of glycerides, sterol esters, and phospholipids, thus promoting changes in the fungal membrane and inhibiting its growth [21].

Treating *Trichophyton interdigitale* H6 (previously identified as *T. rubrum*, and reclassified based on genome sequencing) [47, 48] with UDA resulted in the induction of regulatory genes, such as *AURR1* (DW005378), a transcription factor that regulates aurofusarin biosynthesis, and the cellular regulator DopA (EZF34453.1), which is required for correct cell

morphology [49]. In addition, the susceptibility of *T. interdigitale* to UDA was nutrient-dependent [22].

It has been reported that UDA inhibits the growth of *T. rubrum* in concentrations ranging from 25 to 30 μg/mL [20, 24, 50]. In addition, other assays showed how UDA affects the production of exocellular enzymes by *T. rubrum*, inhibiting lipases and keratinases, which are necessary for the infection process [20]. Molecular studies on the effects of UDA on dermatophytes were performed to elucidate the strategies fungi use to overcome the effects triggered by the entry of UDA into fungal cells. UDA was assumed to alter *T. rubrum* lipid composition by possibly affecting an unknown control mechanism of lipid synthesis or breakdown [21]. The utilization of UDA in phospholipid biosynthesis was corroborated through the upregulation of a sterol carrier protein, followed by the induction of several genes related to FA synthesis and elongation, notably after 3 h of UDA exposure [24]. UDA also led to positive modulation of the beta-oxidation pathway. Fungal cells direct the degradation of FAs through different pathways, such as the beta-oxidation pathway, to overcome toxicity [51]; however, increased beta-oxidation activity significantly induced the overproduction of reactive oxygen species, which led to oxidative stress [24]. Also, ergosterol production was markedly reduced, which was reflected in impaired membrane fluidity. In addition, cellular detoxification pathways were activated to reverse the damage due to oxidative stress. The authors showed that most of these metabolic changes occurred after 3 h of exposure to UDA, which was due to the high toxicity of this FA. As mentioned above, dermatophytes use these strategies to overcome the deleterious effects of UDA that cause remodeling of the cell membrane and cell wall. A vital part of this strategy is the ability to use a sophisticated regulatory mechanism to alter gene expression [24] (Fig. 2).

Cells form integrated systems and, therefore, cellular physiology depends on a delicate balance between the synthesis and degradation of molecules involved in cell maintenance and metabolism. Once this balance is dysregulated, multiple cellular effects are triggered, which cannot be analyzed separately. A broader analysis of these effects is necessary to understand the overall effects of a drug, which may have secondary effects that should be considered. A transcriptomics study of *T. rubrum* exposed to sublethal doses of UDA shed insight on the refined cellular processes triggered by the drug [24]. The processes underlying these effects revealed that cellular-membrane damage had effects on the dermatophyte cell wall. Moreover, coordinated gene regulation might account for restructuring of the cell wall by modifications in its biochemical composition. The glycosyl hydrolase gene was upregulated after a 3-h challenge with UDA, which was a possible response to offset the damage caused by the drug during the early exposure period. However, the gene encoding the protein hydrophobin (TERG_04234), a cysteine-rich protein produced exclusively by filamentous fungi that is related to cell wall remodeling, was downregulated shortly after exposure to UDA. This observation merits attention because of the importance of hydrophobin to cell wall integrity, which was affected by damage to the plasma membrane, demonstrating the breadth of the responses by the fungus to overcome the toxic action of UDA [23].

An attractive approach for antifungal therapy is to target the gene-expression machinery, which is essential, given the network of cellular interactions that occur inside cells. Cells often fine-tune the levels of transcription to generate an appropriate response to a given stimulus. Positive and negative influences on gene expression must be balanced for correct mRNA synthesis [52]. Focusing on specific genes is becoming crucial for the development of drugs, such as transcription factors, which are of primary importance for all organisms [53]. Therefore, a drug capable of affecting transcription factors and disrupting a network of cellular interactions, thereby preventing fungi from responding correctly to developmental and environmental conditions, is an ideal solution. Importantly, the modulation of *T. rubrum* transcription factors is affected by UDA exposure, demonstrating that its toxic effects likewise affect the expression of genes closely related to regulating metabolic pathways in dermatophytes [24].

Taken together, the results of several reports have reinforced UDA as a compound with a broad spectrum of activity that triggers multiple effects in fungal cells, while being non-toxic to mammalian cells in vitro and to *Caenorhabditis elegans* [28, 54].

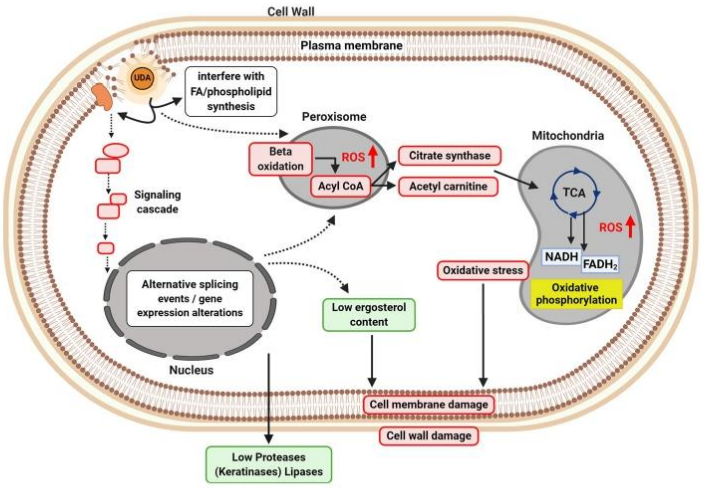

Fig. 2 Proposed mechanism of action of undecanoic acid (UDA) against fungal viability. UDA triggers oxidative stress, leading to changes in fatty acid (FA), phospholipid, and ergosterol synthesis. Increased levels of reactive oxygen species (ROS) cause damage to the cell membrane and cell wall. UDA also decreases the expression and activity of proteases and induces alternative splicing in genes involved in several cellular processes. Inhibited or downregulated processes are represented in green, while increased or upregulated processes are represented in red. Dashed lines represent pathways or processes that have not yet been fully elucidated. (Color figure online)

Fungal Resistance to UDA

A fundamental approach for evaluating the inhibitory potential of antifungals is to investigate the natural resistance mechanisms of fungi [38]. Pathogenic fungi deploy several molecular tools to handle the stress caused by toxic substances produced by host cells or that are present in the environment. For instance, *T. rubrum* responds to UDA mainly by modulating the expression of genes related to FA metabolism, oxidative stress, and proteases [24].

Thus, a mechanism that *T. rubrum* uses against UDA is its incorporation into phospholipid synthesis and degradation of the phospholipids by the β-oxidation enzymes as the acyl oxidase (TERG_02909) and ketoacyl thiolase (TERG_12530) [24]. These enzymes were notably induced after a 3-h exposure to UDA (Table 1). Another vigorous defense involves the induction of antioxidant enzymes to reduce the levels of reactive oxygen species [24].

Analysis of the results obtained through RNA-sequencing (RNA-seq) of *T. rubrum* exposed to acriflavine and UDA revealed upregulation of the ABC and MFS multidrug-resistance (MDR) transporters [23, 55]. MDR transporters are transmembrane components that function as efflux pumps. Overexpression of these proteins results in a resistant phenotype by preventing the over-accumulation of toxic compounds inside cells [56, 57]. Interestingly, the modulation of different transporter genes was observed in the presence of each of these drugs [23, 58], corroborating the idea that an adaptive response occurs in a drug-dependent manner [59]. Previous data revealed that the upregulation of MDR transporters occurred as a rapid response in the first hour after UDA exposure [58]. The presence of several different MDRs in the dermatophyte genome enables it to counteract many classes of drugs, which demonstrates the complexity of such regulation. Furthermore, compensatory expression of *mdr4*, due to the deletion of the *mdr2* gene, was observed in *T. interdigitale* grown in media containing the antifungal medicine griseofulvin [60].

In microorganisms, the biofilm structure is known to provide high resistance against external agents. Indeed, this structure constitutes a significant medical

Table 1 Genes associated with oxidative stress and fatty acid metabolism, grouped in terms of Gene Ontology enrichment

Gene ID	Gene product name	3 h	12 h
GO:0006979—response to oxidative stress			
TERG_01252	Catalase A		2.37
TERG_01463	Cytochrome c peroxidase (*T. tonsurans*)	3.17	2.15
TERG_02735	Fatty acid oxygenase PpoC, putative (*A. benhamiae*)	− 2.06	
TERG_06354	SVP1-like protein (*T. tonsurans*)	1.79	
TERG_08226	hypothetical protein	− 1.79	
GO:0034599—cellular response to oxidative stress			
TERG_01349	Glutathione peroxidase (*T. tonsurans*)	2.41	1.60
TERG_05769	NAD(P)H-dependent D-xylose reductase (*T. equinum*)	1.98	2.02
GO:0006631—fatty acid metabolic process			
TERG_05621	Short-chain dehydrogenase/reductase family oxidoreductase, putative (*A. benhamiae*)	4.02	
TERG_02909	Acyl-CoA oxidase, putative (*T. verrucosum*)	3.81	
TERG_07659	Peroxisomal 3-ketoacyl-coA thiolase (Kat1), putative (*A. benhamiae*)	3.01	
TERG_08170	Fatty acid elongase gig30 (*T. equinum*)	2.27	1.89
TERG_08952	Long-chain-fatty-acid-CoA ligase (*T. equinum*)	1.65	
TERG_06240	Peroxisomal biogenesis factor 2 (*T. tonsurans*)	1.60	
GO:0016747—transferase activity			
TERG_12530	3-Ketoacyl-CoA thiolase peroxisomal A (*T. tonsurans*)	4.19	1.50
TERG_07691	Sterol carrier protein (*T. tonsurans*)	2.73	
TERG_03390	Glutation S-transferase (*T. equinum*)	3.00	
TERG_04960	Glutathione S-transferase Ure2-like, putative (*A. benhamiae*)	6.15	
TERG_00284	Peroxin 14 (*T. tonsurans*)	2.52	
TERG_06361	ATP-dependent protease La	2.13	
TERG_01759	Peroxisome assembly protein 10 (*T. equinum*)	1.94	

Transcriptional modulation is indicated according to the exposure time to undecanoic acid [24]. Gene-expression values are expressed as log2-fold change between the indicated time point and the reference sample (without drug exposure)

problem, since most hospital-acquired infections are associated with biofilms on medical devices such as catheters, dentures, contact lenses, heart valves, and prostheses [61, 62]. Biofilm formation is frequently encountered in fungi; *Candida* spp. have been reported to be proficient in forming biofilms on both biotic and inert surfaces [63]. As mentioned above, combined UDA and QA therapy had a considerable effect on the biofilm structures of *Candida* spp. [28].

Another mechanism of resistance to UDA was described for *A. nidulans*, in which ultraviolet light-induced mutations in the *udaA* gene resulted in the resistant strains *udaA1* and *udaA2* [37]. Interestingly, it was observed that mutations in the *lipA* gene also conferred UDA resistance in *A. nidulans*. In this case, a point mutation in a particular locus caused a Glu-to-Lys substitution during translation, which potentially lowered the rate of enzymatic catalysis or the catalytic affinity of the enzyme for the substrate, or promoted enzymatic inactivation [38]. In addition, a recent study showed that UDA susceptibility was related to chromosome 7 trisomy in *C. albicans* and that resistance was due to chromosomal loss [64]. This study also showed that all susceptible isolates carrying a deletion of the transcription factor DAL81, and that acquired UDA resistance, had lost a copy of chromosome 7. Thus, these data draw a particular, but rather unclear, relationship between aneuploidy and antifungal resistance; a possibility that was corroborated by data from similar studies [65, 66].

A study carried out with a UDA-resistant strain (UDA^r) of *T. interdigitale* demonstrated that tolerance to UDA could also be displayed by a naturally non-resistant strain (H6) under specific nutritional

conditions [22]. Culturing the UDA^r and H6 strains in a protein-rich medium (minimal medium [MM] supplemented with 1% commercial low-fat dry milk) resulted in significant differences in survival rates at UDA concentrations above 50 mg/L. In contrast, culturing the same strains in a lipid-rich medium (MM supplemented with 1% Tween 20 as the sole carbon source) completely prevented the survival effect on the susceptible strain, even at high drug concentrations. The same nullifying effect on the inhibitory potential of UDA was observed when the strains were cultured in a keratin-rich medium (MM supplemented with keratin powder, 2.5 g/L) [22].

The possibility that nutrient conditions are crucial for establishing the susceptibility to a given drug is very relevant for isolating and characterizing resistant strains. Factoring in this possibility is also helpful when screening new antifungal agents [22]. Importantly, resistance acquired by wild-type strains due to environmental conditions (such as the carbon source) can serve as a determinant for the emergence of genetically resistant lineages. This process is a consequence of the population stabilization provided by the resistant phenotype so that mutations, recombination, and selection can occur. Events of environmentally induced resistance occurring before genetic resistance are well described and pose a real challenge for antifungal therapy [67, 68].

Resistance strategies like those described here are adaptive responses that have mostly been shaped by long-term natural selection involving co-evolutionary dynamics with hosts [69]. Despite the activation of common pathways related to stress responses, antifungals can cause high mortality rates, precisely because they correspond to substances that fungi have not experienced prolonged contact with during their evolution. Therefore, the misuse of antifungal drugs exacerbates opportunistic fungal infections by enabling the emergence of resistant strains [70]. Further investigation on this matter will be crucial for better guiding clinical efforts against recidivist pathogenic fungi that are mostly opportunistic.

Effect of UDA Exposure on Pre-mRNA Processing in Dermatophytes

Alternative splicing (AS) is an essential and highly complex process of post-transcriptional regulation that enables increased numbers of transcript isoforms for a single gene [71, 72]. AS powerfully enhances proteome diversity and functionality and thus fulfills paramount functions in adaptive responses [24, 73, 74].

The spliceosome machinery drives RNA processing after detecting exon boundaries (5′ and 3′ splice sites) [75]. The activity of the spliceosome is highly dynamic and coordinated. Splicing factors play essential roles in the activation and maintenance of this machinery [75, 76]. Recent work has shown differences in the modulation of splice factor genes in response to different environmental stimuli in the dermatophyte *T. rubrum* [77], which might ultimately influence the occurrence of AS. Indeed, changes in the relative rates of spliceosome assembly might be a means of AS regulation [78].

Patterns of AS that occur include the use of alternate 5′ or 3′ splice sites, exon skipping, intron retention (IR), and mutually exclusive events [72]. Although AS is not fully understood, fungal pathogens show a higher tendency to undergo AS than non-pathogenic fungi. If we consider only human pathogenic fungi, the relative proportion is even higher [79]. Moreover, evidence suggests the involvement of AS in complex regulatory network wiring in fungal cells that culminates in adaptive responses toward a plethora of stimuli. For example, antifungal signalling, nutrient supply, and host interactions have been reported to influence AS in *Neurospora crassa*, *T. rubrum*, *A. nidulans*, *A. fumigatus*, and *Candida* spp. [24, 73, 80, 81].

The RNA-seq tool consists of a robust and reliable source of data for the analysis of AS because it provides genome-wide information on exon coverage and splice junctions [82, 83]. It is noteworthy that in fungi, IR comprises the most predominant AS pattern [72, 81], and previous reports also demonstrated that only 14% of differentially expressed genes (DEGs) overlap with AS [81], which reinforces that AS occurs as a regulatory mechanism for specific adaptive responses.

Recent RNA-seq data showed the occurrence of AS events (in terms of exon usage and IR) in *T. rubrum* genes after UDA exposure [24]. Approximately 516 genes exhibited differences in exon usage after UDA exposure, distributed among 302 and 214 genes for the 3 h and 12 h time point, respectively (Fig. 3). About 967 genes underwent IR after UDA exposure,

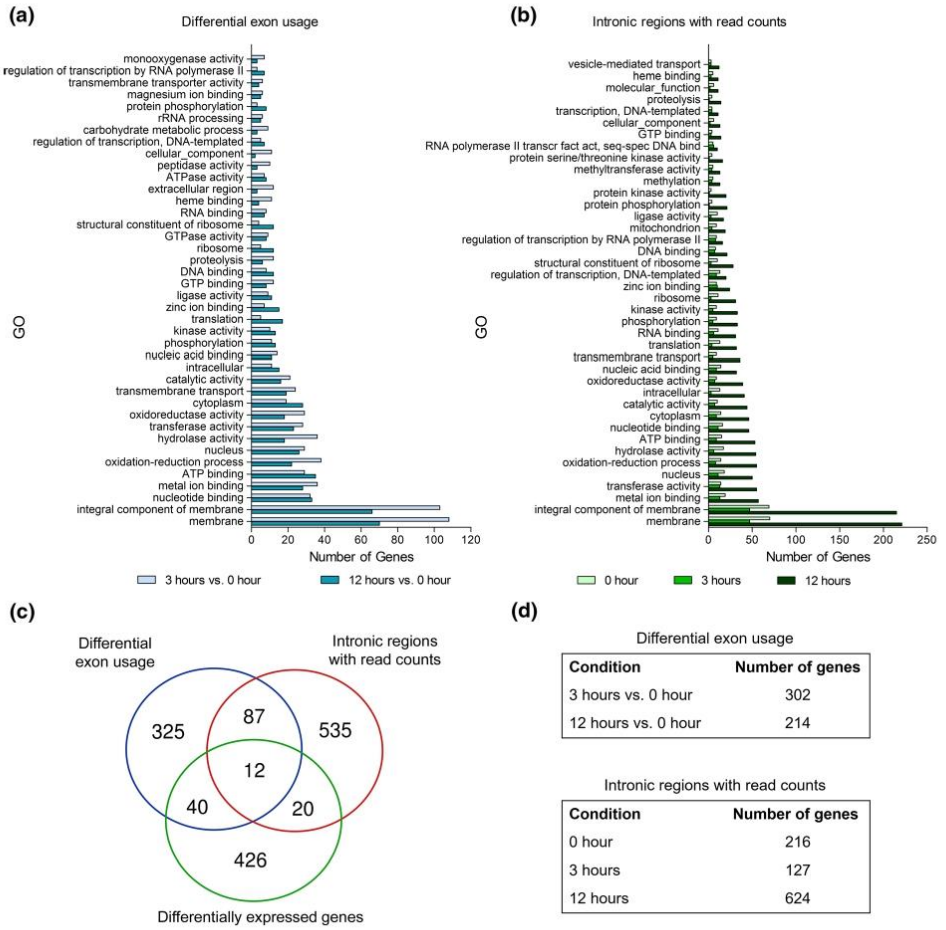

Fig. 3 In silico identification of genes presenting **a** differential exon usage or **b** intron retention, in response to undecanoic acid (UDA) exposure. Analysis was conducted by identifying significantly enriched Gene Ontology terms using previously published RNA-sequencing data [24]. **c** Venn diagram showing the number of transcripts modulated in *Trichophyton rubrum* cells following UDA exposure, and the number of genes that underwent alternative splicing events, differential exon usage, or intron retention. **d** Number of genes presenting differential exon usage and the number of intronic regions with read counts at each time point

distributed among 216 genes at 0 h, 127 genes at 3 h, and 624 genes at 12 h. While exon use events prevailed after a 3 h UDA exposure, IR was observed mainly after 12 h of contact with the drug (Fig. 3d). In both cases, the predominant group of genes subject to AS was related to membrane composition (Fig. 3a, b), associating UDA damage to the membrane with splicing events under the tested conditions. In addition, a small percentage of DEGs (approximately 15%) was associated with a type of AS, IR, or exon skipping (Fig. 3c), reiterating that the aforementioned

regulatory mechanism of AS contributes to adaptive strategies.

It was also reported that pre-mRNA coding for phosphoglucomutase underwent exon skipping and the pre-mRNA coding for inosine monophosphate dehydrogenase underwent IR. In both cases, the encoded enzymes are involved in critical energy metabolism. However, the proteins resulting from either form of AS presented a loss of essential domains and probably had impaired function [24]. These results demonstrated the existence of tight regulation promoted by AS between fungal energy metabolism and cellular signaling in response to UDA exposure. In addition, *T. rubrum* exposed to UDA presented IR events in two genes that encode heat shock proteins (HSPs): Hsp7-like protein (TERG_03206) and Hsp75-like protein (TERG_01883) [26]. In silico analysis revealed that conventional processing of the respective pre-mRNAs of both genes led to functional proteins. In contrast, the AS events caused by IR promoted open reading frame disruptions, resulting in premature mRNA stop codons and the generation of truncated proteins with probable functional impairment. Modulation of the Hsp7-like protein isoforms was compared after *T. rubrum* exposure to UDA and terbinafine. UDA exposure promoted dysregulated gene processing and decreased levels of transcripts coding for functional proteins. In contrast, terbinafine exposure caused increased transcript levels coding for functional proteins after a 3 h UDA exposure, and no difference in modulation of the retained isoform was observed between control and drug-treated cells. These results raised the possibility that a regulatory pathway is involved in HSPs processing, which is probably related to optimization in response to different chemical exposures (cellular conditions). Indeed, refined mechanisms for protein production, co-translation, protein folding, and disposal have been described, each of which plays paramount roles in maintaining cellular homeostasis and proper metabolism [84–86].

The occurrence of IR events in two genes that encode heat shock proteins in *T. rubrum* exposed to UDA was revealed in the pre-mRNA coding for STE/PAKA kinase, as an autoregulatory mechanism for this kinase [25]. Increased IR levels were observed after a 3-h UDA exposure. In silico analyses showed a change in the open reading frame for the kinase due to IR, which was responsible for the production of at least two independent polypeptides. One polypeptide contained the entire kinase catalytic domain, but lacked the regulatory domain. This finding suggests that an alternative pre-mRNA splicing played a role in activating the STE20/PAKA kinase in *T. rubrum*, independent of caspase cleavage or molecular signaling that is normally required for its canonical activation. These results also suggest that the MAPK pathway was activated to varying extents and regulated by different sets of molecules by external stimuli. Based on these lines of evidence, we hypothesize that different sources of isoforms could be generated by AS, leading to potentially functional proteins or proteins with impaired function, which is mainly influenced by the roles each gene plays within cells. In addition, these events rely on a complex signaling cascade that culminates in the optimization of protein production according to the needs of a fungus.

Concluding Remarks and Perspectives

In this review, we highlight known and novel perspectives related to the antifungal properties of UDA. The limited antifungal options currently available have led to increased attention on the potential use of UDA as a therapeutic strategy against fungal infections. This potential use is strengthened by the broad-spectrum activity of UDA, which includes potent antimycotic activity against several human pathogenic fungi, such as *Aspergillus* spp., *Candida* spp., and *Trichophyton* spp. The main effects of UDA exposure on some fungi are compiled in Table 2. Furthermore, UDA is suitable for chemical modifications enabling it to serve as a model scaffold for designing novel and more efficient antimicrobial molecules, it displays synergistic activity with other compounds, and it is non-toxic to mammalian cells and worms. In summary, the data discussed here highlight this overlooked compound as a potentially safe and effective antifungal agent.

Author contributions All authors wrote sections of the manuscript. NM-R, MM, and AR edited the manuscript. All authors read and approved the submitted version.

Funding We thank the Brazilian funding agencies for the continuous support to our projects: São Paulo Research Foundation - FAPESP (proc. Nos. 2019/22596-9, 2018/11319-

Table 2 Main effects observed in some microorganisms following exposure to undecanoic acid

Microorganism	Observed effect	Working doses	References
Trichophyton rubrum	Lipid composition increased when UDA^s was grown in low concentration of UDA	30 μg ml^{-1}	[21]
	Inhibited conidial germination of UDA^s and UDA^r	UDA^s at 30 μg ml^{-1} and UDA^r 120 μg ml^{-1}	[18]
	Inhibited production of exocellular lipase and keratinase	27.5 μg ml^{-1}	[20]
	Inhibited phospholipid metabolism	50 μg ml^{-1}	[19]
	Affected fungal metabolism and pre-mRNA processing regulatory events	17.5 μg mL^{-1}	[24]
Trichophyton interdigitale	Inhibited growth in response to UDA and carbon source for both wild type and UDA^r strains	Concentration is dependent on the carbon source	[22]
	Affected gene-expression profile	50 μg mL^{-1}	[49]
Serratia marcescens	Impaired biofilm formation	ranging from 20 to 160 μg/ml	[43]
Candida albicans		2 μg ml^{-1}	[29]
		QA (50–800 μg mL^{-1}) in combination with UDA (5–80 μg mL^{-1})	[28]
Aspergillus nidulans	Decreased extracellular lipase activity	200 μg mL^{-1}	[37]
	Impaired conidia germination	0 to 300 μg mL^{-1}	[46]
Saccharomyces cerevisiae	Inhibited growth	0.5 mM, 1 mM or 2 mM	[40]
Umbelopsis isabellina	Inhibited biosynthesis of long-chain fatty acids	Concentration is dependent on the carbon source	[44]

QA = quinic acid; UDA = undecanoic acid; UDA^s = UDA sensitive strain; UDA^r = UDA resistant strain

1, 2018/15458-6, 2015/23435-8, 2009/08411-4); National Council for Scientific and Technological Development -CNPq (proc. Nos. 305797/2017-4, and 304989/2017-7); Coordenação de Aperfeiçoamento de Pessoal de Nível Superior - CAPES (Finance Code 001), and Fundação de Apoio ao Ensino, Pesquisa e Assistência - FAEPA.

Declarations

Conflict of interest The authors declare that they have no conflicts of interest.

Research involving human participants and/or animals This manuscript does not contain any studies with human participants or animals performed by any of the authors.

References

1. Martinez-Rossi NM, Bitencourt TA, Peres NTA, Lang EAS, Gomes EV, Quaresemin NR, et al. Dermatophyte resistance to antifungal drugs: mechanisms and prospectus. Front Microbiol. 2018;9:1108.
2. Cordoba S, Vivot W, Szusz W, Albo G. Antifungal activity of essential oils against *Candida* species isolated from clinical samples. Mycopathologia. 2019;184(5):615–23.
3. Lopes AI, Tavaria FK, Pintado ME. Conventional and natural compounds for the treatment of dermatophytosis. Med Mycol. 2020;58(6):707–20.
4. Souza ACO, Amaral AC. Antifungal therapy for systemic mycosis and the nanobiotechnology era: improving efficacy, biodistribution and toxicity. Front Microbiol. 2017;8:336.
5. Drake DR, Brogden KA, Dawson DV, Wertz PW. Thematic review series: skin lipids—antimicrobial lipids at the skin surface. J Lipid Res. 2008;49(1):4–11.
6. Feingold KR. The outer frontier: the importance of lipid metabolism in the skin. J Lipid Res. 2009;50:S417–22.
7. Clark JF. On the toxic effect of deleterious agents on the germination and development of certain filamentous fungi. Bot Gaz. 1899;28(5):289–327.
8. Keeney EL, Ajello L, Broyles EN, Lankford E. Propionate and undecylenate ointments in the treatment of tinea pedis and an *in vitro* comparison of their fungistatic and antibacterial effects with other ointments. Bull Johns Hopkins Hosp. 1944;74:417–39.
9. Shapiro AL, Rothman S. Undecylenic acid in the treatment of dermatomycosis. Arch Dermatol. 1945;119(4):345–50.
10. Peck SM, Russ WR. Propionate-caprylate mixtures in the treatment of dermatomycoses, with a review of fatty acid therapy in general. Arch Derm Syphilol. 1947;56(5):601–13.

11. Kiesel A. Recherches sur L'action de divers acides et sels acides sur le développement de L'*Aspergillus niger*. Ann Inst Pasteur. 1913;27:391–420.
12. Hoffman C, Schweitzer TR, Dalby G. Fungistatic properties of the fatty acids and possible biochemical significance. J Food Sci. 1939;4(6):539–45.
13. Peck SM, Rosenfeld H. The effects of hydrogen ion concentration, fatty acids and vitamin C on the growth of fungi. J Invest Dermatol. 1938;1(4):237–65.
14. Garg AP, Muller J. Fungitoxicity of fatty acids against dermatophytes. Mycoses. 1993;36(1–2):51–63.
15. Vicher EE, Lyon I, White EL. Studies on the respiration of *Trichophyton rubrum*. Mycopathol Mycol Appl. 1959;11:185–95.
16. Vicher EE, Kostiw LL, Lyon I, Bolewicz BM. The effect of sodium propionate and sodium caprylate on the fatty acid content of *Trichophyton rubrum*. Mycopathol Mycol Appl. 1968;35(3):208–14.
17. Samson FE, Katz AM, Harris DL. Effects of acetate and other short-chain fatty acids on yeast metabolism. Arch Biochem Biophys. 1955;54(2):406–23.
18. Das SK, Adhya S, Banerjee AB. Effect of undecanoic acid on germination of microconidia of wild and undecanoic acid resistant mutant of *Trichophyton rubrum*. Mycopathologia. 1977;61(2):121–3.
19. Das SK, Banerjee AB. Effect of undecanoic acid on phospholipid-metabolism in *Trichophyton rubrum*. Sabouraudia-J Med Vet Mycol. 1982;20(4):267–72.
20. Das SK, Banerjee AB. Effect of undecanoic acid on the production of exocellular lipolytic and keratinolytic enzymes by undecanoic acid-sensitive and -resistant strains of *Trichophyton rubrum*. Sabouraudia. 1982;20(3):179–84.
21. Das SK, Banerjee AB. Effect of undecanoic acid on lipid composition of *Trichophyton rubrum*. Mycopathologia. 1983;83(1):35–9.
22. Peres NTA, Cursino-Santos JR, Rossi A, Martinez-Rossi NM. *In vitro* susceptibility to antimycotic drug undecanoic acid, a medium-chain fatty acid, is nutrient-dependent in the dermatophyte *Trichophyton rubrum*. World J Microbiol Biotechnol. 2011;27(7):1719–23.
23. Martins MP, Silva LG, Rossi A, Sanches PR, Souza LDR. Martinez-Rossi NM. Global analysis of cell wall genes revealed putative virulence factors in the dermatophyte *Trichophyton rubrum*. Front Microbiol. 2019;10:2168.
24. Mendes NS, Bitencourt TA, Sanches PR, Silva-Rocha R, Martinez-Rossi NM, Rossi A. Transcriptome-wide survey of gene expression changes and alternative splicing in *Trichophyton rubrum* in response to undecanoic acid. Sci Rep. 2018;8(1):2520.
25. Gomes EV, Bortolossi JC, Sanches PR, Mendes NS, Martinez-Rossi NM, Rossi A. STE20/PAKA protein kinase gene releases an autoinhibitory domain through pre-mRNA alternative splicing in the dermatophyte *Trichophyton rubrum*. Int J Mol Sci. 2018;19(11):3654.
26. Neves-da-Rocha J, Bitencourt TA, de Oliveira VM, Sanches PR, Rossi A, Martinez-Rossi NM. Alternative splicing in heat shock protein transcripts as a mechanism of cell adaptation in *Trichophyton rubrum*. Cells. 2019;8(10):1206.
27. Avrahami D, Shai Y. Bestowing antifungal and antibacterial activities by lipophilic acid conjugation to D, L-amino acid-containing antimicrobial peptides: a plausible mode of action. Biochemistry. 2003;42(50):14946–56.
28. Muthamil S, Balasubramaniam B, Balamurugan K, Pandian SK. Synergistic effect of quinic acid derived from *Syzygium cumini* and undecanoic acid against *Candida* spp. biofilm and virulence. Front Microbiol. 2018;9:2835.
29. Lee JH, Kim YG, Khadke SK, Lee J. Antibiofilm and antifungal activities of medium-chain fatty acids against *Candida albicans* via mimicking of the quorum-sensing molecule farnesol. Microb Biotechnol. 2020.
30. Hastings J, Owen G, Dekker A, Ennis M, Kale N, Muthukrishnan V, et al. ChEBI in 2016: improved services and an expanding collection of metabolites. Nucleic Acids Res. 2016;44(D1):D1214–9.
31. Ammendola S, Lembo A, Battistoni A, Tagliatesta P, Ghisalberti C, Desideri A. 10-undecanhydroxamic acid, a hydroxamate derivative of the undecanoic acid, has strong antimicrobial activity through a mechanism that limits iron availability. FEMS Microbiol Lett. 2009;294(1):61–7.
32. Kabara JJ, Vrable R. Antimicrobial lipids: natural and synthetic fatty acids and monoglycerides. Lipids. 1977;12(9):753–9.
33. Avrahami D, Shai Y. Conjugation of a magainin analogue with lipophilic acids controls hydrophobicity, solution assembly, and cell selectivity. Biochemistry. 2002;41(7):2254–63.
34. Jones AM, Klun JA, Cantrell CL, Ragone D, Chauhan KR, Brown PN, et al. Isolation and identification of mosquito (*Aedes aegypti*) biting deterrent fatty acids from male inflorescences of breadfruit (*Artocarpus altilis* (Parkinson) Fosberg). J Agric Food Chem. 2012;60(15):3867–73.
35. Ali A, Cantrell CL, Bernier UR, Duke SO, Schneider JC, Agramonte NM, et al. *Aedes aegypti* (Diptera: Culicidae) biting deterrence: structure–activity relationship of saturated and unsaturated fatty acids. J Med Entomol. 2012;49(6):1370–8.
36. Cruz-Estrada A, Ruiz-Sanchez E, Cristobal-Alejo J, Gonzalez-Coloma A, Andres MF, Gamboa-Angulo M. Medium-chain fatty acids from *Eugenia winzerlingii* leaves causing insect settling deterrent, nematicidal, and phytotoxic effects. Molecules. 2019;24(9):1724.
37. Brito-Madurro AG, Cuadros-Orellana S, Madurro JM, Martinez-Rossi N, Rossi A. Effect of undecanoic acid on the production of esterases and lipases by *Aspergillus nidulans*. Ann Microbiol. 2005;55(4):291–4.
38. Brito-Madurro AG, Prade RA, Madurro JM, Santos MA, Peres NT, Cursino-Santos JR, et al. A single amino acid substitution in one of the lipases of *Aspergillus nidulans* confers resistance to the antimycotic drug undecanoic acid. Biochem Genet. 2008;46(9–10):557–65.
39. Gershon H, Shanks L. Antifungal activity of fatty acids and derivatives: structure–activity relationships. In: Kabarra JJ, editor. The pharmacological effect of lipids. American Oil Chemists Society; 1978.
40. McDonough V, Stukey J, Cavanagh T. Mutations in *erg4* affect the sensitivity of *Saccharomyces cerevisiae* to medium-chain fatty acids. Biochim Biophys Acta Mol Cell Biol Lipids. 2002;1581(3):109–18.
41. Shi D, Zhao Y, Yan H, Fu H, Shen Y, Lu G, et al. Antifungal effects of undecylenic acid on the biofilm formation of

Candida albicans. Int J Clin Pharmacol Ther. 2016;54(5):343–53.
42. Mionic Ebersold M, Petrovic M, Fong WK, Bonvin D, Hofmann H, Milosevic I. Hexosomes with undecylenic acid efficient against *Candida albicans*. Nanomaterials (Basel). 2018;8(2):91.
43. Salini R, Sindhulakshmi M, Poongothai T, Pandian SK. Inhibition of quorum sensing mediated biofilm development and virulence in uropathogens by *Hyptis suaveolens*. Antonie Van Leeuwenhoek. 2015;107(4):1095–106.
44. Hortmann L, Rehm HJ. Inhibitory effect of undecanoic acid on the biosynthesis of long-chain fatty acids in *Mortierella isabellina*. Appl Microbiol Biotechnol. 1984;20(2):139–45.
45. Reverberi M, Punelli M, Smith CA, Zjalic S, Scarpari M, Scala V, et al. How peroxisomes affect aflatoxin biosynthesis in *Aspergillus flavus*. PLoS ONE. 2012;7(10):e48097.
46. Brito-Madurro AG, Cuadros-Orellana S, Martinez-Rossi NM, Rossi A. Undecanoic acid resistance in filamentous fungi: Identification and linkage mapping of the *Aspergillus nidulans udaA* gene. J Gen Appl Microbiol. 2005;51(1):47–9.
47. Persinoti GF, Martinez DA, Li W, Dogen A, Billmyre RB, Averette A, et al. Whole-genome analysis illustrates global clonal population structure of the ubiquitous dermatophyte pathogen *Trichophyton rubrum*. Genetics. 2018;208(4):1657–69.
48. Chaturvedi V, de Hoog GS. Onygenalean fungi as major human and animal pathogens. Mycopathologia. 2020;185(1):1–8.
49. Paião FG, Segato F, Cursino-Santos JR, Peres NT, Martinez-Rossi NM. Analysis of *Trichophyton rubrum* gene expression in response to cytotoxic drugs. FEMS Microbiol Lett. 2007;271(2):180–6.
50. Das SK, Banerjee AB. Effect of undecanoic acid on cell-permeability and respiration of *Trichophyton rubrum*. Acta Microbiol Pol. 1981;30(3):295–8.
51. Hiltunen JK, Mursula AM, Rottensteiner H, Wierenga RK, Kastaniotis AJ, Gurvitz A. The biochemistry of peroxisomal beta-oxidation in the yeast *Saccharomyces cerevisiae*. FEMS Microbiol Rev. 2003;27(1):35–64.
52. Shelest E. Transcription factors in fungi. FEMS Microbiol Lett. 2008;286(2):145–51.
53. Bahn YS. Exploiting fungal virulence-regulating transcription factors as novel antifungal drug targets. PLoS Pathog. 2015;11(7):e1004936.
54. Li XC, Jacob MR, Khan SI, Ashfaq MK, Babu KS, Agarwal AK, et al. Potent *in vitro* antifungal activities of naturally occurring acetylenic acids. Antimicrob Agents Chemother. 2008;52(7):2442–8.
55. Persinoti GF, Peres NTA, Jacob TR, Rossi A, Vencio RZ, Martinez-Rossi NM. RNA-sequencing analysis of *Trichophyton rubrum* transcriptome in response to sublethal doses of acriflavine. BMC Genomics. 2014;15(Suppl 7):S1.
56. Prasad R, Rawal MK. Efflux pump proteins in antifungal resistance. Front Pharmacol. 2014;5:202.
57. Aneke CI, Rhimi W, Otranto D, Cafarchia C. Synergistic effects of efflux pump modulators on the azole antifungal susceptibility of *Microsporum canis*. Mycopathologia. 2020;185(2):279–88.
58. Martins MP, Rossi A, Sanches PR, Martinez-Rossi NM. Differential expression of multidrug-resistance genes in *Trichophyton rubrum*. J Integr OMICS. 2019;9(2):1–81.
59. Fachin AL, Ferreira-Nozawa MS, Maccheroni W Jr, Martinez-Rossi NM. Role of the ABC transporter TruMDR2 in terbinafine, 4-nitroquinoline N-oxide and ethidium bromide susceptibility in *Trichophyton rubrum*. J Med Microbiol. 2006;55(Pt 8):1093–9.
60. Martins MP, Franceschini AC, Jacob TR, Rossi A, Martinez-Rossi NM. Compensatory expression of multidrug-resistance genes encoding ABC transporters in dermatophytes. J Med Microbiol. 2016;65(7):605–10.
61. Chandra J, Mukherjee PK, Ghannoum MA. *Candida* biofilms associated with CVC and medical devices. Mycoses. 2012;55:46–57.
62. Nett JE, Zarnowski R, Cabezas-Olcoz J, Brooks EG, Bernhardt J, Marchillo K, et al. Host contributions to construction of three device-associated *Candida albicans* biofilms. Infect Immun. 2015;83(12):4630–8.
63. Mayer FL, Wilson D, Hube B. *Candida albicans* pathogenicity mechanisms. Virulence. 2013;4(2):119–28.
64. Ma QX, Ola M, Iracane E, Butler G. Susceptibility to medium-chain fatty acids is associated with trisomy of chromosome 7 in *Candida albicans*. mSphere. 2019;4(3):e00402–19.
65. Selmecki A, Forche A, Berman J. Aneuploidy and isochromosome formation in drug-resistant *Candida albicans*. Science. 2006;313(5785):367–70.
66. Pavelka N, Rancati G, Zhu J, Bradford WD, Saraf A, Florens L, et al. Aneuploidy confers quantitative proteome changes and phenotypic variation in budding yeast. Nature. 2010;468(7321):321–5.
67. Cowen LE, Carpenter AE, Matangkasombut O, Fink GR, Lindquist S. Genetic architecture of Hsp90-dependent drug resistance. Eukaryot Cell. 2006;5(12):2184–8.
68. Cowen LE, Lindquist S. Hsp90 potentiates the rapid evolution of new traits: drug resistance in diverse fungi. Science. 2005;309(5744):2185–9.
69. Decaestecker E, Gaba S, Raeymaekers JAM, Stoks R, Van Kerckhoven L, Ebert D, et al. Host-parasite "Red Queen" dynamics archived in pond sediment. Nature. 2007;450(7171):870-U16.
70. Martinez-Rossi NM, Peres NT, Rossi A. Antifungal resistance mechanisms in dermatophytes. Mycopathologia. 2008;166(5–6):369–83.
71. Kelemen O, Convertini P, Zhang Z, Wen Y, Shen M, Falaleeva M, et al. Function of alternative splicing. Gene. 2013;514(1):1–30.
72. Kempken F. Alternative splicing in ascomycetes. Appl Microbiol Biotechnol. 2013;97(10):4235–41.
73. Mendes NS, Silva PM, Silva-Rocha R, Martinez-Rossi NM, Rossi A. Pre-mRNA splicing is modulated by antifungal drugs in the filamentous fungus *Neurospora crassa*. FEBS Open Bio. 2016;6(4):358–68.
74. Laloum T, Martin G, Duque P. Alternative splicing control of abiotic stress responses. Trends Plant Sci. 2018;23(2):140–50.
75. Chen W, Moore MJ. Spliceosomes. Curr Biol. 2015;25(5):R181-3.
76. Koncz C, Dejong F, Villacorta N, Szakonyi D, Koncz Z. The spliceosome-activating complex: molecular

mechanisms underlying the function of a pleiotropic regulator. Front Plant Sci. 2012;3:9.
77. Bitencourt TA, Oliveira FB, Sanches PR, Rossi A, Martinez-Rossi NM. The prp4 kinase gene and related spliceosome factor genes in *Trichophyton rubrum* respond to nutrients and antifungals. J Med Microbiol. 2019;68(4):591–9.
78. Black DL. Mechanisms of alternative pre-messenger RNA splicing. Annu Rev Biochem. 2003;72:291–336.
79. Grutzmann K, Szafranski K, Pohl M, Voigt K, Petzold A, Schuster S. Fungal alternative splicing is associated with multicellular complexity and virulence: a genome-wide multi-species study. DNA Res. 2014;21(1):27–39.
80. Leal J, Squina FM, Freitas JS, Silva EM, Ono CJ, Martinez-Rossi NM, et al. A splice variant of the *Neurospora crassa hex-1* transcript, which encodes the major protein of the Woronin body, is modulated by extracellular phosphate and pH changes. FEBS Lett. 2009;583(1):180–4.
81. Sieber P, Voigt K, Kammer P, Brunke S, Schuster S, Linde J. Comparative study on alternative splicing in human fungal pathogens suggests its involvement during host invasion. Front Microbiol. 2018;9:2313.
82. Roberts A, Pimentel H, Trapnell C, Pachter L. Identification of novel transcripts in annotated genomes using RNA-Seq. Bioinformatics. 2011;27(17):2325–9.
83. Goldstein LD, Cao Y, Pau G, Lawrence M, Wu TD, Seshagiri S, et al. prediction and quantification of splice events from RNA-Seq data. PLoS ONE. 2016;11(5):e0156132.
84. Hug N, Longman D, Caceres JF. Mechanism and regulation of the nonsense-mediated decay pathway. Nucleic Acids Res. 2016;44(4):1483–95.
85. Yu CH, Dang Y, Zhou Z, Wu C, Zhao F, Sachs MS, et al. Codon usage influences the local rate of translation elongation to regulate co-translational protein folding. Mol Cell. 2016;59(5):744–54.
86. Zhou Z, Dang Y, Zhou M, Yuan H, Liu Y. Codon usage biases co-evolve with transcription termination machinery to suppress premature cleavage and polyadenylation. Elife. 2018;7:29.